DOCTOR OF SCIENCES

LQ-optimal boundary control of infinite-dimensional linear systems

Dehaye, Jérémy

Award date:
2015

Awarding institution:
University of Namur

UNIVERSITÉ DE NAMUR

FACULTÉ DES SCIENCES

DÉPARTEMENT DE MATHÉMATIQUE

LQ-optimal boundary control of infinite-dimensional linear systems

Thèse présentée par
Jérémy Dehaye
pour l'obtention du grade
de Docteur en Sciences

Composition du Jury:

Timoteo CARLETTI
Denis DOCHAIN
Anne-Sophie LIBERT (Présidente du Jury)
Christophe PRIEUR
Joseph WINKIN (Promoteur)

Octobre 2015

Imprimé en Belgique

978-2-87037-916-5
Dépôt légal: D/2015/1881/47

Université de Namur
Faculté des Sciences
Rue de Bruxelles, 61, B-5000 Namur (Belgique)

Commande frontière LQ-optimale de systèmes linéaires en dimension infinie
par Jérémy Dehaye

Résumé : Nous considérons une classe de systèmes avec commande et observation frontière pour lesquels les opérateurs non bornés induisent généralement des difficultés techniques. Un modèle étendu, n'impliquant aucun opérateur non borné à l'exception du générateur, est décrit et analysé. Nous montrons que, sous certaines hypothèses, le modèle est bien posé et, en particulier, que l'opérateur correspondant à la dynamique est le générateur d'un C_0-semigroupe. De plus, nous montrons que le système est observable et conserve certaines propriétés du système nominal, telles que la commandabilité, la stabilisabilité et la détectabilité. Nous présentons une méthode pour la résolution du problème de commande LQ-optimale pour ce modèle, dont la solution fournit un asservissement d'état stabilisant pour le système nominal. Cette méthodologie est basée sur le problème de factorisation spectrale d'une densité spectrale multidimensionnelle à valeurs opératorielles. Elle est appliquée à des systèmes décrits par des équations aux dérivées partielles (EDP) paraboliques ou hyperboliques, modélisant des phénomènes de diffusion-convection-réaction ou un flux de Poiseuille, respectivement. Cette approche semble mener à un bon compromis entre l'investissement théorique requis par la modélisation et l'efficacité des méthodes de résolution de problèmes de commande pour ce type de systèmes.

LQ-Optimal Boundary Control of Infinite-Dimensional Linear Systems
by Jérémy Dehaye

Abstract: A class of boundary control systems with boundary observation is considered, for which the unbounded operators often lead to technical difficulties. An extended model is described and analyzed, which involves no unbounded operator except for the dynamics generator. It is shown that, under suitable conditions, the model is well-posed and, in particular, that the dynamics operator is the generator of a C_0-semigroup. Moreover, the model is shown to be observable and to carry controllability, stabilizability and detectability properties from the nominal system. A method for the resolution of the LQ-optimal control problem for this model is described and the solution provides a stabilizing feedback for the nominal system. This methodology is based on the problem of spectral factorization of a multi-dimensional operator-valued spectral density. It is applied to parabolic and hyperbolic partial differential equations (PDE) systems modeling convection-diffusion-reaction phenomena and a Poiseuille flow, respectively. This approach seems to lead to a good trade-off between the theoretical investment required by the modeling and the efficiency of methods of resolution of control problems for such systems.

Thèse de doctorat en Sciences Mathématiques (Ph.D. thesis in Mathematics)
Date: 08/10/2015
Département de Mathématique
Promoteur (Advisor): Prof. J. WINKIN

Remerciements

Il n'est pas toujours facile, en parcourant le résultat de plusieurs années de recherche, de prendre conscience du rôle qu'ont pu jouer les moments partagés avec de nombreuses personnes. De l'importance et de l'impact que celles-ci ont pu avoir, que ce soit dans le cadre d'une collaboration professionnelle, pour le soutien reçu, ou simplement pour les bons moments passés ensemble.
Avant toute autre chose, je tiens à remercier du fond du coeur mon promoteur, Joseph Winkin, qui m'a donné l'opportunité de passer ces six années enrichissantes et a permis l'aboutissement de ce travail de recherche. Je n'aurais pas retiré autant de cette période de ma vie sans ses qualités, tant humaines que scientifiques, et je lui en suis profondément reconnaissant. Merci pour l'aide immense apportée lors de l'élaboration de ce travail, pour avoir su donner de précieux conseils tout en me laissant toujours une liberté importante dans les choix effectués, pour m'avoir présenté des personnes très intéressantes, et pour les nombreuses discussions (parfois sérieuses et parfois moins) dont je suis toujours ressorti avec le sourire aux lèvres.
Ce travail doit également beaucoup à la collaboration avec les chercheurs du GIPSA-lab de Grenoble. Je remercie en particulier Christophe Prieur, Emmanuel Witrant et Felipe Castillo pour leur accueil remarquable lors de chacun de mes séjours au GIPSA-lab et pour m'avoir donné la possibilité d'effectuer divers travaux de recherche et tests expérimentaux au sein de leurs locaux, pour lesquels ils m'ont apporté une aide précieuse.
Mes remerciements vont aussi à Anne-Sophie Libert pour avoir accepté de présider le jury de thèse ainsi qu'à Denis Dochain, Timoteo Carletti et Christophe Prieur qui ont accepté d'en faire partie et ont apporté une contribution importante à l'amélioration du manuscrit. Par ailleurs, je remercie Denis Dochain et Jean-Charles Delvenne pour avoir constitué le comité d'accompagnement et pour leurs commentaires constructifs et utiles dans le cadre de l'épreuve de confirmation.
Je remercie bien entendu ceux qui m'ont entouré pendant ces magnifiques années, à commencer par mon frère Jon, à qui je dois énormément. Tellement, en fait, qu'en faire la liste ici nécessiterait probablement un chapitre à part, que je me sens trop fainéant pour écrire. Alors, je dirai tout simplement ... merci pour tout, bro.
Je dis merci aux autres membres de ma famille qui, malgré leur affection plutôt limitée pour les mathématiques, m'ont toujours soutenu et encouragé dans mes décisions et ont toujours répondu présents quand j'avais besoin d'eux, ou simplement pour passer de bons moments ensemble. Merci en particulier à Papa, Maman, Papy Michel, Mamy, Papy Hector, Taty, Fabrice, Adrien et Lisa pour tous leurs signes d'affection, les éclats de rire, les encouragements, les sorties en famille, les parties de belote, de whist et de manie endiablées (mais sans tricher !), et tant d'autres choses !
Merci à Charles Hubaux pour les innombrables moments épiques passés en sa compagnie, au bureau comme ailleurs, pour avoir supporté mon désordre légendaire (presque) sans broncher et pour m'avoir aidé à pulvériser tant d'adversaires sur Battlenet. Merci à Martin Gueuning pour avoir su prendre la relève avec brio en tant que collègue de bureau de luxe, pour son humour imparable et inimitable (du génie, je te dis) et pour son soutien inestimable en toutes circonstances. Merci à Sébastien "Chabal" Canart

qui a su autant marquer l'histoire du Cercle Info que mes propres années passées à Namur. Merci à Denis Noël pour être le troll le plus sympa que je connaisse et pour les excellentes soirées jeux passées en sa compagnie. Merci à Jérémy Rekier pour son humour pas toujours si British qui sait faire mouche quand on s'y attend le moins et son implication dans nos très agréables soirées "vieux cons". Merci à Pauline Lucas pour être la belle-soeur dont tout le monde rêve (ou presque) et pour son sens de la répartie et ses taunts cinq étoiles qui me font souvent rire aux éclats. Merci à Eve-Aline Dubois pour ses encouragements dans les périodes de rush, pour avoir réparé mon tableau (espèce de m. d. s. é. !), pour sa Joie (très) communicative et sa faculté à me mettre de bonne humeur, et pour les nombreuses sphères multicolores qui resteront précieusement ancrées dans les dédales de ma mémoire à long terme. Merci à Florence "Floflo" "la Blonde" Peteers pour les taunts réciproques à base de "blondasse" et de "rongeur", pour les moments d'anthologie (avec ou sans tequila) et pour Jimmy qui me tient fidèlement compagnie depuis pas mal de temps maintenant. Merci à Delphine Nicolay pour son ventilateur. Merci à François Lamoline pour tous ces intenses moments de réflexivité (et pour sa cravate). Non, sérieusement, merci à Delphine pour m'avoir toujours permis de squatter son bureau quand je voulais profiter de sa charmante compagnie (sans rire) et pour être la Tristesse la plus blonde, la plus cool et la plus agréable qu'il m'ait été donné de rencontrer. Merci à Johan "Jojo" Barthélémy (qui, pour moi, restera à jamais "Le Président") pour avoir égayé mes journées à l'aide de son humour brutalement efficace et pour avoir été la clef de voûte de la plupart de nos légendaires comités "bidons". Merci à Ambi pour ses nombreux encouragements et pour sa dévotion (parfois exaspérante, souvent amusante et toujours excessive) à essayer de me trouver une future ex-Madame Dehaye. Merci aux autres membres (anciens ou actuels) du staff, et en particulier à Céline Renkens, Charlotte Tannier, Emilie Verheylewegen, Laurie Hollaert, Marie Moriamé, Marie-Alice Poulin, Manon Bataille, Marie Pierard, Morgane Dumont, Marie Leroy, Pauline Thémans et Julien Petit, pour avoir contribué à embellir, chacun et chacune à leur façon, ces semaines, mois et années passés au département. Merci à mes anciens cokotteurs, et en particulier le "noyau dur" (ils se reconnaitront), pour les innombrables moments de pur délire qui se sont transformés en moments de pure nostalgie avec les années. Merci à Mr P. (aka Poney) pour ses nombreuses histoires rocambolesques et son style inimitable pour les raconter. Merci à Pierre Petit et sa courageuse bande de Bac 1 avec qui j'ai apprécié ces petites pauses (dangereuses mais nécessaires) en salle de licence à l'approche de la deadline, ainsi qu'à tous mes autres "petits élèves modèles" sans qui ces années n'auraient pas eu la même saveur.

Merci à toutes et à tous pour avoir marqué ce chapitre important de ma vie ! Il ne reste plus qu'à écrire le suivant.
Et, comme dirait Barney Stinson, it's gonna be legen - wait for it -

Jérémy

Contents

Part I

Introduction

I think we can put our differences behind us.
For science.
You monster.

– GLaDOS

The concept of controlling a system is omnipresent in every day's life, even at the most basic level. Most of the technologies of this age require adapted actions, which are often automated, in order to work as intended. Whether it be for casual, industrial or more specialized usage, regulating, stabilizing or, in general, imposing a desired behaviour to a physical system is often critical in view of many different objectives, such as avoiding a chaotic evolution, maximizing productivity, minimizing waste generation... This involves a wide range of applications, including industrial processes, chemical, mechanical, biological or biomechanical systems, regulation of common devices such as fridges or computers, and many others.
The physical laws governing these systems are often well-known and allow for relatively accurate, or at least efficient, mathematical models. However, though these models may be powerful for predicting the behaviour of the system in the absence of an external influence, it is often much more challenging to design efficient control laws in view of a given objective. One of these challenges arises when one wants to deal with systems that are by nature made to be controlled at one or several specific and punctual locations, or, more generally, on a portion of their physical boundary. In a mathematical formalism, these are often called *boundary control systems*.
Things can become even more complicated when, in addition, the measurements of the considered physical quantities are punctual or done on the boundary as well, which is also reflected by the mathematical model. This is often the case in practice since many sensors or measurement devices are only able to give limited information on the actual state of the system.

When put into this mathematical formalism, *boundary control systems with boundary observation* (BCBO systems) can generally be written as three equations describing the dynamics (including an optional distributed input), the boundary conditions and the observation, respectively. These equations will be studied in more detail later and are given by (1.2.1)-(1.2.3).
These systems typically feature unbounded observation and control linear operators along with the homogeneous dynamics generator and an optional bounded distributed control linear operator. Because of technical difficulties caused by the unboundedness, it is often difficult to solve specific control problems and design control laws for such systems. If possible, this characteristic should then better be avoided in order to achieve an acceptable trade-off between the cost of modeling and the efficiency of analytic and/or numerical methods of resolution of control problems.

The main goal of this work is to pose and solve a *LQ-optimal control problem* for such systems by using the *method of spectral factorization by symmetric extraction*. This problem and more particularly the aforementioned method of resolution for infinite-

dimensional distributed parameter systems have been studied extensively by the Systems and Control team of the University of Namur. In addition of the interesting benefits it may bring to the field, studying the LQ-optimal control problem and developing this methodology as well as the associated results further in the framework of this thesis is a natural and straightforward choice. The solution of this problem is known to be a stabilizing bounded feedback operator and the corresponding control law to be robust in the presence of perturbations. However, the proposed method of resolution, as well as other well-known methods, typically require some relatively strong assumptions on the system, such as the dynamics being well-posed in the sense that the dynamics operator is the generator of a C_0-semigroup, the control and observation operators being bounded or the system being at least stabilizable and detectable.

With these considerations in mind and in order to solve the LQ-optimal control problem, the first step consists of building an extended differential system involving no unbounded operator except for the dynamics generator. For this purpose, we will consider, under suitable conditions, a change of variables for the state and input of the nominal system, as well as a Yosida-type approximation of the output which is based on the resolvent operator of the dynamics generator (Weiss 1994).
This choice yields a well-posed extended system with similar dynamical properties than those of the nominal one. This extended system, described by (1.2.13)-(1.2.14), whose form is well-known in the area of linear systems and control theory, has well-posed dynamics and bounded control and observation operators, which is crucial in order to deal with the aforementioned technical difficulties.
Under suitable initial conditions and inputs, the (extended) state depends on the nominal state, but also on the boundary input and the approximate output which will be included in the state variables for technical reasons. Therefore, one of the novelties of this work is the fact that the boundary input and approximate output trajectories are given jointly by the dynamics equation, thanks to the fact that both are components of the extended state. An important consequence of this choice of model is that the extended input includes the derivative of the nominal boundary input with respect to time. As is detailed in this work, this characteristic implies that any static feedback law designed for the nominal system, including the solution of the LQ-optimal control problem, can be interpreted as a dynamic feedback law for the nominal system.

It is shown that, under suitable conditions, the model is well-posed and, in particular, that the dynamics operator is the generator of a C_0-semigroup. Moreover, the proposed extension is shown to be observable and detectable, and preserves some useful properties of the nominal system, including (approximate) reachability and (exponential) stabilizability (when the nominal system has this property with respect to the distributed input u_d) as well as the spectral structure of the dynamics generator. A part of the analysis is devoted to the case of analytic dynamics generators, which is of particular interest. In fact, the relation between the extended and nominal model relies in particular on the fact that the inputs are sufficiently regular. If analyticity of the nominal dynamics generator is transmitted to the extended one, the relation between both systems holds in closed-loop under feedback laws designed for the extended sys-

tem, in addition of generating regular state, input and output trajectories, which is in general a desirable property.
In the central part of this work, a LQ-optimal control problem is posed for the extended model, which consists of minimizing a quadratic cost functional over the space of inputs.
This problem can be interpreted in the framework of the nominal system, with the time derivative of the boundary input and the approximate output entering the cost functional in addition of the standard terms involving the state and the inputs. The extended model has been designed such that this cost functional, and more particularly the penalization associated to each state, input or output component, can be tuned with a rather large degree of freedom in order to comply with different objectives in practical applications.
It is also shown that this problem has a unique solution and a general method of resolution is then developed. This method is based on the resolution of the problem of spectral factorization of an appropriate operator-valued coercive spectral density and the resolution of a Diophantine equation.
As previously mentioned, it is shown that the solution of the LQ-optimal control problem can be interpreted as a dynamical feedback for the nominal system. One of the key results of this work is that this dynamical feedback designed for the extended system exponentially stabilizes the nominal system in the sense that, in closed-loop, the state trajectories of the nominal system converge to zero exponentially fast.

A semi-heuristic algorithm of spectral factorization by symmetric extraction of pole-zero elementary matrix factors has been developed with an application in mind. This application is a class of parabolic convection-diffusion-reaction systems that is typically used to model a wide range of industrial or natural processes involving phenomena of dispersion, transport and reaction, such as chemical or biochemical reactors. The algorithm is applied successfully in this case, and can readily be extended to a wider class of infinite-dimensional MIMO differential linear systems satisfying some spectral conditions.
The case of hyperbolic systems is treated as well, with two models describing the evolution of a Poiseuille flow, which can be simulated by a test bench. The goal was to implement the control laws derived from the theory with this physical test bench in order to check the feasibility of designing and applying control laws based on this methodology to real life systems.

It is expected that this approach will lead hopefully to a good trade-off between the cost of modeling and the efficiency of methods of resolution of control problems for such systems, like the LQ-optimal control problem.

The idea behind this methodology was introduced for finite-dimensional systems with input derivative constraints, where the time derivative of the input enters the quadratic cost functional for the resolution of a LQ-optimal control problem, see e.g. (Moore and Anderson 1967). In the infinite-dimensional framework, this approach is motivated by the fact that the unboundedness property leads to technical difficulties which

make the modeling and analysis of such systems very hard, see e.g. (Weiss 1994), (Tucsnak and Weiss 2009), (Staffans 2005) and references therein, and the design of control laws as well, especially when boundary control and boundary observation are both present in the model, see e.g. (Weiss and Weiss 1997), or when the control operator is very unbounded, see e.g. (Opmeer 2014) and references therein. A change of variables was already considered for boundary control alone (without observation) in (Fattorini 1968) and (Curtain and Zwart 1995, Section 3.3, pp. 121–128) in order to deal with this problem. Concerning the boundary observation in particular, in (Weiss 1994) and (Tucsnak and Weiss 2009, Section 4.7, p. 147), the Lebesgue and Yosida extensions were presented in the framework of well-posed linear systems.
The LQ-optimal control problem has been studied extensively for systems with bounded control and observation operators, see e.g. (Curtain and Zwart 1995, Chapter 6, pp. 269–334), (Callier and Winkin 1992) and (Aksikas, Winkin and Dochain 2007) (and references therein). A part of the core components of this work has been studied and developed in (Dehaye and Winkin 2013*a*) and (Dehaye and Winkin 2013*b*), upon which many improvements have been made in order to refine the model, methodology, theoretical results and numerical algorithms. For example, in (Dehaye and Winkin 2013*a*), the well-posedness analysis of the model required the C_0-semigroup generated by the dynamics operator to be analytic and the approximate output operator to be weighted by a well-chosen parameter, which could turn out to be hard to determine in practical situations. The assumptions have been weakened and the proofs adapted in consequence in order to obtain a more general model. Moreover, new results concerning the exponential stabilizability and detectability of the extended system have been added. New numerical tests have been performed in order to study the impact of noise on the closed-loop system or the impact of the parameters on the numerical computation of the spectrum of the dynamics generator.

The manuscript is organized as follows.
Part II is dedicated to the main theoretical framework.
In Chapter 1, we introduce a class of abstract differential linear systems with unbounded control and observation operators. We show that they can be described by an extended model that fits in the standard framework with well-posed dynamics and bounded control and observation operators.
In Chapter 2, we present some results concerning the main properties of the extended system, and in particular reachability, observability, stabilizability and detectability. Then, we introduce additional assumptions in order to show that the outputs and transfer functions of both systems are related. More precisely, it is shown that, when some real parameter goes to infinity, the output and transfer function of the nominal system are the limits of the output and transfer function of the extended system, respectively. This important relationship motivates the efforts devoted to the modeling, analysis and control of the extended system.
In Chapter 3, an infinite horizon LQ-optimal control problem is defined for the extended system and we show that it is related to a LQ-optimal control problem for the nominal system. In that chapter, it is also shown that its solution can be interpreted as a dynamical feedback for the nominal system.

Part III focuses on illustrating the theoretical results presented in Part II by the numerical resolution of a particular LQ-optimal control problem for two classes of infinite-dimensional differential linear systems.
A class of convection-diffusion-reaction systems with distributed control along with boundary control and observation is studied first in Chapter 4. The corresponding extended model is constructed and analyzed. An algorithm of spectral factorization by symmetric extraction that can be extended to a wider class of infinite-dimensional MIMO systems is presented and implemented for the numerical resolution of a LQ-optimal (pure boundary or mixed) control problem.
In Chapter 5, theoretical, numerical and experimental results are presented for two models of hyperbolic systems which describe the behaviour of a Poiseuille flow test bench.

Finally, in Part IV, we make some concluding remarks and give some perspectives for future work.

Contributions

Boundary control systems have been a topic of interest in the field of systems and control for many years. The approach presented in this thesis has its roots in the development of models that allow boundary control systems to be considered in the standard framework with bounded linear control operators. These developments were pioneered in (Fattorini 1968) and considered in several other works, such as (Curtain and Zwart 1995). However, this formalism does not take boundary observation into account, which leads to additional difficulties when combined with boundary control, and the question of well-posedness naturally arises in this case. The design of specific control laws and the case of closed-loop systems in this formalism are still largely unexplored as well.
This work brings several contributions in the field of systems and control, and in particular boundary control systems with boundary observation. Some of the core results and methods of this thesis have been developed and established in several published or submitted conference or journal papers.

The first developments concerning our class of boundary control systems with boundary observation were presented in (Dehaye and Winkin 2013*a*), which was published in the proceedings of the first IFAC Workshop on Control of Systems Modeled by Partial Differential Equations (CPDE). That paper introduced the main framework and the extended model that is used throughout this work and focused on its well-posedness. It also showed how a given class of convections-diffusion-reaction systems can fit in this framework.

Some of the central results involving control, and more precisely LQ-optimal control, based on this model were presented and established in (Dehaye and Winkin 2013*b*), which was published in the proceedings of the 52nd Conference on Decision and

Control (CDC) after a review process as well. That paper showed how a LQ-optimal control problem for the extended model can be related to a similar problem for a class of boundary control systems with boundary observation. One of the main additions of this work is the resolution of this problem by spectral factorization with assumptions less restrictive than those in (Callier and Winkin 1992) and (Aksikas et al. 2007), and the proof that its solution can be interpreted as a stabilizing dynamical feedback for the nominal system. In that work, a general methodology for the resolution of this problem, based on the resolution of a problem of spectral factorization, was presented. A semi-heuristic algorithm of spectral factorization by symmetric extraction for a class of MIMO systems was developed in view of solving such a problem numerically. This methodology was illustrated with numerical tests involving the previously mentioned class of convection-diffusion-reaction systems.

Another article concerning this work and entitled "LQ-Optimal Boundary Control of Infinite-Dimensional Systems with Yosida-Type Approximate Boundary Observation" has been submitted to Automatica as a regular paper. This paper improved and extended both the theoretical and numerical results developed previously by weakening the assumptions required for the well-posedness, establishing a stronger link between the nominal and extended model with a comparison between the approximate and effective outputs and transfer functions, extending the results and methodology to the case of LQ-optimal pure boundary control, and bringing additional numerical results in order to further illustrate some robustness, stabilization or convergence properties.

This work is built on the foundations of these contributions while improving the previously established framework and results, and adding a new application to hyperbolic systems. In particular, this manuscript offers an overview of the differences that can arise between pure boundary control and mixed boundary and distributed control, with a detailed methodology and corresponding theoretical results for both cases. It also offers a more in depth analysis of some important theoretic properties of the convection-diffusion-reaction system, like e.g. stabilizability and reachability. Moreover, several new numerical results have been added. The application to hyperbolic systems helps demonstrating that the proposed framework and methodology cover a wide range of infinite-dimensional differential linear systems. It also includes the results of experimental tests that were performed in the GIPSA-lab of Grenoble on a test bench simulating a Poiseuille flow on the basis of the method presented here.

A more detailed list of the most important contributions can be found below.

- J. R. Dehaye, J. J. Winkin, *Boundary control systems with Yosida type approximate boundary observation*, Proceedings of the first IFAC Workshop on Control of Systems Modeled by Partial Differential Equations (CPDE), paper no. 61 (Paris, France, 25-27 September 2013) (Dehaye and Winkin 2013*a*) (with invited presentation)

- J. R. Dehaye, J. J. Winkin, *LQ-optimal control by spectral factorization of extended semigroup boundary control systems with approximate boundary observation*, Proceedings of the 52nd IEEE Conference on Decision and Control (CDC), pp. 1071-1076 (Florence, Italy, 10-13 December 2013) (Dehaye and Winkin 2013*b*) (with invited presentation)

- J. R. Dehaye, J. J. Winkin, *LQ-optimal boundary control of infinite-dimensional systems with Yosida-type approximate boundary observation*, Automatica ; provisionally accepted as Regular Paper, under revision (2014)

- Participation in an international group project supervised by Professor Delio Mugnolo (Institute of Analysis, University of Ulm, Ulm, Germany) and presentation at the ISEM 2011 workshop: *Further semigroup methods for control systems: controllability and observability* (Blaubeuren, Germany, 5-11 June 2011)

- Presentation of a poster at the 8th Workshop on Control of Distributed Parameter Systems (CDPS): *Boundary control systems with Yosida type approximate boundary observation* (Craiova, Romania, 1-5 July 2013)

Part II

Boundary control systems with boundary observation

Chapter 1

Modeling

1.1 Motivation

Most physical systems involved in practical applications, such as cooling or heating systems, disinfection and purification processes, or industrial processes, including for example beer or yogurt fermentation and many others, need to be controlled efficiently in order to yield interesting results. Controlling such systems often requires acting on a physical boundary. Though this may seem simpler at first glance, several problems arise when one attempts to model these systems in a mathematical form.
A notable example, for which a particular case will be studied later in detail, is a class of convection-diffusion-reaction systems with boundary control and observation which is notably useful for modeling chemical and biochemical reactors, see e.g. (Dramé, Dochain and Winkin 2008), (Winkin, Dochain and Ligarius 2000), (Delattre, Dochain and Winkin 2003). The equations governing this system are given by

$$\left\{\begin{array}{rcl} \frac{\partial x}{\partial t}(z,t) & = & D\frac{\partial^2 x}{\partial z^2}(z,t) - v\frac{\partial x}{\partial z}(z,t) + f(x(z,t)) \\ & & +\chi_{[s_u-\varepsilon_l, s_u+\varepsilon_r]}(z)u_d(t) \\ -D\frac{\partial x}{\partial z}(0,t) & = & v(u_b(t) - x(0,t)) \\ \frac{\partial x}{\partial z}(L,t) & = & 0 \\ x(z,0) & = & x_0(z) \\ y(t) & = & x(L,t) \end{array}\right. \tag{1.1.1}$$

where $t \geq 0$ and $z \in [0,L]$ denote the time and the spatial variable, respectively, $L > 0$ is the length of the spatial domain, x is the state, such that for all $t \geq 0$, $x(\cdot,t) \in X$, where X is a Banach or Hilbert space (e.g. $X = L^2(0,L)$, with $L > 0$), $f : D \subset \mathbb{R} \to \mathbb{R}$ is in general a nonlinear function, D and v are constants and $s_u \in [0,1]$, $\varepsilon_l \geq 0$ and $\varepsilon_r \geq 0$ are parameters representing the distributed control window. The state variable x may represent for example temperatures, concentrations of reactants or products involved in one or more biochemical reactions. The function f corresponds to the reaction and is based in general on a physical or chemical law depending on the framework of the application, such as e.g. the law of mass action, the Arrhenius law or Haldane

kinetics. A distributed control input u_d is introduced in the second order partial differential equation describing the dynamics, and more precisely in the spatial window $[s_u - \varepsilon_l, s_u + \varepsilon_r]$ located inside the physical setup and of arbitrary width $\varepsilon_l + \varepsilon_r$. This input may represent for example the action of a cooling system allowing a cooling fluid to be in contact with the tube (or a part of the tube) of a chemical reactor via an adapted interface. Moreover, a boundary control input u_b is involved in the first boundary condition. This kind of input may be used to represent for example the introduction of a specific concentration of reactant at the inlet of the tube.
An example of biochemical system with a nonlinear reaction rate based on modified Haldane kinetics is studied in (Dramé et al. 2008) and is presented in Chapter 4.

Another application of interest for this work is the evolution of air density, speed and pressure in a Poiseuille flow (see e.g. (Castillo, Witrant and Dugard 2013), (Castillo, Witrant, Prieur and Dugard 2012) and references therein), for which a test bench is available in the GIPSA-lab in Grenoble, France. The physical setup is composed of a horizontal tube attached to a heating column with one fan at each end of the tube. The fans are used to regulate the air flow speed and propagate heat or humidity along the tube. Several sensors are available in order to take temperature, hygrometry or speed measurements.
The full mathematical model considered for this application is given by

$$\left\{\begin{array}{rcl} \frac{\partial \rho}{\partial t}(x,t) & = & -u(x,t)\frac{\partial \rho}{\partial x}(x,t) - \rho(x,t)\frac{\partial u}{\partial x}(x,t) \\ \frac{\partial u}{\partial t}(x,t) & = & -u(x,t)\frac{\partial u}{\partial x}(x,t) - \frac{1}{\rho(x,t)}\frac{\partial p}{\partial x}(x,t) - G \\ \frac{\partial p}{\partial t}(x,t) & = & -a^2\rho(x,t)\frac{\partial u}{\partial x}(x,t) - u(x,t)\frac{\partial p}{\partial x}(x,t) \\ & & -(\gamma-1)\rho(x,t)(q+u(x,t)G) \end{array}\right. \tag{1.1.2}$$

where $t \geq 0$ is the time variable, $x \in [0,1]$ is the space variable, ρ is the gas density, u is the flow speed, p is the pressure in the tube, a is the speed of sound in the gas, G represents the friction losses, q represents the heat exchanges and γ is the ratio between the specific heat constants of the gas at constant pressure and at constant volume.
The boundary conditions have the following structure:

$$\left\{\begin{array}{rcl} \rho(0,t) & = & \rho_{\text{in}}(t) \\ Au(0,t) & = & K_f C_0(t)[p(0,t) - p_{\text{in}}] \\ Au(L,t) & = & K_f C_1(t)[p_{\text{out}} - p(L,t)] \end{array}\right.$$

where K_f is a coefficient, ρ_{in} is the density at the inlet of the tube, C_0 and C_1 are the rotation speeds of the fans and p_{in} and p_{out} are the pressures at the inlet and the outlet of the tube respectively. More details about the mathematical model can be found in e.g. (Castillo et al. 2013).
A simplified version of this model will be studied in Part III.

The main objective of this work is to pose and solve specific control problems for a class of dynamical system with boundary and distributed control and boundary observation that can be used to model a wide range of physical or industrial processes,

including (1.1.1) and (1.1.2).
The aim of this chapter is to present a way of modeling such systems that avoids the aforementioned difficulties without requiring too restrictive additional assumptions, which allows to treat practical applications.

This chapter gives the background, theoretical requirements, modeling and first results about *boundary control systems with boundary observation (BCBO) systems*. It also provides a comparison between the extended and nominal systems when a real parameter in the model goes to infinity.

1.2 Construction of the model

1.2.1 BCBO systems: definition

The starting point of this work is to consider a class of mathematical models that feature interesting properties that will be used in the sequel. The abstract boundary control model with boundary observation which we are interested in is described by

$$\begin{cases} \dot{x}(t) = \mathscr{A}x(t) + B_d u_d(t), \quad x(0) = x_0 & (1.2.1) \\ \mathscr{B}x(t) = u_b(t) & (1.2.2) \\ y(t) = \mathscr{C}x(t) & (1.2.3) \end{cases}$$

where, for all $t \geq 0$, $x(t) \in X$, $u_d(t) \in U_d$, $u_b(t) \in U_b$ and $y(t) \in Y$ and where X, U_d, U_b and Y are Hilbert spaces.
The dynamics of the system are described by (1.2.1), where $\mathscr{A}$ is generally called the *dynamics generator* and B_d is the *distributed control operator* which represents the action of a control input on a spatial domain of the physical system. Even though the distributed control operator B_d is important and may bring interesting properties, it is not required to perform the following analysis. Hence, throughout this section, it can be considered as 0 when one wants to deal with pure boundary control without affecting the main results which remain valid in this particular case.
The boundary conditions are described by (1.2.2), where $\mathscr{B}$ is the *boundary control operator* and represents the action of a control input on a physical boundary of the system.
Finally, the operator $\mathscr{C}$ in the observation equation (1.2.3) describes the measurements of the available sensors, the quantity that we want to penalize in a cost criterion, or both at the same time.
Keeping practical applications in mind, we assume throughout this manuscript that the dynamics operator $\mathscr{A} : D(\mathscr{A}) \subset X \to X$ is in general an unbounded linear operator and $B_d \in \mathscr{L}(U_d, X)$ is a bounded linear operator. The main difficulty comes from the fact that $\mathscr{B}$ and $\mathscr{C}$ are assumed to be unbounded linear operators on X taking values in U_b and Y respectively, and whose domains contain the one of the operator $\mathscr{A}$, i.e. $D(\mathscr{A}) \subset D(\mathscr{B})$ and $D(\mathscr{A}) \subset D(\mathscr{C})$.

We start by recalling the very important definition of C_0-semigroup, see e.g. (Jacob and Zwart 2012, Definition 5.1.2. p. 53).

Definition 1 *Let X be a Hilbert space. $(T(t))_{t\geq 0}$ is called a strongly continuous semigroup (or C_0-semigroup) if the following conditions hold:*

1. *For all $t \geq 0$, $T(t) \in \mathscr{L}(X)$, i.e. $T(t)$ is a bounded linear operator on X ;*
2. *$T(0) = I$;*
3. *$T(t+s) = T(t)T(s)$ for all $t,s \geq 0$;*
4. *For all $x \in X$, we have that $\lim_{t\to 0^+} \|T(t)x - x\|_X = 0$, i.e. the mapping $t \mapsto T(t)$ is strongly continuous at zero.*

In what follows, the kernel (or null space) of any operator S is denoted by Ker S.
In order to develop our theory, we need to introduce some additional assumptions which are not too restrictive for practical applications. This is what motivates the following important definition on which this work is based.

Definition 2 *An abstract boundary control model (1.2.1)-(1.2.3) is said to be a boundary control system with boundary observation (BCBO) if the following conditions hold:*

[C1] *the operator $A : D(A) \to X$ defined by $Ax = \mathscr{A}x$ for all x in its domain $D(A) = D(\mathscr{A}) \cap$ Ker $\mathscr{B}$ is the infinitesimal generator of a C_0-semigroup $(T(t))_{t\geq 0}$ of bounded linear operators on X,*

[C2] *the operator $\mathscr{B}$ is onto, such that there exists a bounded linear operator $B_b \in \mathscr{L}(U_b, X)$ such that for all $u \in U_b$, $B_b u \in D(\mathscr{A})$, the operator $\mathscr{A}B_b \in \mathscr{L}(U_b, X)$ and for all $u \in U_b$, $\mathscr{B}B_b u = u$,*

[C3] *there exist constants $a, b \geq 0$ such that, for all $x \in D(A)$,*

$$\|\mathscr{C}x\| \leq a\|Ax\| + b\|x\|. \tag{1.2.4}$$

Condition **[C3]** is equivalent to the fact that $\mathscr{C} \in \mathscr{L}(X_1, Y)$, where $X_1 = D(A)$ equipped with the norm $\|x\|_1 = \|(\beta I - A)x\|$ for some β in the resolvent set $\rho(A)$ of the operator A.

These crucial assumptions are not too restrictive in general. In fact, both the parabolic and hyperbolic systems studied in Part III satisfy conditions **[C1]**-**[C3]**, which will be checked systematically in Chapters 4 and 5.

1.2.2 Approximation of the output operator

The first step consists of building a bounded approximation of the observation operator $\mathscr{C}$. This new operator is based on a real parameter that dictates the precision of the approximation and can be adjusted depending on the available computational resources and robustness of the numerical algorithms.
Formally, for any parameter α in $\rho(A)$, let us define the operator C_α by

$$C_\alpha : X \to Y \; : \; x \mapsto C_\alpha x := \alpha \mathscr{C}(\alpha I - A)^{-1} x. \tag{1.2.5}$$

Observe that, by condition **[C3]**, $C_\alpha \in \mathscr{L}(X,Y)$, i.e. C_α is a bounded observation operator from X to Y. This operator (more specifically, its limit as the parameter α tends to infinity, whenever it exists) is useful in the analysis of the well-posedness of infinite-dimensional systems with an unbounded observation operator, see e.g. (Weiss 1994), (Tucsnak and Weiss 2009) and references therein. It is related to a concept known in the literature as the *Yosida approximation*, which plays an important role in the proof of the Hille-Yosida theorem, see e.g. (Curtain and Zwart 1995, Theorem 2.1.12, p. 26), (Jacob and Zwart 2012, Theorem 6.1.3, p.66). The idea behind this operator is that, for a class of abstract differential systems which covers most real-life applications, the approximate output equation

$$y_\alpha(t) = C_\alpha x(t)$$

will produce an approximate output that tends towards $y(t)$ for almost every nonnegative time t when α goes to infinity along the real axis. This allows for the development of numerical algorithms where $\mathscr{C}$ is replaced by C_α with α large enough in order to obtain a satisfying approximation.
This relationship between both outputs will be studied more in depth in Chapter 2, Section 2.2.
In the sequel, the operator C_α will be interpreted as a *Yosida type approximate boundary observation operator*.

1.2.3 Construction of the extended system

The next step consists of performing a change of variables by including the boundary input and the approximate output in an extended state, whose central component is an affine transformation of the nominal state $x(t)$. This transformation yields an extended model which is related to the BCBO system (1.2.1)-(1.2.3) and can be used as an intermediate tool in the resolution of specific control problems by avoiding the technical difficulties inherent to the unboundedness of the operators $\mathscr{B}$ and $\mathscr{C}$.
In order to build this new system, we consider, under the conditions presented in the previous sections, the following abstract differential equations:

$$\begin{cases} \dot{v_1}(t) = Av_1(t) - B_b\dot{u}_b(t) + \mathscr{A}B_b u_b(t) + B_d u_d(t) & (1.2.6) \\ v_1(0) = v_{1_0}, & (1.2.7) \\ \dot{v_2}(t) = C_\alpha A v_1(t) + C_\alpha \mathscr{A} B_b u_b(t) + C_\alpha B_d u_d(t) & (1.2.8) \\ v_2(0) = v_{2_0}. & (1.2.9) \end{cases}$$

The question of the well-posedness of these equations will be studied and answered positively in Section 1.3.

Then one can define the following extended system, which is one of the pillars of this work:

$$\begin{cases} \dot{x}_1^e(t) = u_e^1(t) & (1.2.10)\\ \dot{x}_2^e(t) = \mathscr{A}B_b x_1^e(t) + Ax_2^e(t) - B_b u_1^e(t) + B_d u_2^e(t) & (1.2.11)\\ \dot{x}_3^e(t) = C_\alpha \mathscr{A}B_b x_1^e(t) + C_\alpha A x_2^e(t) + C_\alpha B_d u_2^e(t) & (1.2.12)\\ \\ y_1^e(t) = \rho_1 x_1^e(t) \\ y_2^e(t) = \rho_2 B_b x_1^e(t) + \rho_2 x_2^e(t) \\ y_3^e(t) = \rho_3 x_3^e(t) \end{cases}$$

with the initial condition

$$x^e(0) = \begin{pmatrix} x_{0_1}^e \\ x_{0_2}^e \\ x_{0_3}^e \end{pmatrix},$$

which can be rewritten under the more compact form

$$\begin{cases} \dot{x}^e(t) = A^e x^e(t) + B^e u^e(t)\,, \quad x^e(0) = \left(x_{0_1}^e\,, x_{0_2}^e\,, x_{0_3}^e\right)^T & (1.2.13)\\ y^e(t) = C^e x^e(t) & (1.2.14) \end{cases}$$

on the extended state space $\widetilde{X}^e := U_b \oplus X \oplus Y$, where the (extended) state is defined, under suitable initial conditions and inputs, by

$$\begin{aligned} x^e(t) &= (u_b(t)\ \ v_1(t)\ \ v_2(t))^T & (1.2.15)\\ &= (u_b(t)\ \ x(t) - B_b u_b(t)\ \ y_\alpha(t))^T\,, & (1.2.16) \end{aligned}$$

the (extended) input is defined by

$$\boxed{u^e(t) = (\dot{u}_b(t)\ \ u_d(t))^T \ \in\ U^e := U_b \oplus U_d} \qquad (1.2.17)$$

and where

$$A^e = \begin{pmatrix} 0 & 0 & 0 \\ \mathscr{A}B_b & A & 0 \\ C_\alpha \mathscr{A}B_b & C_\alpha A & 0 \end{pmatrix}, \tag{1.2.18}$$

$$B^e = \begin{pmatrix} I & 0 \\ -B_b & B_d \\ 0 & C_\alpha B_d \end{pmatrix}, \quad C^e = \begin{pmatrix} \rho_1 I & 0 & 0 \\ \rho_2 B_b & \rho_2 I & 0 \\ 0 & 0 & \rho_3 I \end{pmatrix}. \tag{1.2.19}$$

The domain of the operator A^e is given by $D(A^e) := U_b \oplus D(A) \oplus Y$ and ρ_i, $i = 1,2,3$, are nonnegative weighting factors. The observation operator C^e is considered with a view to solving an LQ-optimal feedback control problem with a quadratic cost involving the (extended) output $y^e(t)$. The structure of C^e has been chosen such that the norm of the corresponding output $y^e(t)$ can be interpreted as the sum of the weighted norms of $u_b(t)$, $x(t)$ and $y_\alpha(t)$ with arbitrarily chosen weighting factors. The penalization of y^e in a given cost criterion can then be seen as an arbitrary penalization of these input, state and output components independently of each other. This problem and its resolution are studied more extensively in Chapter 3.

At this point, it should be noted that equations (1.2.13)-(1.2.19) are equivalent to (1.2.1)-(1.2.3) with $\mathscr{C}$ replaced by C_α, as shown in Theorem 1.3.2 b). However, the crucial relations (1.2.15)-(1.2.16) are not straightforward and only hold with a suitable initial condition and sufficiently regular inputs. The result showing the relationship between the extended and nominal systems is stated and proved in Section 1.3.

Concerning the inclusion of y_α in the extended state, at first glance, one may be worried that it is not recommended to differentiate $y(t)$ (or its approximation) because measurement noise may be amplified by the differentiation of the output in the model. However, it is shown later that, when designing a state feedback control law, the dynamics of the output are only used in the computation of the feedback operator. Without loss of generality, the control law can then be rewritten as acting only on the boundary input and the state of the nominal system (see (3.2.9)). The approximate output y_α is not used directly in the feedback, which is useful to avoid such problems in practical applications.

1.3 Well-posedness

In the previous sections, BCBO systems were introduced and it was shown that they can be extended in such a way that the control and observation operators become bounded. However, it is still unclear at this point whether the dynamics of the extended system are well-posed.

The goal of this section is to provide a positive answer to this question by showing that the dynamics operator A^e is the generator of a C_0-semigroup of bounded linear operators on the extended state space X^e.

The first step consists of showing that the abstract differential equations (1.2.6)-(1.2.7) and (1.2.8)-(1.2.9) are well-posed and have a unique classical solution for sufficiently regular inputs. This result acts as a lemma for the main theorem of this section,

which is the second step. It mainly states that the extended dynamics generate a C_0-semigroup and that, under a sufficiently regular input given by (1.2.17) and suitable initial conditions, the relations (1.2.15)-(1.2.16) hold.
The well-posedness analysis of the extended model of a BCBO system (1.2.13)-(1.2.19) is based on the following preliminary definitions and results.

Definition 3 *For a given linear operator $\Gamma : D(\Gamma) \subset X \to X$ on a Banach space X, a linear operator $\Delta : D(\Delta) \subset X \to X$ is said to be Γ-bounded if $D(\Gamma) \subset D(\Delta)$ and if there exist nonnegative constants γ and δ such that, for all $x \in D(\Gamma)$,*

$$\|\Delta x\| \leq \gamma \|\Gamma x\| + \delta \|x\| . \tag{1.3.1}$$

The Γ-bound of the operator Δ is given by

$$\gamma_0 := \inf\{\gamma \geq 0 : \text{ there exists } \delta \geq 0 \text{ such that } (1.3.1) \text{ holds}\}.$$

This definition can be extended to operators with values in a Banach space Y. In view of condition (**C3**), the operator $\mathscr{C}$ is A-bounded with A-bound less than or equal to a.

Observe that the abstract differential equation (1.2.12) should correspond to the dynamics of the output trajectories of equations (1.2.10)-(1.2.11) through the output operator C_α. In order to take this feature into account in the description of the extended system, let us consider the bounded linear operator $C \in \mathscr{L}(U_b \oplus X, Y)$ defined for all $(x_1^e, x_2^e) \in U_b \oplus X$ by $C\,(x_1^e, x_2^e)^T = (C_\alpha B_b \;\; C_\alpha)\,(x_1^e, x_2^e)^T = C_\alpha(x_2^e + B_b x_1^e)$. Thanks to the fact that the graph $G(C)$ of the operator C is a closed subspace of $\widetilde{X}^e$, from now on, we will use $X^e := G(C) \subset \widetilde{X}^e = U_b \oplus X \oplus Y$ as new extended (Hilbert) state space for the extended system. This restriction is particularly useful when analyzing some subsequent properties such as stability, reachability and stabilizability, since, as it will be studied later, the state-output relationship $y_\alpha = C_\alpha(v + B_b u_b) = C_\alpha x$ always holds in X^e.
The proof of the following result, and more particularly the well-posedness of (1.2.6)-(1.2.9), is based on (Engel and Nagel 2006, Corollary 1.5, p. 119) and follows the lines of (Dehaye and Winkin 2013*a*, Lemma 4, Lemma 5 and Theorem 6) with a less restrictive operator C_α.

Lemma 1.3.1 *Let the operators $\mathscr{A}$, $\mathscr{B}$ and $\mathscr{C}$ define a BCBO system (1.2.1)-(1.2.3) such that conditions (**C1**)-(**C3**) hold.*
Consider the operator C_α given by (1.2.5).
Then, for any distributed input $u_d \in C^1([0,\tau], U_d)$ and for any boundary input $u_b \in C^2([0,\tau], U_b)$, where $\tau > 0$ is any fixed final time, the abstract differential equations (1.2.6)-(1.2.7) and (1.2.8)-(1.2.9) are well-posed, i.e. for all initial conditions $v_{1_0} \in D(A)$ and $v_{2_0} \in Y$, the Cauchy problems (1.2.6)-(1.2.7) and (1.2.8)-(1.2.9) have unique classical solutions $v_1 \in C^1([0,\tau], X)$ and $v_2 \in C^1([0,\tau], Y)$, respectively, with $v_1(t) \in D(A)$ and $v_2(t) \in Y$ for all $t \in [0,\tau]$.

Proof. By (Curtain and Zwart 1995, Theorem 3.1.3, p.103) and by (Engel and Nagel 2006, Corollary 1.5, p.119) applied to the operators

$$\Gamma = \begin{pmatrix} A & 0 \\ 0 & 0 \end{pmatrix} \text{ and } \Delta = \begin{pmatrix} 0 & 0 \\ C_\alpha A & 0 \end{pmatrix},$$

with $D(\Gamma) = D(\Delta) = D(A) \oplus Y$, the result follows directly from condition (**C1**) and from the fact that, thanks to conditions (**C2**) and (**C3**), the operator $C_\alpha A$ is A-bounded and the operators B_b, $\mathscr{A}B_b$, B_d, $C_\alpha \mathscr{A} B_b$ and $C_\alpha B_d$ are bounded. ■

Theorem 1.3.2 *[Well-posedness of the extended system]*
a) The restriction of the operator A^e, given by (1.2.18), (1.2.5), to the subspace $X^e = G(C)$, whose domain is given by $D(A^e) \cap G(C)$, is the infinitesimal generator of a C_0-semigroup $(T^e(t))_{t\geq 0}$ of bounded linear operators on X^e.

b) For any distributed input $u_d \in C^1([0,\tau], U_d)$ and for any boundary input $u_b \in C^2([0,\tau], U_b)$, where $\tau > 0$ is any fixed final time, the dynamics (1.2.13) of the extended system (1.2.13)-(1.2.19) are well-posed, i.e. the abstract differential equation

$$\dot{x^e}(t) = A^e x^e(t) + B^e u^e(t)$$

with initial condition

$$x^e(0) = x_0^e = \begin{pmatrix} x_{0_1}^e \\ x_{0_2}^e \\ x_{0_3}^e \end{pmatrix} = \begin{pmatrix} u_b(0) \\ v_{1_0} \\ v_{2_0} \end{pmatrix} \in D(A^e) \cap G(C)$$

and input given by (1.2.17), has the unique classical solution

$$x^e(t) = \begin{pmatrix} u_b(t) \\ v_1(t) \\ v_2(t) \end{pmatrix}$$

where $v_1(t)$ and $v_2(t)$ are the unique classical solutions of the abstract differential equations (1.2.6)-(1.2.7) and (1.2.8)-(1.2.9), respectively.

Moreover, if $x_0 = v_{1_0} + B_b u_b(0)$, hence $v_{2_0} = C_\alpha x_0$, then the state trajectory $x(t)$ of the BCBO system (1.2.1)-(1.2.3) is related to the one of the extended system (1.2.13)-(1.2.19), for all $t \geq 0$, by

$$x(t) = v_1(t) + B_b u_b(t) \quad \text{and} \quad v_2(t) = C_\alpha x(t). \tag{1.3.2}$$

Proof. a) First observe that the operator A^e, with domain $D(A^e) = U_b \oplus D(A) \oplus Y$, is the infinitesimal generator of a C_0-semigroup (of bounded linear operators) on $\widetilde{X}^e$. Indeed, let us define the operator

$$A_0^e = \begin{pmatrix} 0 & 0 & 0 \\ 0 & A & 0 \\ 0 & 0 & 0 \end{pmatrix}$$

on its domain $D(A_0^e) = D(A^e)$, and the perturbation operators

$$P_1^e = \begin{pmatrix} 0 & 0 & 0 \\ 0 & 0 & 0 \\ 0 & C_\alpha A & 0 \end{pmatrix}, \quad P_2^e = \begin{pmatrix} 0 & 0 & 0 \\ \mathscr{A}B_b & 0 & 0 \\ C_\alpha \mathscr{A}B_b & 0 & 0 \end{pmatrix}.$$

Since A is the infinitesimal generator of a C_0-semigroup $(T(t))_{t\geq 0}$ on X, the operator A_0^e is the infinitesimal generator of the C_0-semigroup $(T_0^e(t))_{t\geq 0}$ on $\widetilde{X}^e$, given for all $t \geq 0$ by

$$T_0^e(t) = \begin{pmatrix} I & 0 & 0 \\ 0 & T(t) & 0 \\ 0 & 0 & I \end{pmatrix}.$$

Observe that Ran $P_1^e \subset D(A_0^e)$, where Ran P_1^e is the range of the operator P_1^e.
Moreover, let $\beta \in \rho(A_0^e)$. For any $x^e \in D(A_0^e) = D(A^e)$,

$$\begin{aligned} \|(\beta I - A_0^e)P_1^e x^e\| &\leq |\beta| \|P_1^e x^e\| + \|A_0^e P_1^e x^e\| \\ &= |\beta| \|P_1^e x^e\|, \end{aligned}$$

which implies that $(\beta I - A_0^e)P_1^e \in \mathscr{L}(X_1^e, \widetilde{X}^e)$ since P_1^e is A_0^e-bounded. Hence $P_1^e \in \mathscr{L}(X_1^e)$, where $X_1^e = D(A_0^e) = D(A^e)$. By (Engel and Nagel 2006, Corollary 1.5, p.119), the operator $A_0^e + P_1^e$ (with domain $D(A^e)$) is the infinitesimal generator of a C_0-semigroup.
Since $P_2^e \in \mathscr{L}(\widetilde{X}^e)$, the operator $A^e = A_0^e + P_1^e + P_2^e$ is the infinitesimal generator of a C_0-semigroup $(\widetilde{T}^e(t))_{t\geq 0}$ on $\widetilde{X}^e$.
The conclusion follows by (Engel and Nagel 2006, Corollary p. 48), since X^e is a $\widetilde{T}^e(t)$-invariant closed subspace of $\widetilde{X}^e$. In fact, $\widetilde{T}^e(t)$ is given by

$$\widetilde{T}^e(t) = \begin{pmatrix} I & 0 & 0 \\ S_1(t) & T(t) & 0 \\ S_2(t) & S_3(t) & I \end{pmatrix}$$

where

$$\begin{aligned} S_1(t)u_b &= \int_0^t T(s)\mathscr{A}B_b u_b ds, \\ S_2(t)u_b &= \int_0^t [S_3(s) + C_\alpha]\mathscr{A}B_b u_b ds, \\ S_3(t)v &= \int_0^t C_\alpha A T(s) v ds \end{aligned}$$

and for all $x^e \in G(C)$,

$$\widetilde{T}^e(t)x^e = \begin{pmatrix} x_1^e \\ S_1(t)x_1^e + T(t)x_2^e \\ S_2(t)x_1^e + S_3(t)x_2^e + x_3^e \end{pmatrix}$$

is such that $x_1^e \in U_b$, $S_1(t)x_1^e + T(t)x_2^e \in X$ and

$$S_2(t)x_1^e + S_3(t)x_2^e + x_3^e = C_\alpha B_b x_1^e + C_\alpha [S_1(t)x_1^e + T(t)x_2^e].$$

b) First, we assume that $v_1(t)$ is a classical solution of (1.2.6)-(1.2.7) and we show that $x(t)$ defined by (1.3.2) is a classical solution of (1.2.1)-(1.2.3).
Since $v_1(t)$ is a classical solution of (1.2.6)-(1.2.7), $v_1(t) \in D(A) \subset D(\mathscr{A}) \subset D(\mathscr{B})$ for all $t \geq 0$.
Moreover, for all $t \geq 0$, $B_b u_b(t) \in D(\mathscr{A}) \subset D(\mathscr{B})$ by assumption. Hence,

$$\begin{aligned} \mathscr{B}x(t) &= \mathscr{B}[v_1(t) + B_b u_b(t)] \\ &= \mathscr{B}v_1(t) + \mathscr{B}B_b u_b(t) \\ &= u_b(t) \end{aligned}$$

by condition **[C2]** and since $v(t) \in \text{Ker}\, \mathscr{B}$.
Furthermore, we see that

$$\begin{aligned} \dot{x}(t) &= \dot{v}_1(t) + B_b \dot{u}_b(t) \\ &= Av_1(t) - B_b \dot{u}_b(t) + \mathscr{A}B_b u_b(t) + B_d u_d(t) + B_b \dot{u}_b(t) \\ &= Av_1(t) + \mathscr{A}B_b u_b(t) + B_d u_d(t) \\ &= \mathscr{A}v_1(t) + \mathscr{A}B_b u_b(t) + B_d u_d(t) \\ &= \mathscr{A}[v_1(t) + B_b u_b(t)] + B_d u_d(t) \\ &= \mathscr{A}x(t) + B_d u_d(t) \end{aligned}$$

where the first equality comes from the fact that $B_b \in \mathscr{L}(U_b, X)$.
Thus, $x(t)$ defined by (1.3.2) is a classical solution of (1.2.1)-(1.2.3).
The other implication is proved similarly.
Now, let us consider the first two equations of (1.2.13)-(1.2.19), which define the operators

$$\tilde{A}^e = \begin{pmatrix} 0 & 0 \\ \mathscr{A}B_b & A \end{pmatrix} \quad \text{and} \quad \tilde{B}^e = \begin{pmatrix} I & 0 \\ -B_b & B_d \end{pmatrix}$$

with $\tilde{A}^e$ generating a C_0-semigroup on $U_b \oplus X$. By (Curtain and Zwart 1995, Lemma 3.2.2), the mild solution of the differential system formed by the first two equations of (1.2.13)-(1.2.19) (i.e. by $\tilde{A}^e$ and $\tilde{B}^e$) is given by

$$\begin{aligned} \tilde{x}^e(t) &= \begin{pmatrix} I & 0 \\ S(t) & T(t) \end{pmatrix} \begin{pmatrix} x^e_{0_1} \\ x^e_{0_2} \end{pmatrix} \\ &\quad + \int_0^t \begin{pmatrix} I & 0 \\ S(t-s) & T(t-s) \end{pmatrix} \begin{pmatrix} I & 0 \\ -B_b & B_d \end{pmatrix} \begin{pmatrix} \dot{u}_b(s) \\ u_d(s) \end{pmatrix} ds \end{aligned}$$

where

$$S(t)x = \int_0^t T(t-s)\mathscr{A}B_b x ds = \int_0^t T(s)\mathscr{A}B_b x ds.$$

This implies that

$$x^e_1(t) = x^e_{0_1} + \int_0^t \dot{u}_b(s) ds = u_b(0) + \int_0^t \dot{u}_b(s) ds = u_b(t).$$

Since $u_b \in C^2([0,\tau],U_b)$, we have that $\dot{u}_b \in C^1([0,\tau],U_b)$, and since $\tilde{x}^e(0) \in D(\tilde{A}^e)$, by (Curtain and Zwart 1995, Theorem 3.1.3), the differential system formed by $\tilde{A}^e$ and $\tilde{B}^e$ has a unique classical solution that satisfies

$$\dot{x}_1^e(t) = \dot{u}_b(t)$$

and

$$\begin{aligned} \dot{x}_2^e(t) &= \mathscr{A}B_b x_1^e(t) + Ax_2^e(t) - B_b\dot{u}_b(t) + B_d u_d(t) \\ &= \mathscr{A}B_b u_b(t) + Ax_2^e(t) - B_b\dot{u}_b(t) + B_d u_d(t), \end{aligned}$$

which is (1.2.6). Since $x_{0_2}^e = v_{1_0}$, we have that for all $t \geq 0$, $x_2^e(t) = v_1(t)$, where $v_1(t)$ is the unique classical solution of (1.2.6)-(1.2.7).
Finally, it suffices to observe that the third component $x_3^e(t)$ of the extended state is the solution of the abstract differential equation (1.2.8)-(1.2.9) with initial condition $v_{2_0} = x_{0_3}^e = C_\alpha x_0$, hence $x_3^e(t) = v_2(t) = C_\alpha x(t)$ for all $t \geq 0$ since $C_\alpha \in \mathscr{L}(X,Y)$. ■

The proof of the main part of b) follows the lines of (Curtain and Zwart 1995, Section 3.3, pp. 121–128), where there is no distributed control in the dynamics of (1.2.1)-(1.2.3) and the approximate output is not included in the extended state.
We conclude this chapter by reminding that the well-posedness of some specific classes of boundary control systems, in particular port-hamiltonian systems, has been studied in detail in several existing works, see e.g. (Jacob and Zwart 2012),(Le Gorrec, Maschke, Villegas and Zwart 2006),(Villegas 2007).

1.4 Analytic case

The previous result does not state that the extension preserves interesting properties of the C_0-semigroup generated by A. However, in the case where the C_0-semigroup $(T(t))_{t\geq 0}$ is *analytic* in condition **[C1]**, the previous results can be slightly adjusted such that A^e is the generator of an *analytic C_0-semigroup*. This property is of particular interest due to the fact that the state trajectories associated with an analytic C_0-semigroup are smooth, or more precisely, for all $t > 0$ and $x \in X$, the map $t \mapsto T(t)x$ is infinitely many times differentiable. As shown later in Theorem 3.2.2, this characteristic guarantees that the closed-loop extended system maintains its relationship with the nominal system under an appropriate state feedback. This fact will be exploited in Chapter 4 since the differential operator associated with convection-diffusion-reaction dynamics is known to be the generator of an analytic C_0-semigroup on $L^2(a,b)$.
We start by recalling the definition of an analytic C_0-semigroup (see e.g. (Engel and Nagel 2000, Definition 4.5, p. 101)). In what follows, for any $\delta > 0$, Σ_δ denotes the sector $\{z \in \mathbb{C} : |\arg z| < \delta\} \setminus \{0\}$ of the complex plane.

Definition 4 *A family of operators* $(T(z))_{z\in\Sigma_\delta\cup\{0\}}\subset\mathscr{L}(X)$ *is called an* analytic semigroup *(of angle* $\delta\in(0,\pi/2]$*) if*

(*i*) $T(0)=I \quad$ *and* $\quad T(z_1+z_2)=T(z_1)T(z_2) \quad$ *for all* $z_1,z_2\in\Sigma_\delta$*;*

(*ii*) *The map* $z\mapsto T(z)$ *is analytic in* Σ_δ*;*

(*iii*) $\lim\limits_{\substack{z\to 0\\ z\in\Sigma_{\delta'}}} T(z)x=x \quad$ *for all* $x\in X$ *and* $0<\delta'<\delta$.

If, in addition,

(*iv*) $\|T(z)\|$ *is bounded in* $\Sigma_{\delta'}$ *for every* $0<\delta'<\delta$,

we call $(T(z))_{z\in\Sigma_\delta\cup\{0\}}$ *a* bounded analytic semigroup.

In order to achieve our goal, we need to use a suitable scaling of the operators C_α. More precisely, we consider a weighted approximate output operator defined for every $x\in X$ by

$$\widetilde{C}_\alpha x := \rho_\alpha C_\alpha x \tag{1.4.1}$$

where $\rho_\alpha>0$ is a real parameter which has to be chosen sufficiently small.
The abstract differential equation (1.2.8)-(1.2.9) is replaced by

$$\begin{aligned} \dot{v_2}(t) &= \widetilde{C}_\alpha A v_1(t)+\widetilde{C}_\alpha\mathscr{A}B_b u_b(t)+\widetilde{C}_\alpha B_d u_d(t)\\ v_2(0) &= v_{2_0}\end{aligned}$$

and (1.2.18) naturally becomes

$$A^e=\begin{pmatrix} 0 & 0 & 0\\ \mathscr{A}B_b & A & 0\\ \widetilde{C}_\alpha\mathscr{A}B_b & \widetilde{C}_\alpha A & 0\end{pmatrix}. \tag{1.4.2}$$

In order to preserve the relationship between the extended output and the approximate output, we must also consider the corresponding scaled extended output operator defined by

$$C^e=\begin{pmatrix} \rho_1 I & 0 & 0\\ \rho_2 B_b & \rho_2 I & 0\\ 0 & 0 & \rho_3\rho_\alpha^{-1}I\end{pmatrix}$$

in (1.2.19).
The main result for the analytic case is based on the following lemmas.

Lemma 1.4.1 *(Engel and Nagel 2006, Lemma 2.6, p. 127) Let $(A,D(A))$ be an operator whose resolvent exists for all $\lambda \in \overline{\Sigma}_\delta := \{z \in \mathbb{C} : |\arg z| \leq \delta\}$ such that $\lambda \neq 0$ and satisfies*

$$\|R(\lambda,A)\| \leq \frac{M}{|\lambda|}$$

for some constants $\delta \geq 0$ and $M \geq 1$. Moreover, assume $(B,D(B))$ to be A-bounded with A-bound

$$a_0 < \frac{1}{M+1}.$$

Then there exists constants $r \geq 0$ and $\tilde{M} \geq 1$ such that

$$\overline{\Sigma}_\delta \cap \{z \in \mathbb{C} : |z| > r\} \subset \rho(A+B)$$

and

$$\|R(\lambda,A+B)\| \leq \frac{\tilde{M}}{|\lambda|}$$

for all $\lambda \in \overline{\Sigma}_\delta \cap \{z \in \mathbb{C} : |z| > r\}$.

Lemma 1.4.2 *(Engel and Nagel 2006, Theorem 2.10, p. 130) Let the linear operator $\Gamma : D(\Gamma) \subset X \to X$ be the infinitesimal generator of an analytic C_0-semigroup $(T(z))_{z\in\Sigma_\delta\cup\{0\}}$ on a Banach space X.*
Then
a) there exists a constant $c > 0$ such that $\Gamma + \Delta : D(\Gamma) \to X$ is the infinitesimal generator of an analytic C_0-semigroup for every Γ-bounded operator Δ having Γ-bound $\gamma_0 < c$;
b) for every Γ-bounded operator Δ, the operator $\Gamma + \rho\Delta$ is the infinitesimal generator of an analytic C_0-semigroup provided that the parameter $\rho \in \mathbb{R}$ be such that $|\rho|$ is sufficiently small.

Sketch of the proof. a) If $(T(z))_{z\in\Sigma_\delta\cup\{0\}}$ is bounded, it follows from (Engel and Nagel 2000, Theorem 4.6, p. 101) that Γ is sectorial. From this, it is possible to show that, with a suitable c, the assumptions of Lemma 1.4.1 are satisfied with $\delta := \pi/2 + \delta'$, where $\delta' \in (0,\pi/2]$. By combining the conclusion of this lemma with (Engel and Nagel 2000, Exercise 4.12(6), p. 108), one obtains that $\Gamma + \Delta$ generates an analytic semigroup.
If $(T(z))_{z\in\Sigma_\delta\cup\{0\}}$ is not bounded, it is easy to show that any Γ-bounded operator Δ is also $\Gamma - wI$-bounded with the same Γ-bound γ_0 for any $w \in \mathbb{R}$. It remains to observe that $\Gamma - wI$ is the generator of an analytic semigroup by (Engel and Nagel 2006, Proposition 1.12, p. 122), which is bounded in Σ_δ for w sufficiently large. By applying the first step of the proof to $\Gamma - wI$, one deduces that $\Gamma + \Delta - wI$ and hence $\Gamma + \Delta$ generates an analytic C_0-semigroup.

b) The assertion directly follows from a). ■

Lemma 1.4.2 is the key result in the proof of the following theorem, which corresponds to Theorem 1.3.2 a).

Theorem 1.4.3 *The restriction of the operator A^e, given by (1.4.2), (1.4.1), where $\rho_\alpha \in \mathbb{R}$ is such that $|\rho_\alpha|$ is sufficiently small, to the subspace $X^e = G(C)$, whose domain is given by $D(A^e) \cap G(C)$, is the infinitesimal generator of an analytic C_0-semigroup $(T^e(t))_{t\geq 0}$ of bounded linear operators on X^e.*

Proof. First, observe that the operator A^e, with domain $D(A^e) = U_b \oplus D(A) \oplus Y$, is the infinitesimal generator of a C_0-semigroup (of bounded linear operators) on $\widetilde{X}^e$. Indeed, let us define the operator

$$A_0^e = \begin{pmatrix} 0 & 0 & 0 \\ 0 & A & 0 \\ 0 & 0 & 0 \end{pmatrix}$$

on its domain $D(A_0^e) = D(A^e)$, and the perturbation operators

$$P_1^e = \begin{pmatrix} 0 & 0 & 0 \\ 0 & 0 & 0 \\ 0 & C_\alpha A & 0 \end{pmatrix}, \quad \widetilde{P}_2^e = \begin{pmatrix} 0 & 0 & 0 \\ \mathscr{A}B_b & 0 & 0 \\ \widetilde{C}_\alpha \mathscr{A}B_b & 0 & 0 \end{pmatrix}.$$

Since A is the infinitesimal generator of an analytic C_0-semigroup $(T(t))_{t\geq 0}$ on X, the operator A_0^e is the infinitesimal generator of the analytic C_0-semigroup $(T_0^e(t))_{t\geq 0}$ on $\widetilde{X}^e$, given for all $t \geq 0$ by

$$T_0^e(t) = \begin{pmatrix} I & 0 & 0 \\ 0 & T(t) & 0 \\ 0 & 0 & I \end{pmatrix}.$$

It follows from the fact that the operator P_1^e is A_0^e-bounded that, by Lemma 1.4.2b), the operator $A_0^e + \rho_\alpha P_1^e$ (with domain $D(A^e)$) is still the infinitesimal generator of an analytic C_0-semigroup for $|\rho_\alpha|$ sufficiently small.
Since $\widetilde{P}_2^e \in \mathscr{L}(\widetilde{X}^e)$, the operator $A^e = A_0^e + \rho_\alpha P_1^e + \widetilde{P}_2^e$ is the infinitesimal generator of an analytic C_0-semigroup $(T^e(t))_{t\geq 0}$ on $\widetilde{X}^e$ by (Engel and Nagel 2006, Proposition 1.12, p. 122).
The conclusion follows by (Engel and Nagel 2006, Corollary, p. 48), since X^e is a $T^e(t)$-invariant closed subspace of $\widetilde{X}^e$. ■

It should be noted that, when the analytic C_0-semigroup $(T(z))_{z\in\Sigma_\delta\cup\{0\}}$ is bounded, it is possible to choose ρ_α more precisely. In fact, with A satisfying

$$\|R(\lambda, A)\| \leq \frac{M}{|\lambda|}$$

for all $\lambda \in \rho(A)$, it suffices to choose ρ_α such that $\rho_\alpha P_1^e$ has a A_0^e-bound lower than $\dfrac{1}{M+1}$.

At this point, it is interesting to emphasize the fact that the well-posedness of the extended system is not studied for itself, but for the benefits it brings, in particular from Chapter 3 on. In fact, as can be seen in Theorem 1.3.2 b), under suitable initial conditions and inputs, the extended system is basically a tool describing the behaviour of the nominal system under one differential equation and one simple output equation. This tool will be used extensively in Chapters 3, 4 and 5, where its properties, including the well-posedness, will be crucial for the resolution of a LQ-optimal control problem that can be interpreted in the framework of the nominal system.

Chapter 2

Analysis

2.1 Properties of the extended system

This section deals with the analysis of system theoretic properties of the extended system, namely exact controllability and observability, (approximate) reachability and observability, and (exponential) stabilizability and detectability.
These properties are highly desirable. Stabilizability makes the LQ-optimal control problem solvable and reachability, in addition of allowing the state trajectories to become arbitrarily close to any given state, makes the solution unique. Detectability is useful in practical applications as well since the state variables are usually measured via relatively limited sensors which do not provide access to the whole state. In this situation, it is generally useful to build a state observer for which the error of estimation exponentially converges to zero. The existence of such an observer is guaranteed by the detectability. Finally, observability allows the knowledge of the output to uniquely determine the initial state, which can be useful in problems where this initial state is unknown and has to be reconstituted.
The main result of this section gives sufficient conditions on the nominal system for these properties to hold for the extended system. Basically, as one could expect, the extended system inherits some properties of the nominal one, while systematically adding others due to the structure of the extended output operator C^e.
We recall some important definitions here, see e.g. (Curtain and Zwart 1995, Definitions 4.1.3 a., p. 143, 4.1.12 a., p. 154, 4.1.17, p. 157) for the definitions of (approximate) reachability and (approximate) observability, and (Curtain and Zwart 1995, Definition 5.2.1, p. 227) for the definitions of (exponential) stabilizability and (exponential) detectability.
In what follows, the closure of a set $E \subset X$ in the corresponding normed space X will be denoted by $\overline{E}$.

Definition 5 *For a control system associated with an abstract Cauchy problem*

$$\begin{cases} \dot{x}(t) &= Ax(t)+Bu(t), \quad x(0)=x_0 \\ y(t) &= Cx(t) \end{cases}$$

with state space X, input space U and output space Y, and where A is the infinitesimal generator of a C_0-semigroup $(T(t))_{t\geq 0}$ of bounded linear operators on X, the control operator $B \in \mathscr{L}(U,X)$, and the observation operator $C \in \mathscr{L}(X,Y)$, let $\mathscr{B}_t \in \mathscr{L}(L^p([0,t],U),X)$ be the controllability map *defined for all $t \geq 0$ and for all $u(\cdot) \in L^p([0,t],U)$ by*

$$\mathscr{B}_t[u(\cdot)] := \int_0^t T(t-\tau)Bu(\tau)d\tau$$

and $\mathscr{C}_t : X \to L^p([0,t],Y)$ be the observability map *defined for all $t \geq 0$ and for all $x \in X$ by*

$$\mathscr{C}_t x(\cdot) := CT(\cdot)x.$$

1. *The system is* (exactly) controllable *if*

$$\bigcup_{t>0} Ran\ \mathscr{B}_t = X.$$

2. *The system is* (approximately) reachable *if*

$$\overline{\bigcup_{t>0} Ran\ \mathscr{B}_t} = X.$$

3. *The system is* (approximately) observable *if*

$$\bigcap_{t>0} Ker\ \mathscr{C}_t = \{0\}.$$

4. *The system is* (exponentially) stabilizable *if there exists a feedback operator $K \in \mathscr{L}(X,U)$ such that the C_0-semigroup generated by $A+BK$ is (exponentially) stable, i.e. its growth bound is less than* 0.

5. *The system is* (exponentially) detectable *if there exists an output injection operator $L \in \mathscr{L}(Y,X)$ such that the C_0-semigroup generated by $A+LC$ is (exponentially) stable, i.e. its growth bound is less than* 0.

The analysis is based on the following auxiliary lemma. This result states that the reachability of the pair (A,B_d) is transmitted to the first two equations of the extended system describing the dynamics of the boundary input and the transformed state, where A is the dynamics generator defined by condition **[C1]** in Definition 2 and B_d is the distributed control operator introduced in (1.2.1).

Lemma 2.1.1 *a) If the pair (A,B_d) is (exactly) controllable, then the pair $(\tilde{A}^e,\tilde{B}^e)$ given by*

$$\tilde{A}^e = \begin{pmatrix} 0 & 0 \\ \mathscr{A}B_b & A \end{pmatrix}, \quad \tilde{B}^e = \begin{pmatrix} I & 0 \\ -B_b & B_d \end{pmatrix} \tag{2.1.1}$$

is controllable.

b) If the pair (A,B_d) is (approximately) reachable, then the pair $(\tilde{A}^e,\tilde{B}^e)$ given by (2.1.1) is reachable.

Proof. a) First, observe that the operator $\tilde{A}^e$ is the infinitesimal generator of a C_0-semigroup $(\tilde{T}^e(t))_{t\geq 0}$ of the following form:

$$\tilde{T}^e(t) = \begin{pmatrix} I & 0 \\ \tilde{S}(\cdot) & T(\cdot) \end{pmatrix},$$

where $(T(t))_{t\geq 0}$ is the C_0-semigroup generated by A.
The goal is to show that

$$\bigcup_{t>0} \text{Ran } \tilde{\mathscr{B}}_t^e = U_b \oplus X, \tag{2.1.2}$$

where the extended controllability map is given by

$$\begin{aligned} \tilde{\mathscr{B}}_t^e[\tilde{u}^e(\cdot)] &= \int_0^t \tilde{T}^e(t-\tau)\tilde{B}^e\tilde{u}^e(\tau)d\tau \\ &= \int_O^t \begin{pmatrix} I & 0 \\ \tilde{S}(t-\tau) & T(t-\tau) \end{pmatrix} \begin{pmatrix} I & 0 \\ -B_b & B_d \end{pmatrix} \begin{pmatrix} \tilde{u}_1^e(\tau) \\ \tilde{u}_2^e(\tau) \end{pmatrix} d\tau \\ &= \int_O^t \begin{pmatrix} I & 0 \\ \tilde{S}(t-\tau) - T(t-\tau)B_b & T(t-\tau)B_d \end{pmatrix} \begin{pmatrix} \tilde{u}_1^e(\tau) \\ \tilde{u}_2^e(\tau) \end{pmatrix} d\tau. \end{aligned}$$

Now, the controllability map associated with the pair (A,B_d) is given by

$$\mathscr{B}_t[u(\cdot)] = \int_0^t T(t-\tau)B_d u(\tau)d\tau.$$

Since the pair (A,B_d) is exactly controllable, we have that

$$\bigcup_{t>0} \text{Ran } \mathscr{B}_t = X,$$

from which it is easy to deduce that (2.1.2) holds.

b) Observe that the dual observability map is given for all $\tilde{x}^e = (x_1^e\ x_2^e)^T \in U_b \oplus X$ by

$$\tilde{\mathscr{B}}_t^e\tilde{x}^e = (\tilde{B}^e)^*(\tilde{T}^e(\cdot))^*\tilde{x}^e = \begin{pmatrix} x_1^e + (\tilde{S}(\cdot))^*x_2^e + -B_b^*(T(\cdot))^*x_2^e \\ B_d^*(T(\cdot))^*x_2^e \end{pmatrix}.$$

Hence $\tilde{\mathscr{B}}_t^e\tilde{x}^e = 0$ if and only if $\tilde{x}^e = 0$.
The conclusion follows by a standard duality argument, see e.g. (Curtain and Zwart 1995). ■

The following proposition gives sufficient conditions for the reachability and stabilizability of the extended system. More precisely, these properties are transmitted from the pair (A,B_d) of the nominal system. Moreover, it states that the extended system is observable and detectable.

Proposition 2.1.2 *a) If the pair (A,B_d) is exactly controllable, then the extended system (1.2.13)-(1.2.19), i.e. the pair (A^e,B^e), is exactly controllable.*

b) If the pair (A,B_d) is reachable, then the extended system (1.2.13)-(1.2.19), i.e. the pair (A^e,B^e), is reachable.

c) If $\rho_i \neq 0$, $i=1,2,3$, then the extended system (1.2.13)-(1.2.19), i.e. the pair (C^e,A^e), is observable.

d) If the pair (A,B_d) is stabilizable, then the extended system (1.2.13)-(1.2.19), i.e. the pair (A^e,B^e), is stabilizable.

e) If $\rho_i \neq 0$, $i=1,2,3$, then the extended system (1.2.13)-(1.2.19), i.e. the pair (C^e,A^e), is detectable.

Proof. a) For any fixed time $t>0$ and any state $z=(z_1,z_2,z_3)=(z_1,z_2,C(z_1,z_2))\in X^e$, it should be shown that there exists an input function $u^e(\cdot)$ (defined on the time interval $[0,t]$) such that $x^e(t)=z$, where $x^e(\cdot)$ is the state trajectory of the extended system corresponding to the input $u^e(\cdot)$ with zero initial condition.
Now, by Lemma 2.1.1 a), there exists an input function $u^e(\cdot)$ such that $(x_1^e(t)\ x_2^e(t))^T = (z_1\ z_2)^T$.
Moreover, since $x^e(t)\in X^e = G(C)$, we see that

$$\begin{aligned} x_3^e(t) &= C\begin{pmatrix} x_1^e(t) \\ x_2^e(t)\end{pmatrix} \\ &= C\begin{pmatrix} z_1 \\ z_2\end{pmatrix} \\ &= z_3. \end{aligned}$$

b) For any fixed time $t>0$ and any state $z=(z_1,z_2,z_3)=(z_1,z_2,C(z_1,z_2))\in X^e$, it should be shown that, for an arbitrarily fixed $\varepsilon>0$, there exists an input function $u^e(\cdot)$ (defined on the time interval $[0,t]$) such that

$$\|x^e(t)-z\|<\varepsilon, \tag{2.1.3}$$

where, as in the proof of a), $x^e(\cdot)$ is the state trajectory of the extended system corresponding to the input $u^e(\cdot)$ with zero initial condition.
Since $C\in\mathscr{L}(U_b\oplus X,Y)$, one can define

$$\widetilde{\varepsilon} := \frac{\varepsilon}{\sqrt{1+\|C\|^2}} > 0.$$

By Lemma 2.1.1 b), there exists an input function $u^e(\cdot)$ such that

$$\|(x_1^e(t),x_2^e(t))-(z_1,z_2)\|<\widetilde{\varepsilon}.$$

It follows that

$$\begin{aligned} \|x_3^e(t) - z_3\| &= \|C(x_1^e(t), x_2^e(t)) - C(z_1, z_2)\| \\ &\leq \|C\| \, \widetilde{\varepsilon}, \end{aligned}$$

whence (2.1.3) holds.

c) First observe that the C_0-semigroup $(T^e(t))_{t\geq 0}$ generated by A^e has the following form:

$$T^e(t) = \begin{pmatrix} I & 0 & 0 \\ S_1(\cdot) & T(\cdot) & 0 \\ S_2(\cdot) & S_3(\cdot) & I \end{pmatrix}.$$

It follows that the observability map is given for all $x^e \in X^e$ by

$$\mathscr{C}_t^e x^e = C^e T^e(\cdot) x^e = \begin{pmatrix} \rho_1 x_1^e \\ \rho_2(B_b x_1^e + S_1(\cdot) x_1^e + T(\cdot) x_2^e) \\ \rho_3(S_2(\cdot) x_1^e + S_3(\cdot) x_2^e + x_3^e) \end{pmatrix}.$$

Hence $\mathscr{C}_t^e x^e = 0$ if and only if $x^e = 0$.

d) Since (A, B_d) is stabilizable, there exists a stabilizing feedback operator $K_d \in \mathscr{L}(X, U_d)$ such that $A + B_d K_d$ is the generator of a stable C_0-semigroup on X.
Hence the operator $K^e \in \mathscr{L}(X^e, U^e)$ defined by

$$K^e = \begin{pmatrix} -I & 0 & 0 \\ 0 & K_d & 0 \end{pmatrix}$$

is a stabilizing feedback operator for the pair (A^e, B^e).
Indeed, the operator

$$A^e + B^e K^e = \begin{pmatrix} -I & 0 & 0 \\ (\mathscr{A} + I) B_b & A + B_d K_d & 0 \\ C_\alpha \mathscr{A} B_b & C_\alpha (A + B_d K_d) & 0 \end{pmatrix}$$

is the generator of a stable C_0-semigroup on X^e. For this purpose, observe that, in closed loop, the first two equations generate a stable C_0-semigroup on $U_b \oplus X$. Hence, there exist $M_1, M_2 > 0$ and $\alpha_1, \alpha_2 < 0$ such that for all $(x_{1_0}^e, x_{2_0}^e) \in U_b \oplus D(A)$ and for all $t \geq 0$,

$$\|x_1^e(t)\| \leq M_1 e^{\alpha_1 t} \|x_{1_0}^e\|$$

and

$$\|x_2^e(t)\| \leq M_2 e^{\alpha_2 t} \|x_{2_0}^e\|,$$

where x_1^e and x_2^e are the state trajectories corresponding to the C_0-semigroup generated by

$$\begin{pmatrix} -I & 0 \\ (\mathscr{A} + I) B_b & A + B_d K_d \end{pmatrix}.$$

Now, observe that, on X^e, for all $t \geq 0$,

$$\begin{aligned} \|x_3^e(t)\| &= \|C_\alpha(x_2^e(t) + B_b x_1^e(t))\| \\ &\leq \|C_\alpha\|(M_2 e^{\alpha_2 t}\|x_{2_0}^e\| + \|B_b\|M_1 e^{\alpha_1 t}\|x_{1_0}^e\|). \end{aligned}$$

Finally, taking the max norm $\|\cdot\|_\infty$ on the product space $U_b \oplus X \oplus Y$ yields the inequality

$$\|(x_1^e(t), x_2^e(t), x_3^e(t))\|_\infty \leq [(1 + \|C_\alpha\|\|B_b\|)M_1 + (1 + \|C_\alpha\|)M_2]e^{\alpha t}\|(x_{1_0}^e, x_{2_0}^e, x_{3_0}^e)\|_\infty,$$

where $\alpha := \max\{\alpha_1, \alpha_2\}$.

e) Consider the operator $L^e := -\kappa I \in \mathscr{L}(Y^e, X^e)$, where $\kappa \geq 0$. It is easy to see that the operator

$$A^e + L^e C^e = \begin{pmatrix} -\kappa\rho_1 I & 0 & 0 \\ (\mathscr{A} - \kappa\rho_2 I)B_b & A - \kappa\rho_2 I & 0 \\ C_\alpha \mathscr{A} B_b & C_\alpha A & -\kappa\rho_3 I \end{pmatrix}$$

is the generator of a stable C_0-semigroup on X^e if κ is chosen large enough. ■

Similar questions are studied in (Curtain and Zwart 1995, Exercise 5.25., pp. 262–264) for a boundary control system without distributed input and with a bounded observation operator. In particular, the stabilizability of the extended system is related to the stabilizability of the nominal system with respect to the boundary input.
The previous proposition emphasizes the crucial role of the distributed input operator B_d in the dynamics. This result is of particular importance for the uniqueness and optimality of the solution of a LQ-optimal control problem, which is studied in Chapter 3. In fact, in general, the extended system without distributed input is not reachable. However, as stated in that chapter, the distributed control operator, though important, is not necessarily required to obtain a certain form of optimality which is still very interesting in practice when the nominal system is reachable with respect to a sufficiently smooth boundary input.
In the sequel, the extended system (1.2.13)-(1.2.19) will be considered on the state space X^e as in Theorem 1.3.2.

2.2 Comparison with the nominal system

In this section, we introduce additional assumptions such that the nominal system (1.2.1)-(1.2.3) is a well-posed linear system, whose definition can be found in e.g. (Weiss 1994). It will be shown later that this definition is indeed satisfied under these additional assumptions.
Our aim is to show that the extended system becomes close in some sense to the nominal one when the parameter α goes to infinity. This would ensure that the resolution of some control problems for the extended system would provide a good estimation of the solution for the nominal one when α is large enough.

Under this assumption, the state trajectories are almost everywhere in the domain of the Yosida extension, i.e. for all $x_0 \in D(A)$ and for almost all $t \geq 0$, $C_\alpha x(t) \to \mathscr{C}x(t)$ when $\alpha \to +\infty$ along the real axis.

First, as in (Weiss 1994), let us define the Yosida extension $C_\Lambda : D(C_\Lambda) \subset X \to Y$ given by

$$C_\Lambda x_0 = \lim_{\alpha \to +\infty} C_\alpha x_0 \tag{2.2.1}$$

where $\alpha \in \mathbb{R}$, for all x_0 in its domain

$$D(C_\Lambda) = \{x_0 \in X : \text{the limit in (2.2.1) exists}\}.$$

It should be noted that the operator C_Λ is an extension of the operator C_L defined by

$$C_L x_0 = \lim_{\tau \to 0} \mathscr{C} \frac{1}{\tau} \int_0^\tau \mathbb{T}_\sigma x_0 d\sigma \tag{2.2.2}$$

on its domain

$$D(C_L) = \{x_0 \in X : \text{the limit in (2.2.2) exists}\},$$

which is often referred to as the *Lebesgue extension* of $\mathscr{C}$, in the sense that $D(C_L) \subset D(C_\Lambda) \subset X$ and for all $x \in D(C_L)$, $C_\Lambda x = C_L x$, see (Weiss 1994), where it is also emphasized that in most cases C_L and C_Λ are interchangeable and one can choose the most suitable one. In this case, the Yosida extension C_Λ was chosen because of the importance and the recurrent role of the frequency domain and the resolvent operator of A in this theory. In fact, the computation of the resolvent operator of A (and hence of A^e) is a crucial step in order to obtain the right coprime fraction (3.2.5)-(3.2.6) and the spectral density (3.2.4) which are introduced in Chapter 3 and play a central role in the resolution of the LQ-optimal control problem.
Now, we assume that

1) the operator $(\mathscr{A} - A)B_b$ is an admissible control operator for the semigroup $\mathbb{T} = (\mathbb{T}_t)_{t \geq 0} = (T(t))_{t \geq 0}$ (see condition **[C1]** in Definition 2), i.e. for some $\tau > 0$, Ran $\tilde{\Phi}_\tau \subset X$, where for all $u_b \in U_b$,

$$\tilde{\Phi}_\tau u_b = \int_0^\tau T(\tau - \sigma)(\mathscr{A} - A)B_b u_b(\sigma) d\sigma,$$

2) the operator $\mathscr{C}$ is an admissible observation operator for $\mathbb{T}$, i.e. for some $\tau > 0$, there exists a constant $K_\tau \geq 0$ such that for all $x \in D(A)$,

$$\int_0^\tau \|\mathscr{C}T(t)x\|_Y^2 dt \leq K_\tau^2 \|x\|_X^2.$$

Under these conditions, the BCBO system (1.2.1)-(1.2.3) is a *well-posed linear system* whose state, input-state, state-output and input-output mappings defined in (Weiss 1994) are given by $\mathbb{T}_\tau = T(\tau)$ for all $\tau \geq 0$,

$$\begin{aligned} \Phi_\tau u &= \int_0^\tau T(\tau - \sigma)(\mathscr{A} - A)B_b u_b(\sigma) d\sigma \\ &\quad + \int_0^\tau T(\tau - \sigma) B_d u_d(\sigma) d\sigma \end{aligned}$$

for all $\tau \geq 0$ and $u \in \Omega = L^2([0,+\infty),U)$, where $U := U_b \oplus U_d$,

$$(\Psi_\tau x)(t) = \begin{cases} \mathscr{C}T(t)x & \text{if} \quad t \in [0,\tau) \\ 0 & \text{if} \quad t \geq \tau \end{cases}$$

for all $\tau > 0$ and $x \in D(A)$, with $\Psi_0 = 0$, and

$$(\mathbb{F}_\tau u)(t) = \begin{cases} \mathscr{C}\int_0^t [T(t-\sigma)\mathscr{A} - AT(t-\sigma)]B_b u_b(\sigma)d\sigma \\ +\mathscr{C}\int_0^t T(t-\sigma)B_d u_d(\sigma)d\sigma \quad \text{if } t \in [0,\tau) \\ 0 \quad \text{if } t \geq \tau \end{cases}$$

for all $\tau \geq 0$ and $u \in \Omega$, with $\mathbb{F}_0 = 0$, respectively.

Observe that both C_L and C_Λ defined by (2.2.2) and (2.2.1), respectively, are extensions of the admissible observation operator $\mathscr{C}$, which can be written as

$$\mathscr{C}x = \lim_{t\to 0} \frac{1}{t}\int_0^t (\Psi_\tau x)(\sigma)d\sigma$$

for all $x \in X_1$.

In what follows, for any Hilbert space W, for all $u,v \in L^2([0,+\infty),W)$ and for all $\tau \geq 0$, the τ-concatenation of u and v is defined by

$$(u \underset{\tau}{\diamond} v)(t) = \begin{cases} u(t) & \text{if} \quad t \in [0,\tau) \\ v(t-\tau) & \text{if} \quad t \geq \tau. \end{cases}$$

The mappings introduced above satisfy the assumptions of (Weiss 1994), hence the conditions of the definition of a well-posed linear system hold in this case. Indeed,

(i) $\mathbb{T} = (\mathbb{T}_t)_{t\geq 0} = (T(t))_{t\geq 0}$ is a C_0-semigroup of bounded linear operators on X.

(ii) The family $\Phi = (\Phi_t)_{t\geq 0}$ is a family of bounded linear operators from Ω to X.
Indeed, $(\mathscr{A}-A)B_b \in \mathscr{L}(U_b, X_{-1})$ since, for all $u_b \in U_b$,

$$\begin{aligned} \|(\mathscr{A}-A)B_b u_b\|_{-1} &= \|(\beta I - A)^{-1}(\mathscr{A}-A)B_b u_b\| \\ &\leq \left(\|(\beta I-A)^{-1}\mathscr{A}B_b\| + |\beta|\|(\beta I-A)^{-1}B_b\| + \|B_b\|\right)\|u_b\| \end{aligned}$$

where $\beta \in \rho(A)$.
Moreover, $(\mathscr{A}-A)B_b$ is admissible by assumption, hence we deduce from (Tucsnak and Weiss 2009, Proposition 4.2.2., p. 126) that for all $t \geq 0$, $\Phi_t \in \mathscr{L}(\Omega, X)$.
In addition, for all $u_1, u_2 \in \Omega$ and for all $\tau, t \geq 0$,

$$\begin{aligned} \Phi_{\tau+t}(u_1 \underset{\tau}{\diamond} u_2) &= T(t)\Phi_\tau u_1 + \Phi_t u_2 \\ &= \mathbb{T}_t \Phi_\tau u_1 + \Phi_t u_2 \end{aligned}$$

(iii) The family $\Psi = (\Psi_t)_{t\geq 0}$ is a family of bounded linear operators from X to $\Gamma = L^2([0,+\infty),Y)$.
Indeed, since $\mathscr{C} \in \mathscr{L}(X_1,Y)$ is admissible, it follows by (Tucsnak and Weiss 2009, Proposition 4.3.2., p. 132) that for all $t \geq 0$, $\Psi_t \in \mathscr{L}(X,\Gamma)$.
Moreover, since $(T(t))_{t\geq 0}$ satisfies the semigroup property, it is easy to check that for all $x \in X$ and for all $\tau, t \geq 0$,

$$\begin{aligned}\Psi_{\tau+t}x &= \Psi_\tau x \underset{\tau}{\diamond} \Psi_t T(\tau)x \\ &= \Psi_\tau x \underset{\tau}{\diamond} \Psi_t \mathbb{T}_\tau x.\end{aligned}$$

Finally, $\Psi_0 = 0$.

(iv) The family $\mathbb{F} = (\mathbb{F}_t)_{t\geq 0}$ is a family of bounded linear operators from Ω to Γ, which follows from (ii) and (iii), and for all $u_1, u_2 \in \Omega$ and for all $\tau, t \geq 0$,

$$\mathbb{F}_{\tau+t}(u_1 \underset{\tau}{\diamond} u_2) = \mathbb{F}_\tau u_1 \underset{\tau}{\diamond} (\Psi_t \Phi_\tau u_1 + \mathbb{F}_t u_2).$$

Finally, $\mathbb{F}_0 = 0$.

Proposition 2.2.1 *Let us assume that*

(i) *the transfer function of the nominal system (1.2.1)-(1.2.3) given by*

$$\hat{H}(s) = \begin{pmatrix} C_\Lambda (sI - A)^{-1}(\mathscr{A}B_b - sB_b) + C_\Lambda B_b & C_\Lambda (sI-A)^{-1}B_d \end{pmatrix}$$

has a strong limit along the real axis, i.e., for all $u = (u_b, u_d) \in U_b \oplus U_d$,

$$\lim_{\substack{s\to\infty \\ s\in\mathbb{R}}} \hat{H}(s)u \in Y,$$

which implies that the system is regular, and

(ii) *for all $(u_b,u_d) \in U_b \oplus U_d$, $B_b u_b \in D(C_\Lambda)$ and*

$$\lim_{\alpha\to+\infty} C_\alpha B_b u_b = \mathscr{C} B_b u_b,$$

$$\lim_{\alpha\to+\infty} C_\alpha (sI-A)^{-1} B_b u_b = \mathscr{C}(sI-A)^{-1} B_b u_b,$$

$$\lim_{\alpha\to+\infty} C_\alpha (sI-A)^{-1} B_d u_d = \mathscr{C}(sI-A)^{-1} B_d u_d.$$

Then, the following properties hold:

a) for all state trajectories $x(\cdot)$ of the BCBO system and for a.e. $t \geq 0$, $x(t)$ is in the domain of the Yosida extension, i.e. $y_\alpha(t) = C_\alpha x(t)$ converges in Y as α goes to $+\infty$, and

$$\lim_{\alpha\to+\infty} y_\alpha(t) = \lim_{\alpha\to+\infty} C_\alpha x(t) = \mathscr{C}x(t),$$

b) for all $s \in \rho(A)$,

$$\lim_{\alpha \to +\infty} \hat{\tilde{G}}^e_\alpha(s) = \hat{G}(s),$$

where the input-output transfer functions $\hat{G}(s)$ *and* $\hat{\tilde{G}}^e_\alpha$ *of the nominal and extended systems respectively are defined by*

$$\hat{y}(s) = \hat{G}(s) \begin{pmatrix} \hat{u}_b(s) \\ \hat{u}_d(s) \end{pmatrix}$$

and

$$\hat{y}_\alpha(s) = \hat{\tilde{G}}^e_\alpha(s) \begin{pmatrix} \hat{u}_b(s) \\ \hat{u}_d(s) \end{pmatrix}.$$

Proof. Since (1.2.1)-(1.2.3) is a well-posed linear system, a) follows immediately from (Weiss 1994, Theorem 5.8.) and (Weiss 1994, Remark 6.2.).

b) follows from (ii) and (Weiss 1994, Theorem 5.8.) since the regularity implies that for all $s \in \rho(A)$ and for all $(u_b, u_d) \in U_b \oplus U_d$, $(sI-A)^{-1}B_b u_b$, $(sI-A)^{-1}\mathscr{A}B_b u_b$ and $(sI-A)^{-1}B_d u_d \in D(C_\Lambda)$. ■

Transfer functions and input-output maps have been studied for boundary control systems in factor form with an admissible observation operator in (Grabowski and Callier 2001).

Chapter 3

LQ-optimal control

3.1 Objectives

This central chapter provides results and a general method of resolution for the *LQ-optimal control problem* associated with BCBO systems.
Many physical systems are naturally unstable and in general this instability is inherited by the mathematical system. This characteristic is often undesirable and one may want to design a control law that stabilizes the system around an equilibrium of interest. However, it is sometimes interesting to conceive this control law such that it optimizes a given criterion, which is generally based on the state and input trajectories of the system and has a physical interpretation in terms of energy, for example.

More specifically, we consider the following optimization problem for the extended system (1.2.13)-(1.2.19), which is assumed from now on to be reachable and stabilizable:

$$\min_{u^e} J(u^e, x_0^e, \infty) \tag{3.1.1}$$

where the *quadratic cost functional* is given by

$$\begin{aligned} J(u^e, x_0^e, \infty) &= \frac{1}{2}\int_0^{+\infty} \left[\|y^e(t)\|^2 + u^e(t)^* Q u^e(t)\right] dt \\ &= \frac{1}{2}\int_0^{+\infty} \left[\|C^e x^e(t)\|^2 + u^e(t)^* Q u^e(t)\right] dt \end{aligned} \tag{3.1.2}$$

where Q is a positive-definite weighting matrix operator of appropriate dimension.
This problem has been studied extensively for finite and infinite-dimensional systems with bounded control and observation operators, see e.g. (Curtain and Zwart 1995). However, it is still relatively unexplored for boundary control systems with boundary observation, where these operators are unbounded. Our goal is to use the extended model presented and analyzed in the previous chapters in order to establish a connection between the standard theory and the resolution of the LQ-optimal control problem for BCBO systems.

The rest of this chapter is divided into two sections, which correspond to the cases where only a boundary input is present in the model ($B_d = 0$) or where a distributed input is present as well ($B_d \neq 0$). The control design methodology is similar in both cases, but some computations, consequences and results are adapted in order to reflect the nature of the control inputs.

3.2 Boundary LQ-optimal control

3.2.1 Interpretation of the cost functional

Due to the nature of a wide range of physical systems, it is often hard or impossible to control them at every spatial position. For example, heating a three-dimensional object often consists in introducing heat in the object via its external layer, or, in other words, its physical boundary. In many biochemical systems, not only the temperature but also the concentration of reactants and / or substrate is regulated via the inlet of the reactor. For these kinds of systems, we need an adapted methodology in order to design efficient control laws.

In this section, we consider the case where no distributed input is present in the model ($B_d = 0$) and we focus on LQ-optimal pure boundary control.
We consider the LQ-optimal control problem (3.1.1) with the cost functional (3.1.2), where the input weighting coefficient operator is given by $Q = \eta I > 0$. By using the structure of the operator C^e given by (1.2.19) and the relation (1.3.2), the cost functional (3.1.2) can be written as

$$
\begin{aligned}
& J(u^e, x_0^e, \infty, \eta) \\
= \; & \frac{1}{2}\int_0^{+\infty} \left[\| (\rho_1 u_b(t) \quad \rho_2(v_1(t) + B_b u_b(t)) \quad \rho_3 v_2(t))^T \|^2 + \overline{\dot{u}_b(t)} \eta I \dot{u}_b(t) \right] dt \\
= \; & \frac{1}{2}\int_0^{+\infty} \left[\rho_1 \|u_b(t)\|^2 + \rho_2 \|v_1(t) + B_b u_b(t)\|^2 + \rho_3 \|v_2(t)\|^2 + \eta \|\dot{u}_b(t)\|^2 \right] dt \\
= \; & \frac{1}{2}\int_0^{+\infty} \left[\rho_1 \|u_b(t)\|^2 + \rho_2 \|x(t)\|^2 + \rho_3 \|y_\alpha(t)\|^2 + \eta \|\dot{u}_b(t)\|^2 \right] dt \qquad (3.2.1)
\end{aligned}
$$

for a suitable initial condition, where the weighting parameters ρ_1, ρ_2, ρ_3 and η are positive and the dependence to η is written explicitly. The fact that ρ_2 and η can be chosen small should be emphasized at this point. In fact, as a consequence, with suitably chosen parameters, the cost functional for the extended system can be interpreted as a cost functional for the nominal system, with a non standard term involving the norm of the variation rate of the boundary input $u_b(t)$ for which the corresponding parameter η can be adjusted. When η goes to zero, this non standard term vanishes, which can be written as

$$\lim_{\eta \to 0^+} J(u^e, x_0^e, \infty, \eta) = J(u, x, \infty)$$

whenever this limit exists, where

$$J(u,x,\infty)=\frac{1}{2}\int_0^{+\infty}\left[\rho_1\|u_b(t)\|^2+\rho_2\|x(t)\|^2+\rho_3\|y_\alpha(t)\|^2\right]dt$$

is a standard cost functional for the nominal system (1.2.1)-(1.2.3) with a penalization of the boundary input, the state and the approximate output. However, one has to be careful with any practical implementation of a method of resolution for this problem with η being very small, since the problem may become badly conditioned from a numerical point of view. In particular, in Step 3 of the algorithm presented in Section 4.3, the research of zeros of the determinant of the spectral density becomes harder as the parameter η becomes smaller. More precisely, in this case, the MATLAB implementation of this algorithm encounters huge numerical instabilities when η gets close to 0.01 and is also dependent on the ratio ρ_1/η. Despite these numerical difficulties, the evolution of the behaviour of the boundary input corresponding to the solution of (3.1.1) can be observed in Figure 4.8 (in Section 4.3), where the parameter ρ_1 is fixed and the parameter η becomes gradually smaller.

3.2.2 General methodology

The following methodology and results show how this problem can be solved when Q is the identity operator, i.e. $\eta=1$, by solving a problem of spectral factorization of an appropriate spectral density, or Popov function. More precisely, we use the methodology of (Callier and Winkin 1992) extended to possibly infinite-dimensional input and output Hilbert spaces. The main result was reported in (Dehaye and Winkin 2013*b*) for the particular case of an analytic extended C_0-semigroup.

General methodology:

1. *Computation and instability of the open-loop transfer function:*

   The resolvent operator of A^e has the form

$$(sI-A^e)^{-1}=\begin{pmatrix}\frac{1}{s}I & 0 & 0\\ \frac{1}{s}(sI-A)^{-1}\mathscr{A}B_b & (sI-A)^{-1} & 0\\ \frac{1}{s}C_\alpha(sI-A)^{-1}\mathscr{A}B_b & \frac{1}{s}C_\alpha A(sI-A)^{-1} & \frac{1}{s}I\end{pmatrix}.$$

   The transfer function of the extended system is then given by

$$\begin{aligned}\hat{G}^e(s) &= C^e(sI-A^e)^{-1}B^e\\ &= \begin{pmatrix}\rho_1\frac{1}{s}I\\ \rho_2E(s)\\ \rho_3C_\alpha E(s)\end{pmatrix}\end{aligned}$$

   where

$$E(s)=\frac{1}{s}\left[(sI-A)^{-1}\mathscr{A}-A(sI-A)^{-1}\right]B_b.$$

This transfer function is unstable due to $\hat{G}^e_{11}(s)$.

2. *Stabilizing feedback and closed-loop dynamics:*

Since the transfer function $\hat{G}^e(s)$ is unstable, the next step consists of prestabilizing the system in order to find a right coprime fraction of $\hat{G}^e(s)$. For this purpose, let us consider any stabilizing feedback

$$K^e = \begin{pmatrix} k_1 & k_2 & k_3 \end{pmatrix} \tag{3.2.2}$$

where $k_1 \in \mathscr{L}(U_b)$, $k_2 \in \mathscr{L}(X,U_b)$ and $k_3 \in \mathscr{L}(Y,U_b)$.
The corresponding stable closed-loop dynamics generator is given by

$$A^e + B^e K^e = \begin{pmatrix} k_1 & k_2 & k_3 \\ \mathscr{A}B_b - B_b k_1 & A - B_b k_2 & -B_b k_3 \\ C_\alpha \mathscr{A} B_b & C_\alpha A & 0 \end{pmatrix}.$$

3. *Right coprime fraction:*

A right coprime fraction of $\hat{G}^e(s)$ is then given by

$$\begin{aligned} \hat{N}^e(s) &= C^e(sI - A^e - B^e K^e)^{-1} B^e, \\ \hat{D}^e(s) &= I + K^e(sI - A^e - B^e K^e)^{-1} B^e. \end{aligned}$$

4. *Spectral factorization:*

Then, one can compute the spectral density

$$\hat{F}^e(s) = \hat{N}^e_*(s)\hat{N}^e(s) + \hat{D}^e_*(s)\hat{D}^e(s)$$

and solve the spectral factorization problem, i.e. find $\hat{R}^e \in H^\infty(\mathscr{L}(U_b))$ such that $(\hat{R}^e)^{-1} \in H^\infty(\mathscr{L}(U_b))$ and for all $\omega \in \mathbb{R}$,

$$\hat{F}^e(j\omega) = \hat{R}^e_*(j\omega)\hat{R}^e(j\omega).$$

It is known that this problem admits a solution if the operator spectral density $\hat{F}^e(s)$ is (uniformly) coercive on the imaginary axis, i.e. there exists $\eta > 0$ such that for all $\omega \in \mathbb{R}$,

$$\hat{F}^e(j\omega) \geq \eta I,$$

see e.g. (Rosenblum and Rovnyak 1985).
When the input space is finite-dimensional, this solution is known to be in $\mathrm{Mat}(\hat{\mathscr{A}_-})$, whose definition is recalled here, together with its inverse, see e.g. (Callier and Winkin 1992), (Callier and Winkin 1999).

Definition 6 *a) Let $\sigma \leq 0$. A complex-valued Laplace-transformable impulse response f is said to be in $\mathscr{A}(\sigma)$ if for all $t < 0$, $f(t) = 0$ and for all $t \geq 0$, $f(t) = f_a(t) + f_{sa}(t)$ where*

(i) the regular functional part f_a satisfies

$$\int_0^{+\infty} |f_a(t)| e^{-\sigma t} dt < \infty,$$

(ii) the singular atomic part $f_{sa} := \sum_{i=0}^{+\infty} f_i \delta(\cdot - t_i)$, where $t_0 = 0$, $t_i > 0$ for all $i \in \mathbb{N}$ and $f_i \in \mathbb{C}$ for all $i \in \mathbb{N}$, satisfies

$$\sum_{i=0}^{+\infty} |f_i| e^{-\sigma t_i} < \infty.$$

b) An impulse response f is said to be in $\mathscr{A}_-$ if $f \in \mathscr{A}(\sigma)$ for some $\sigma < 0$. The set of Laplace transforms of elements of $\mathscr{A}_-$ is denoted by $\hat{\mathscr{A}}_-$. The set of matrices with entries in $\hat{\mathscr{A}}_-$ is denoted by $Mat(\hat{\mathscr{A}}_-)$.

It is well-known that $\mathscr{A}_- \subset H^\infty := H^\infty(\mathbb{C})$. See ((Curtain and Zwart 1995), Appendix 6 and 7) for more detail.

For the existence of a spectral factor $\hat{R}^e \in H^\infty(\mathscr{L}(U_b \oplus U_d))$, see (Weiss and Weiss 1997), which is based on (Rosenblum and Rovnyak 1985, Theorem 3.7).

5. *Diophantine equation:*

Finally, one has to find a constant solution $(\mathscr{U}, \mathscr{V})$ of the diophantine equation

$$\mathscr{U} \hat{D}^e(s) + \mathscr{V} \hat{\mathscr{N}}^e(s) = \hat{R}^e(s), \tag{3.2.3}$$

where

$$\hat{\mathscr{N}}^e(s) := (sI - A^e - B^e K^e)^{-1} B^e.$$

Since A^e is the generator of a C_0-semigroup by Theorem 1.3.2, the pair (C^e, A^e) is detectable by Proposition 2.1.2 and the pair (A^e, B^e) is assumed to be reachable and stabilizable, this solution is unique and the optimal feedback can be computed as

$$K_0^e = -\mathscr{U}^{-1} \mathscr{V} = -\mathscr{U}^* \mathscr{V}.$$

Remark 1 *In a slightly simpler context, a Diophantine equation generally corresponds to a polynomial equation, typically in two or more unknowns, for which only integer solutions are allowed. By analogy, in (3.2.3), $D^e(s)$, $\hat{\mathscr{N}}^e(s)$ and $\hat{R}^e(s)$ can be seen as known operator-valued coefficients and, instead of an integer solution, we look for a solution $(\mathscr{U}, \mathscr{V})$ which is a couple of bounded linear operators.*

6. *Feedback structure:*

   Without loss of generality, any state feedback $K^e = (k_1\ k_2\ k_3)$ is such that $k_3 = 0$. This fact can be explained by the dependence of the third state component, which corresponds to the approximate output, with respect to the first two state components. Hence any feedback operator acting on the whole state can be rewritten as an operator acting on the first two components only.
   More precisely, since the state trajectories are such that $x^e(t) \in G(C)$ for all $t \geq 0$, we have that

$$x_3^e(t) = C_\alpha(x_2^e(t) + B_b x_1^e(t)).$$

   Hence, for all $t \geq 0$,

$$K^e x^e(t) = \begin{pmatrix} k_1 + k_3 C_\alpha B_b & k_2 + k_3 C_\alpha & 0 \end{pmatrix} \begin{pmatrix} x_1^e(t) \\ x_2^e(t) \\ x_3^e(t) \end{pmatrix}$$

   where B_b and C_α are bounded linear operators.

The computation of the spectral factor and the constant solution of the diophantine equation often requires adapted numerical schemes, such as the algorithm presented in Chapter 4.

This methodology is summarized in the following result.

Theorem 3.2.1 *Consider the extended system (1.2.13)-(1.2.19) with $B_d = 0$. Assume that the pair (A^e, B^e) is reachable and stabilizable.*
Let us consider the LQ-optimal control problem (3.1.1) with the cost functional (3.1.2) where $Q = I$.
Consider

a) a stabilizing feedback K^e and the spectral density given by

$$\hat{F}^e(s) = \hat{N}_*^e(s)\hat{N}^e(s) + \hat{D}_*^e(s)\hat{D}^e(s), \tag{3.2.4}$$

where the pair $(\hat{N}^e, \hat{D}^e)$ defined by

$$\hat{N}^e(s) = C^e(sI - A^e - B^e K^e)^{-1} B^e \tag{3.2.5}$$
$$\hat{D}^e(s) = I + K^e(sI - A^e - B^e K^e)^{-1} B^e \tag{3.2.6}$$

is a right coprime fraction of the operator-valued transfer function $\hat{G}^e(s) = C^e(sI - A^e)^{-1}B^e$, and

b) the spectral factorization problem

$$\hat{F}^e(j\omega) = \hat{R}_*^e(j\omega)\hat{R}^e(j\omega) \tag{3.2.7}$$

and the (standard) invertible stable spectral factor $\hat{R}^e \in H^\infty(\mathscr{L}(U_b \oplus U_d))$ *such that* $(\hat{R}^e)^{-1} \in H^\infty(\mathscr{L}(U_b \oplus U_d))$ *and* $\hat{R}^e(\infty) = I$.

Then the solution of the LQ-optimal control problem (3.1.1) is the stabilizing feedback control law $u^e = K_0^e x^e$ *with the state feedback operator*

$$K_0^e = \begin{pmatrix} k_{0_1} & k_{0_2} & k_{0_3} \end{pmatrix} \tag{3.2.8}$$

where $k_{0_1} \in \mathscr{L}(U_b)$, $k_{0_2} \in \mathscr{L}(X, U_b)$ *and* $k_{0_3} \in \mathscr{L}(Y, U_b)$ *are bounded linear operators.*
Without loss of generality, the solution has the following structure:

$$K_0^e = \begin{pmatrix} k_{0_1} & k_{0_2} & 0 \end{pmatrix}. \tag{3.2.9}$$

The feedback operator K_0^e *is given by*

$$K_0^e = -\mathscr{U}^{-1}\mathscr{V} = -\mathscr{U}^*\mathscr{V} \tag{3.2.10}$$

where $(\mathscr{U}, \mathscr{V})$ *is the unique constant solution of the Diophantine equation*

$$\mathscr{U}\hat{D}^e(s) + \mathscr{V}\hat{\mathscr{N}}^e(s) = \hat{R}^e(s) \tag{3.2.11}$$

with $\hat{\mathscr{N}}^e(s) := (sI - A^e - B^e K^e)^{-1} B^e$.

The proof of Theorem 3.2.1 is a direct consequence of the methodology detailed above in combination with the fact that (A^e, B^e) is reachable and stabilizable by assumption and that (C^e, A^e) is detectable by Proposition 2.1.2. It is also a direct adaptation of the proof of (Dehaye and Winkin 2013*b*, Theorem 1).
This result is an extension of the results established in (Callier and Winkin 1992) and (Aksikas et al. 2007), where the input space is assumed to be finite-dimensional and the C_0-semigroup is assumed to be stable, respectively. In this work, the theorem is stated without these assumptions. This extension is rather straightforward by combining proofs and results from (Callier and Winkin 1992), (Aksikas et al. 2007), (Rosenblum and Rovnyak 1985) and (Weiss and Weiss 1997). However, the computational methodology on which the proof is based for the extended system considered in this work is new and specific to the structure of the system described by (1.2.13)-(1.2.19). It provides some explicit and potentially useful computational details in steps 1,2,3 and 6 in view of a practical implementation of the proposed method of resolution of a LQ-optimal control problem. Even more details can be found in the methodology presented in Section 3.3 when distributed control is present in the model and the pair (A, B_d) is stabilizable.

This theorem is stated for the normalized case, i.e. where the weighting operator Q is the identity. However, one can define the positive-definite weighting operator $\tilde{Q} := \eta I$, where $\eta > 0$, and the modified bounded control operator $\tilde{B}^e = B^e \tilde{Q}^{-\frac{1}{2}}$ such that the input is given by $\tilde{u}^e = \tilde{Q}^{\frac{1}{2}} u^e$. Hence

$$\tilde{u}^{e*}\tilde{u}^e = u^{e*} Q u^e = \eta \|u^e\|^2,$$

which allows the general case to be treated as well.

It is important to notice that in general, for infinite-dimensional systems, reachability does not imply stabilizability (see e.g. (Curtain and Zwart 1995, Example 5.2.2, p. 228)). Similarly, by duality, observability does not guarantee that detectability holds. In Theorem 3.2.1, stabilizability is crucial for the existence of a solution of the LQ-optimal control problem, while reachability guarantees the uniqueness of the solution of the Diophantine equation (3.2.11), which is not necessarily the case in general, and hence of the optimal feedback operator. For these reasons, both these properties have to be considered in the assumptions of this result.
However, it should be noted that, even without the reachability assumption, any constant solution of (3.2.11) provides the reachable restriction of the optimal feedback operator. In these conditions, (3.2.10) only holds on the reachable subspace, i.e. for all x^e in the reachable subspace $\mathscr{R}(A^e, B^e)$,

$$K_0^e x^e = -\mathscr{U}^{-1}\mathscr{V}x^e = -\mathscr{U}^*\mathscr{V}x^e,$$

see (Callier and Winkin 1992), (Aksikas et al. 2007).

Remark 2 *The reachability and the stabilizability of the pair (A^e, B^e) may seem relatively difficult to check in general. However, in some cases, these properties can be established on basis of some straightforward tests on the nominal system.*
For example, in (Curtain and Zwart 1995, Exercise 4.20., p. 201-204), it is stated that, if $\mathscr{A}B_b = 0$, the pair (A^e, B^e) is reachable if and only if the pair (A, B_b) is. Even though this model does not include the approximate output in the state, it can be easily generalized to fit the BCBO system.
Stabilizability can be achieved as well in this case when the pair (A, B_b) is stabilizable, without the requirement of distributed control in the model, as seen in (Curtain and Zwart 1995, Exercise 5.25., pp. 262–264).
More generally, if $0 \in \rho(A)$ and (A, B_b) is stabilizable, stabilizability of the extended system holds if and only if

$$Ker\ (sI\ \ (\mathscr{A}B_b)^*) \cap Ker\ (0\ \ sI - A^*) \cap Ker\ (I\ \ -B_b^*) = \{0\} \tag{3.2.12}$$

for all $s \in \overline{\mathbb{C}_0^+}$.

It is well known that, under suitable assumptions, the LQ-optimal control problem can alternatively be solved by the resolution of an operator algebraic Riccati equation, see e.g. (Curtain and Zwart 1995, Section 6.2, pp. 292–303), (Pritchard and Salamon 1987) and (Alizadeh Moghadam, Aksikas, Dubljevic and Forbes 2013). Efficient numerical methods, including standard and modified Newton-Kleinman algorithms, were developed and analyzed in order to solve this problem for approximate finite-dimensional systems in practical applications, in particular for distributed parameter systems where the dynamics are described by partial differential equation, see e.g. (Grad and Morris 1996), (Morris and Navasca 2010) and references therein.

3.2.3 Interpretation of the optimal feedback law

So far, it has been shown that the LQ-optimal control problem is solvable for the extended system. However, it is still unclear at this point how its solution is useful for the stabilization of the nominal one. The following crucial theorem shows that the (static) optimal feedback for the extended system can be seen as a stabilizing dynamical feedback compensator for the nominal system, with an exponential rate of convergence, provided that the C_0-semigroup $(T(t))_{t\geq 0}$ generated by A is analytic or, more generally, immediately differentiable, which means that the map $t \mapsto T(t)x$ is differentiable on $(0,+\infty)$ for every $x \in X$ (see e.g. (Engel and Nagel 2000, Definition 4.13, p. 109)).

Definition 7 *A C_0-semigroup $(T(t))_{t\geq 0}$ on a Banach space X is called* eventually differentiable *if there exists $t_0 \geq 0$ such that the orbit maps $\xi_x : t \mapsto T(t)x$ are differentiable on $(t_0,+\infty)$ for every $x \in X$.*
The C_0-semigroup is called immediately differentiable *if t_0 can be chosen as $t_0 = 0$.*

Theorem 3.2.2 *Assume that the C_0-semigroup $(\mathbb{T}_t)_{t\geq 0} = (T(t))_{t\geq 0}$ generated by A is analytic.*

Then, under the assumptions of Theorem 3.2.1, the optimal control law for the extended system

$$\dot{u}_b(t) = K_0^e \begin{pmatrix} u_b(t) \\ x(t) - B_b u_b(t) \\ y_\alpha(t) \end{pmatrix} \tag{3.2.13}$$

is given by the dynamic compensator for the nominal system described by

$$\dot{u}_b(t) = (k_{0_1} - k_{0_2} B_b) u_b(t) + k_{0_2} x(t) \tag{3.2.14}$$

with $u_b(0)$ satisfying $x_0 - B_b u_b(0) \in D(A)$, whose state is the boundary input $u_b(t)$ and with input $x(t)$.

In addition, this dynamic compensator is (exponentially) stabilizing, i.e. in closed loop, there exist $M > 0$ and $\alpha < 0$ such that the state trajectory $x(t)$ given by (1.3.2) is such that for all $t \geq 0$,

$$\|x(t)\| \leq M e^{\alpha t} r(x_0),$$

where $r(x_0) > 0$ depends on $x_0 = x(0) \in D(\mathscr{A})$.

Moreover, this compensator is optimal with respect to the cost (3.2.1) for the nominal system among all dynamic compensators of the form (3.2.14) where k_{0_1} and k_{0_2} are bounded linear operators.

Proof. First, we show that the assumptions of Theorem 1.3.2b) hold for the closed-loop system, more specifically the fact that $u_b \in C^2([0,+\infty), U_b)$. For this purpose, let

us consider the auxiliary homogeneous differential system

$$\dot{\tilde{x}}(t) = \tilde{A}\tilde{x}(t) \tag{3.2.15}$$

with the initial condition

$$\tilde{x}(0) = \tilde{x}_0 = (u_b(0)\ ,\ x_0 - B_b u_b(0))^T \in D(\tilde{A}),$$

where $\tilde{A} : D(\tilde{A}) \subset U_b \oplus X \to U_b \oplus X$ is defined by

$$\tilde{A} = \begin{pmatrix} k_{0_1} & k_{0_2} \\ \mathscr{A}B_b - B_b k_{0_1} & A - B_b k_{0_2} \end{pmatrix} \tag{3.2.16}$$

on its domain $D(\tilde{A}) = U_b \oplus D(A)$.
Now, let us consider the perturbation operator

$$\begin{aligned} P &= \tilde{A} - \mathrm{diag}(0,A) \\ &= \begin{pmatrix} k_{0_1} & k_{0_2} \\ \mathscr{A}B_b - B_b k_{0_1} & -B_b k_{0_2} \end{pmatrix}. \end{aligned}$$

Since A is the generator of an analytic C_0-semigroup on X, the operator $\mathrm{diag}(0,A)$ is the generator of an analytic C_0-semigroup on $U_b \oplus X$. And, since $P \in \mathscr{L}(U_b \oplus X)$, the operator $\tilde{A} = \mathrm{diag}(0,A) + P$ is the generator of an analytic C_0-semigroup $(\tilde{T}(t))_{t\geq 0}$ on $U_b \oplus X$, see e.g. (Engel and Nagel 2000, Theorem 2.10, p. 176).
Hence, the classical solution of (3.2.15)-(3.2.16) satisfies

$$\tilde{x}(\cdot) = \tilde{T}(\cdot)\tilde{x}_0 \in C^\infty([0,+\infty), U_b \oplus X).$$

Observe that the second equation of (3.2.15)-(3.2.16) is equivalent to (1.2.6) under (3.2.13) with $v_1 := \tilde{x}_2$ and $u_b := \tilde{x}_1$. Since $\tilde{x}_{0_2} = x_0 - B_b u_b(0)$ and $\tilde{x} \in C^\infty([0,+\infty), U_b \oplus X)$ (hence $\tilde{x}_1 \in C^2([0,+\infty), U_b \oplus X)$), the classical solution is given for all $t \geq 0$ by

$$\tilde{x}_2(t) = x(t) - B_b u_b(t)$$

by Theorem 1.3.2b).
The first equation of (3.2.15)-(3.2.16) is then equivalent to the dynamics of (3.2.14), which shows that (1.3.2) holds for the closed-loop system.
Now, it is well known that the solution of the LQ-optimal control problem is a stabilizing feedback operator. Hence, there exist $M_u, M_v > 0$ and $\alpha_u, \alpha_v < 0$ such that, in closed loop, for all $t \geq 0$,

$$\|u_b(t)\| \leq M_u e^{\alpha_u t}\|u_b(0)\|$$

and

$$\|v_1(t)\| \leq M_v e^{\alpha_v t}\|v_1(0)\|.$$

Since $x(t) = v_1(t) + B_b u_b(t)$ by (1.3.2), for all $t \geq 0$,

$$\|x(t)\| \leq M e^{\alpha t} r(x_0),$$

where

$$M := 2\max\{\|B_b\|M_u, M_v\} > 0,$$

$$\alpha := \max\{\alpha_u, \alpha_v\} < 0$$

and

$$r(x_0) := \max\{\|u_b(0)\|, \|v_1(0)\|\}.$$

Finally, since it has been shown that (1.3.2) holds for the closed-loop system, any dynamic compensator of the form (3.2.14) can be interpreted as a static feedback law of the form (3.2.9) for the extended system. Hence (3.2.14), where k_{0_1} and k_{0_2} form the optimal feedback operator, minimizes the cost (3.2.1). ■

The assumption that the C_0-semigroup generated by A is analytic, which is the case for the application studied in Chapter 4, can be replaced by the following:

(i) the C_0-semigroup $(\mathbb{T}_t)_{t\geq 0} = (T(t))_{t\geq 0}$ generated by A is immediately differentiable,

$$(ii)\ \limsup_{t\to 0^+} \frac{t\log\|AT(t)\|}{\log\left(\frac{1}{t}\right)} = 0,$$

see e.g. (Engel and Nagel 2000, Definition 4.13, p. 109), (Doytchinov, Hrusa and Watson 1997, Theorem 1).
The first assumption is satisfied in particular when the C_0-semigroup is analytic. However, the converse is not true. Some multiplication semigroups, for example, are immediately differentiable but not analytic, see e.g. (Engel and Nagel 2000, Counterexample 4.33, p. 123).

Theorem 3.2.2 is illustrated by the following diagrams, which show the three interpretations of the closed-loop system with the LQ-optimal control law.
The first diagram represents the closed-loop extended system, which acts as an intermediate computational tool and for which the LQ-optimal control law is given by the static state feedback K_0^e.
The second diagram illustrates the closed-loop nominal system, for which the LQ-optimal control law becomes a dynamical state and approximate output feedback.
Finally, the third diagram shows the nominal system again with the output feedback included in the state feedback via the bounded operator C_α.

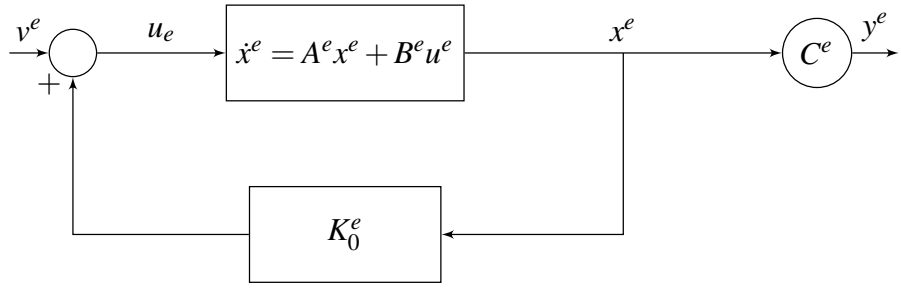

Figure 3.1: Static interpretation of the LQ-optimal feedback with boundary control for the extended system

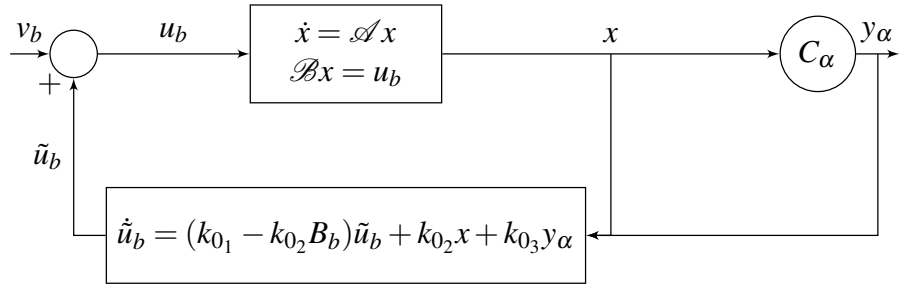

Figure 3.2: Dynamical interpretation of the LQ-optimal state and approximate output feedback with boundary control for the nominal system

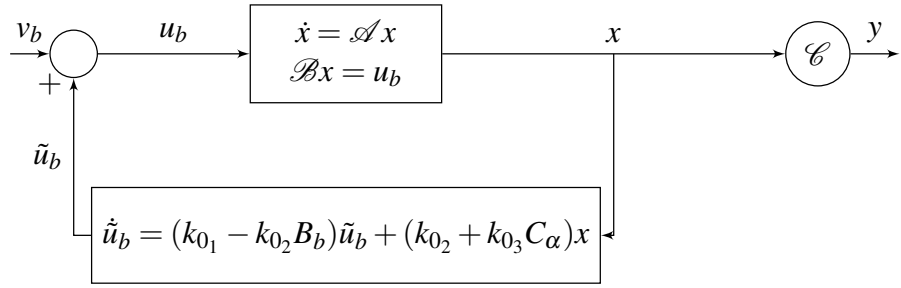

Figure 3.3: Dynamical interpretation of the LQ-optimal state feedback with boundary control for the nominal system

As a consequence of this result, in closed loop, the nominal system becomes

$$\left\{\begin{array}{rcl} \dot{x}(t) & = & \mathscr{A}x(t), \\ \mathscr{B}x(t) & = & u_b(t), \\ \dot{u}_b(t) & = & (k_{0_1} - k_{0_2}B_b)u_b(t) + k_{0_2}x(t), \end{array}\right.$$

with the initial conditions $x(0) = x_0$ and $u_b(0) = \mathscr{B}x_0$, where the interconnection between both dynamics only appears in the boundary conditions as expected. It should be observed that an additional constraint of this approach is the fact that the initial condition for the dynamic compensator has to be compatible with the boundary conditions at the time $t = 0$.

In general, one can expect that this dynamic feedback law is not optimal with respect to the standard cost for the nominal system. However, it has been shown that, under the assumptions of Theorem 3.2.2, the dynamic compensator minimizes the modified cost (3.2.1). The question of optimality with respect to a modified performance index has been studied in detail for finite-dimensional systems, see e.g. (Ikeda and Šiljak 1990) for nonlinear systems and (Moore and Anderson 1967) for linear systems with input derivative constraints.

3.3 Boundary and distributed LQ-optimal control

3.3.1 Interpretation of the cost functional

Even though a wide range of physical systems only allow punctual control, many others can be acted upon via their entire spatial domain, or at least via a distributed actuation on a portion of this domain. Again, a basic case is a heated metal bar, but instead of introducing heat only at one end, the whole bar (or at least a portion of the latter) is heated at the same time, with a possibly different intensity at each point. In the industry, this is also the case for some chemical reactors for example, where the tube is contained in a bed filled with cooling fluid, allowing to act on the reactions via variations of temperature along the tube.

In this section, we assume that a distributed control is present in the model ($B_d \neq 0$). Similarly as in the previous section, we consider the LQ-optimal control problem (3.1.1), where, this time, the positive-definite weighting matrix operator Q in (3.1.2) is given by $Q = \mathrm{diag}(\eta_1 I, \eta_2 I)$, with $\eta_1 > 0$ and $\eta_2 > 0$. The cost functional (3.1.2) can be written as

$$\begin{array}{rcl} J(u^e, x_0^e, \infty) & = & \dfrac{1}{2}\displaystyle\int_0^{+\infty} \big[\rho_1\|u_b(t)\|^2 + \rho_2\|x(t)\|^2 + \rho_3\|y_\alpha(t)\|^2 \\ & & +\eta_1\|\dot{u}_b(t)\|^2 + \eta_2\|u_d(t)\|^2\big]\, dt \end{array} \tag{3.3.1}$$

for a suitable initial condition, where ρ_2 and η_1 can be chosen small. The developments leading to this expression are similar to those of (3.2.1) with $u^e = (\dot{u}_b \;\; u_d)^T$ instead of $u^e = \dot{u}_b$.

3.3.2 General methodology

In the sequel, we present the corresponding methodology, which is applicable when Q is the identity operator, i.e. $\eta_1 = \eta_2 = 1$ but can also be easily adapted for a more general weighting matrix operator Q.

General methodology:

1. *Computation and instability of the open-loop transfer function:*

   The resolvent operator of A^e has the form

   $$(sI - A^e)^{-1} = \begin{pmatrix} \frac{1}{s}I & 0 & 0 \\ \frac{1}{s}(sI-A)^{-1}\mathscr{A}B_b & (sI-A)^{-1} & 0 \\ \frac{1}{s}C_\alpha(sI-A)^{-1}\mathscr{A}B_b & \frac{1}{s}C_\alpha A(sI-A)^{-1} & \frac{1}{s}I \end{pmatrix}.$$

   The transfer function of the extended system is given by

   $$\begin{aligned} \hat{G}^e(s) &= C^e(sI-A^e)^{-1}B^e \\ &= \begin{pmatrix} \rho_1\frac{1}{s}I & 0 \\ \rho_2 E(s) & \rho_2(sI-A)^{-1}B_d \\ \rho_3 C_\alpha E(s) & \rho_3 C_\alpha(sI-A)^{-1}B_d \end{pmatrix} \end{aligned}$$

   where

   $$E(s) = \frac{1}{s}\left[(sI-A)^{-1}\mathscr{A} - A(sI-A)^{-1}\right]B_b.$$

   This transfer function is unstable due to $\hat{G}^e_{11}(s)$.

2. *Stabilizing feedback and closed-loop dynamics:*

   Since the transfer function $\hat{G}^e(s)$ is unstable, the next step consists of prestabilizing the system in order to find a right coprime fraction of $\hat{G}^e(s)$. For this purpose, let us consider any stabilizing feedback

   $$K^e = \begin{pmatrix} k_{11} & k_{12} & k_{13} \\ k_{21} & k_{22} & k_{23} \end{pmatrix} \tag{3.3.2}$$

   where $k_{11} \in \mathscr{L}(U_b)$, $k_{21} \in \mathscr{L}(U_b, U_d)$, $k_{12} \in \mathscr{L}(X, U_b)$, $k_{22} \in \mathscr{L}(X, U_d)$, $k_{13} \in \mathscr{L}(Y, U_b)$ and $k_{23} \in \mathscr{L}(Y, U_d)$.
   In particular, if the pair (A, B_d) is stabilizable, the feedback can be chosen as

   $$K^e = \begin{pmatrix} k_1 & 0 & 0 \\ 0 & k_2 & 0 \end{pmatrix} \tag{3.3.3}$$

where $k_1 \in \mathscr{L}(U_b)$ is the bounded infinitesimal generator of a stable C_0-semigroup on U_b (such an operator always exists, take e.g. $k_1 = -I$) and $k_2 \in \mathscr{L}(X, U_d)$ is a stabilizing feedback for the pair (A, B_d).
In this case, the corresponding stable closed-loop dynamics generator is given by

$$A^e + B^e K^e = \begin{pmatrix} k_1 & 0 & 0 \\ \mathscr{A}B_b - B_b k_1 & A + B_d k_2 & 0 \\ C_\alpha \mathscr{A} B_b & C_\alpha (A + B_d k_2) & 0 \end{pmatrix}.$$

3. *Right coprime fraction:*

With the stabilizing feedback (3.3.3), a right coprime fraction of $\hat{G}^e(s)$ is then given by

$$\begin{aligned} \hat{N}^e(s) &= C^e(sI - A^e - B^e K^e)^{-1} B^e \\ &= \begin{pmatrix} \rho_1 M(s) \\ \rho_2 [I - J(s)(sI - \mathscr{A})] B_b M(s) \\ \rho_3 C_\alpha [I - J(s)(sI - \mathscr{A})] B_b M(s) \end{pmatrix}, \\ \hat{D}^e(s) &= I + K^e(sI - A^e - B^e K^e)^{-1} B^e \\ &= \begin{pmatrix} I + K_1 M(s) & 0 \\ -K_2 J(s)(sI - \mathscr{A}) B_b M(s) & I + K_2 J(s) B_d \end{pmatrix} \end{aligned}$$

where $M(s) = (sI - K_1)^{-1}$ and $J(s) = (sI - A - B_d K_2)^{-1}$.

4. *Spectral factorization:*

Then, one can compute the spectral density

$$\hat{F}^e(s) = \hat{N}_*^e(s)\hat{N}^e(s) + \hat{D}_*^e(s)\hat{D}^e(s)$$

and solve the spectral factorization problem, i.e. find $\hat{R}^e \in H^\infty(\mathscr{L}(U_b \oplus U_d))$ such that $(\hat{R}^e)^{-1} \in H^\infty(\mathscr{L}(U_b \oplus U_d))$ and for all $\omega \in \mathbb{R}$,

$$\hat{F}^e(j\omega) = \hat{R}_*^e(j\omega)\hat{R}^e(j\omega),$$

with

$$\hat{F}^e(s) = \begin{pmatrix} \hat{F}_1(s) & \hat{F}_2(s) \\ \hat{F}_{2*}(s) & \hat{F}_4(s) \end{pmatrix}$$

and

$$\hat{R}^e(s) = \begin{pmatrix} \hat{R}_1(s) & \hat{R}_2(s) \\ \hat{R}_3(s) & \hat{R}_4(s) \end{pmatrix}.$$

It is known that this problem admits a solution if the operator spectral density $\hat{F}^e(s)$ is (uniformly) coercive on the imaginary axis, i.e. there exists $\eta > 0$ such that for all $\omega \in \mathbb{R}$,

$$\hat{F}^e(j\omega) \geq \eta I.$$

When the input space is finite-dimensional, this solution is known to be in $\mathrm{Mat}(\hat{\mathscr{A}}_-)$ together with its inverse, see e.g. (Callier and Winkin 1992), (Callier and Winkin 1999). For the existence of a spectral factor $\hat{R}^e \in H^\infty(\mathscr{L}(U_b \oplus U_d))$, see (Weiss and Weiss 1997), which is based on (Rosenblum and Rovnyak 1985, Theorem 3.7).

5. *Diophantine equation:*

Finally, one has to find a constant solution $(\mathscr{U}, \mathscr{V})$ of the diophantine equation

$$\mathscr{U}\hat{D}^e(s) + \mathscr{V}\hat{\mathscr{N}}^e(s) = \hat{R}^e(s),$$

where

$$\hat{\mathscr{N}}^e(s) := (sI - A^e - B^e K^e)^{-1} B^e.$$

Since A^e is the generator of a C_0-semigroup by Theorem 1.3.2, the pair (C^e, A^e) is detectable by Proposition 2.1.2 and the pair (A^e, B^e) is assumed to be reachable and stabilizable (in particular if the pair (A, B_d) is), this solution is unique and the optimal feedback can be computed as

$$K_0^e = -\mathscr{U}^{-1}\mathscr{V} = -\mathscr{U}^*\mathscr{V}.$$

6. *Feedback structure:*

Observe that, without loss of generality, any state feedback of the form (3.3.2) is such that $k_{13} = k_{23} = 0$.
Indeed, since the state trajectories are such that $x^e(t) \in G(C)$ for all $t \geq 0$, we have that

$$x_3^e(t) = C_\alpha(x_2^e(t) + B_b x_1^e(t)).$$

Hence, for all $t \geq 0$,

$$K^e x^e(t) = \begin{pmatrix} k_{11} + k_{13}C_\alpha B_b & k_{12} + k_{13}C_\alpha & 0 \\ k_{21} + k_{23}C_\alpha B_b & k_{22} + k_{23}C_\alpha & 0 \end{pmatrix} \begin{pmatrix} x_1^e(t) \\ x_2^e(t) \\ x_3^e(t) \end{pmatrix}$$

where B_b and C_α are bounded linear operators.

Theorem 3.2.1 is applicable in this case. However, due to the distributed input, the optimal feedback operator (3.2.8) becomes

$$K_0^e = \begin{pmatrix} k_{0_{11}} & k_{0_{12}} & k_{0_{13}} \\ k_{0_{21}} & k_{0_{22}} & k_{0_{23}} \end{pmatrix}$$

and, without loss of generality, has the following structure:

$$K_0^e = \begin{pmatrix} k_{0_{11}} & k_{0_{12}} & 0 \\ k_{0_{21}} & k_{0_{22}} & 0 \end{pmatrix}. \tag{3.3.4}$$

Again, the result is stated for the normalized case but one can define the positive-definite weighting operator $\tilde{Q} := \mathrm{diag}(\eta_1 I, \eta_2 I)$, where $\eta_1 > 0$ and $\eta_2 > 0$, and the modified bounded control operator $\tilde{B}^e = B^e \tilde{Q}^{-\frac{1}{2}}$ such that the input is given by $\tilde{u}^e = \tilde{Q}^{\frac{1}{2}} u^e$. Hence

$$\tilde{u}^{e*}\tilde{u}^e = u^{e*}Qu^e = \eta_1 \|u_1^e\|^2 + \eta_2 \|u_2^e\|^2.$$

As in the case with boundary control only, Proposition 2.1.2 can help establish reachability and / or stabilizability of the extended system.

3.3.3 Interpretation of the optimal feedback law

Theorem 3.2.2 can be adapted for the case where $B_d \neq 0$ and is illustrated by Figure 3.4, where the black part corresponds to the distributed input and can be plugged out when the system only features boundary control.

Theorem 3.3.1 *Assume that the C_0-semigroup $(\mathbb{T}_t)_{t\geq 0} = (T(t))_{t\geq 0}$ generated by A is analytic.*

Then, under the assumptions of Theorem 3.2.1, the optimal control law for the extended system

$$\begin{pmatrix} \dot{u}_b(t) \\ u_d(t) \end{pmatrix} = K_0^e \begin{pmatrix} u_b(t) \\ x(t) - B_b u_b(t) \\ y_\alpha(t) \end{pmatrix} \tag{3.3.5}$$

is given by the dynamic compensator for the nominal system described by

$$\left\{ \begin{array}{rcl} \dot{u}_b(t) & = & (k_{0_{11}} - k_{0_{12}} B_b) u_b(t) + k_{0_{12}} x(t) \\ u_d(t) & = & (k_{0_{21}} - k_{0_{22}} B_b) u_b(t) + k_{0_{22}} x(t), \end{array} \right. \tag{3.3.6}$$

with $u_b(0)$ satisfying $x_0 - B_b u_b(0) \in D(A)$, whose state is the boundary input $u_b(t)$ and with input $x(t)$ and output $u_d(t)$.

In addition, this dynamic compensator is (exponentially) stabilizing, i.e. in closed loop, there exist $M > 0$ and $\alpha < 0$ such that the state trajectory $x(t)$ given by (1.3.2) is such that for all $t \geq 0$, $\|x(t)\| \leq M e^{\alpha t} r(x_0)$, where $r(x_0) > 0$ depends on $x_0 = x(0) \in D(\mathscr{A})$.

Moreover, this compensator is optimal with respect to the cost (3.3.1) for the nominal system among all dynamic compensators of the form (3.3.6) where the $k_{0_{ij}}$, $i, j = 1, 2$, are bounded linear operators.

Proof. First, we show that the assumptions of Theorem 1.3.2b) hold for the closed-loop system, more specifically the fact that $u_d \in C^1([0,+\infty), U_d)$ and $u_b \in C^2([0,+\infty), U_b)$. For this purpose, let us consider the auxiliary homogeneous differential system

$$\dot{\tilde{x}}(t) = \tilde{A}\tilde{x}(t) \tag{3.3.7}$$

with the initial condition

$$\tilde{x}(0) = \tilde{x}_0 = (u_b(0)\ ,\ x_0 - B_b u_b(0))^T \in D(\tilde{A}),$$

where $\tilde{A} : D(\tilde{A}) \subset U_b \oplus X \to U_b \oplus X$ is defined by

$$\tilde{A} = \begin{pmatrix} k_{0_{11}} & k_{0_{12}} \\ \mathscr{A}B_b - B_b k_{0_{11}} + B_d k_{0_{21}} & A - B_b k_{0_{12}} + B_d k_{0_{22}} \end{pmatrix} \tag{3.3.8}$$

on its domain $D(\tilde{A}) = U_b \oplus D(A)$. Now, let us consider the perturbation operator

$$\begin{aligned} P &= \tilde{A} - \mathrm{diag}(0,A) \\ &= \begin{pmatrix} k_{0_{11}} & k_{0_{12}} \\ \mathscr{A}B_b - B_b k_{0_{11}} + B_d k_{0_{21}} & -B_b k_{0_{12}} + B_d k_{0_{22}} \end{pmatrix}. \end{aligned}$$

Since A is the generator of an analytic C_0-semigroup on X, the operator $\mathrm{diag}(0,A)$ is the generator of an analytic C_0-semigroup on $U_b \oplus X$. And, since $P \in \mathscr{L}(U_b \oplus X)$, the operator $\tilde{A} = \mathrm{diag}(0,A) + P$ is the generator of an analytic C_0-semigroup $(\tilde{T}(t))_{t\geq 0}$ on $U_b \oplus X$, see e.g. (Engel and Nagel 2000, Theorem 2.10, p. 176).
Hence, the classical solution of (3.3.7)-(3.3.8) satisfies

$$\tilde{x}(\cdot) = \tilde{T}(\cdot)\tilde{x}_0 \in C^\infty([0,+\infty), U_b \oplus X).$$

Observe that the second equation of (3.3.7)-(3.3.8) is equivalent to (1.2.6) under (3.3.5) with $v_1 := \tilde{x}_2$, $u_b := \tilde{x}_1$ and $u_d := k_{21}\tilde{x}_1 + k_{22}\tilde{x}_2$. Since $\tilde{x}_{0_2} = x_0 - B_b u_b(0)$ and $\tilde{x} \in C^\infty([0,+\infty), U_b \oplus X)$ (hence $\tilde{x}_1 \in C^2([0,+\infty), U_b \oplus X)$ and $u_d \in C^1([0,+\infty), U_d)$), the classical solution is given for all $t \geq 0$ by

$$\tilde{x}_2(t) = x(t) - B_b u_b(t)$$

by Theorem 1.3.2b).
The first equation of (3.3.7)-(3.3.8) is then equivalent to the dynamics of (3.3.6) and the relation

$$u_d := k_{21}\tilde{x}_1 + k_{22}\tilde{x}_2$$

is equivalent to the output equation of (3.3.6), which shows that (1.3.2) holds for the closed-loop system.
Now, it is well known that the solution of the LQ-optimal control problem is a stabilizing feedback operator. Hence, there exist $M_u, M_v > 0$ and $\alpha_u, \alpha_v < 0$ such that, in closed loop, for all $t \geq 0$,

$$\|u_b(t)\| \leq M_u e^{\alpha_u t}\|u_b(0)\|$$

and

$$\|v_1(t)\| \leq M_v e^{\alpha_v t}\|v_1(0)\|.$$

Since $x(t) = v_1(t) + B_b u_b(t)$ by (1.3.2), for all $t \geq 0$,

$$\|x(t)\| \leq M e^{\alpha t} r(x_0),$$

where

$$M := 2\max\{\|B_b\|M_u, M_v\} > 0,$$
$$\alpha := \max\{\alpha_u, \alpha_v\} < 0$$

and

$$r(x_0) := \max\{\|u_b(0)\|, \|v_1(0)\|\}.$$

Finally, since it has been shown that (1.3.2) holds for the closed-loop system, any dynamic compensator of the form (3.3.6) can be interpreted as a static feedback law of the form (3.3.4) for the extended system. Hence (3.3.6), where the k_{ij}, $i,j = 1,2$, form the optimal feedback operator, minimizes the cost (3.3.1). ■

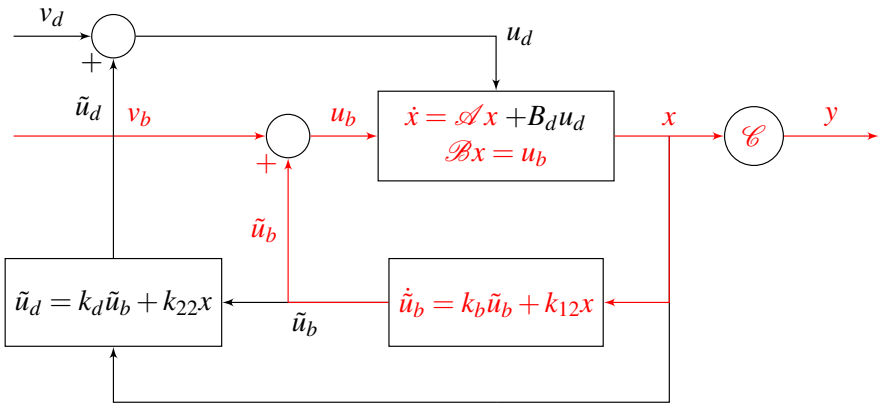

Figure 3.4: Dynamical interpretation of the LQ-optimal feedback with boundary and distributed control

Even though the proof has to be slightly adjusted due to the presence of the distributed control u_d, Theorem 3.3.1 can be seen as a corollary of Theorem 3.2.2, which is only valid with pure boundary control.

When distributed control is present in the model, the boundary control u_b plays the role of the state of the dynamic compensator (3.3.6), whereas the distributed control u_d is its output and the closed-loop nominal system becomes

$$\begin{cases} \dot{x}(t) &= (\mathscr{A} + k_{0_{22}})x(t) + B_d(k_{0_{21}} - k_{0_{22}}B_b)u_b(t), \\ \mathscr{B}x(t) &= u_b(t), \\ \dot{u}_b(t) &= (k_{0_{11}} - k_{0_{12}}B_b)u_b(t) + k_{0_{12}}x(t), \end{cases}$$

where the control input u_b now acts both in the boundary conditions and in the dynamics via a bounded operator and u_d is uniquely determined by u_b and x.

Part III

Applications: parabolic and hyperbolic systems

Chapter 4

Parabolic system

4.1 Description and analysis

This section introduces the parabolic convection-diffusion-reaction (CDR) system as an application, shows that it is a BCBO system and gives some of its main properties.

4.1.1 Description of the CDR system

The results of Part II are illustrated by a Sturm-Liouville system which is inspired by the literature and may correspond to a linearization around a stable or unstable equilibrium. The systems on which this application is based are notably useful for modeling chemical and biochemical reactors, see e.g. (Dramé et al. 2008) for an application to a biochemical reactor model, or (Winkin et al. 2000), (Delattre et al. 2003) for the analysis of distributed parameter tubular reactor models or Sturm-Liouville systems in general and their relation with Riesz-spectral systems.

Let us consider a convection-diffusion-reaction system with boundary control and observation of the form

$$\left\{\begin{array}{rcl} \frac{\partial x}{\partial t}(z,t) & = & D\frac{\partial^2 x}{\partial z^2}(z,t) - v\frac{\partial x}{\partial z}(z,t) - kx(z,t) + \chi_{[1-\varepsilon_u,1]}(z)u_d(t) \\ -D\frac{\partial x}{\partial z}(0,t) & = & v(u_b(t) - x(0,t)) \\ \frac{\partial x}{\partial z}(1,t) & = & 0 \\ x(z,0) & = & x_0(z) \\ y(t) & = & x(1,t) \end{array}\right. \tag{4.1.1}$$

where $t \geq 0$ and $z \in [0,1]$ denote the time and the spatial variable, respectively, D, v and k are the diffusion, convection and reaction parameters, respectively, and $\varepsilon_u \in [0,1]$ is a parameter which corresponds to the length of the distributed input window located at the end of the spatial domain. The parabolic equation describing the dynamics represents the conservation of mass in the system.

The stability of the CDR system (4.1.1) depends on the reaction parameter k. When the reaction rate is already linear, a negative reaction parameter makes no sense from a physical point of view, and a nonnegative reaction parameter leads to a stable system. However, for nonlinear CDR systems, a linearization around an unstable equilibrium profile can yield a system of the form (4.1.1) or a similar one with $k < 0$.
For example, in (Dramé et al. 2008), it is seen that CDR dynamics can be used to describe the evolution of substrate in a biochemical reactor. We consider a slightly modified system with a normalized length and where the boundary condition at 0 features the additional variable u_b, which is the actual control variable. The partial differential equations (PDE's) describing the dynamics of the system are given by

$$\left\{\begin{array}{rcl} \frac{\partial S}{\partial \tau}(\zeta,\tau) & = & D\frac{\partial^2 S}{\partial \zeta^2}(\zeta,\tau) - v\frac{\partial S}{\partial \zeta}(\zeta,\tau) - k\mu(S,X)X(\zeta,\tau) \\ \frac{\partial X}{\partial \tau}(\zeta,\tau) & = & -k_d X(\zeta,\tau) + \mu(S,X)X(\zeta,\tau) \end{array}\right.$$

with the boundary conditions

$$\left\{\begin{array}{rcl} -D\frac{\partial S}{\partial \zeta}(0,\tau) & = & v[(1-u_b(\tau))S_{\text{in}} - S(0,\tau)] \\ \frac{\partial S}{\partial \zeta}(1,t) & = & 0 \end{array}\right.$$

for all $\tau \geq 0$, where τ is the time variable, $\zeta \in [0,1]$ is the space variable, $S(\zeta,\tau)$ is the limiting substrate concentration and $X(\zeta,\tau)$ is the living biomass and S_{in} and k_d are positive parameters.
The substrate inhibition law is

$$\mu(S,X) = \mu_0 \frac{S}{K_S X + S + \frac{1}{K_i}S^2}$$

where μ_0, K_S and K_i are positive parameters.
In the first boundary condition, u_b can be seen as a control input used to regulate the inlet substrate concentration S_{in}.
An appropriate change of variables yields the following system of PDE's:

$$\left\{\begin{array}{rcl} \frac{\partial x_1}{\partial t}(z,t) & = & \frac{1}{P^e}\frac{\partial^2 x_1}{\partial z^2}(z,t) - \frac{\partial x_1}{\partial z}(z,t) - k\tilde{\mu}(x_1,x_2)x_2(z,t) \\ \frac{\partial x_2}{\partial t}(z,t) & = & -\gamma x_2(z,t) + \tilde{\mu}(x_1,x_2)x_2(z,t) \end{array}\right.$$

with the boundary conditions

$$\left\{\begin{array}{rcl} \frac{1}{P_e}\frac{\partial x_1}{\partial z}(0,t) & = & x_1(0,t) - u_b(t) \\ \frac{\partial x_1}{\partial z}(1,t) & = & 0 \end{array}\right.$$

for all $t \geq 0$, where $P_e = \dfrac{v}{D}$ is the Peclet number and $\gamma = \dfrac{k_d}{v}$. The modified substrate inhibition law is

$$\tilde{\mu}(x_1,x_2) = \beta \frac{1-x_1}{K_S x_2 + (1-x_1) + \alpha(1-x_1^2)}$$

where $\alpha = \dfrac{S_{\text{in}}}{K_i}$ and $\beta = \dfrac{\mu_0}{v}$.
In that paper, and more precisely in Proposition 4.1, it is shown that this system has at least two non trivial equilibria if D is sufficiently large and if v is sufficiently small. These equilibria can be computed as the solutions of a system composed of an algebraic equation and an ordinary differential equation (ODE) with initial and final conditions described by

$$\begin{cases} \dfrac{1}{P_e}\overline{x}_1'' - \overline{x}_1' + k\tilde{\mu}(\overline{x}_1,\overline{x}_2)\overline{x}_2 = 0 & (4.1.2) \\ -\gamma\overline{x}_2 + \tilde{\mu}(\overline{x}_1,\overline{x}_2)\overline{x}_2 = 0 & \\ \dfrac{1}{P_e}\overline{x}_1'(0) - \overline{x}_1(0) = 0 & (4.1.3) \\ \overline{x}_1'(1) = 0. & (4.1.4) \end{cases}$$

From the second equation, it can be seen that the non trivial solutions such that $\overline{x}_2 \neq 0$ satisfy

$$\tilde{\mu}(\overline{x}_1,\overline{x}_2) = \gamma$$

which yields the relationship

$$\overline{x}_2 = \frac{(1-\overline{x}_1)(M+\alpha k_d \overline{x}_1)}{k_d K_S} \tag{4.1.5}$$

where $M = \mu_0 - k_d - \alpha k_d < 0$.
Moreover, the corresponding modified substrate inhibition law equilibrium is

$$\tilde{\mu}(\overline{x}_1,\overline{x}_2) = \beta \frac{1-\overline{x}_1}{K_S\overline{x}_2 + (1-\overline{x}_1) + \alpha(1-\overline{x}_1^2)}.$$

Equation (4.1.5) can then be plugged into (4.1.2)-(4.1.4), which yields a second order nonlinear ODE in the variable $\overline{x}_1$.
It is also shown that at least one of these equilibria, around which the system can be linearized, is unstable, which motivates the choice for a negative reaction parameter for the CDR system considered in this chapter.

Both the cases $k \geq 0$ and $k < 0$ are considered in Section 4.3 for numerical simulations.

4.1.2 The CDR system as a BCBO system

This dynamical system can be interpreted as an abstract boundary control model with boundary observation described by (1.2.1)-(1.2.3). In this case, the operator $\mathscr{A} : D(\mathscr{A}) \subset X = L^2(0,1) \to L^2(0,1)$ is given by

$$\mathscr{A}x = D\frac{d^2x}{dz^2} - v\frac{dx}{dz} - kx$$

on its domain $D(\mathscr{A})$, which is defined as the set of all $x \in L^2(0,1)$ such that x and $\dfrac{dx}{dz}$ are absolutely continuous (a.c.), $\dfrac{d^2x}{dz^2} \in L^2(0,1)$ and $\dfrac{dx}{dz}(1) = 0$.
The distributed control operator $B_d : U_d = \mathbb{R} \to L^2(0,1)$ is given for all $u_d \in U_d$ and $z \in [0,1]$, by

$$(B_d u_d)(z) = \chi_{[1-\varepsilon_u,1]}(z) u_d \,, \tag{4.1.6}$$

where $\chi_{[1-\varepsilon_u,1]}$ denotes the characteristic function of the interval $[1-\varepsilon_u, 1]$. The boundary conditions correspond to the operator $\mathscr{B} : D(\mathscr{B}) \supset D(\mathscr{A}) \to U_b = \mathbb{R}$, which is given by

$$\mathscr{B}x = -\frac{D}{v}\frac{dx}{dz}(0) + x(0).$$

Finally, the boundary observation operator $\mathscr{C} : D(\mathscr{C}) \supset D(\mathscr{A}) \to Y = \mathbb{R}$ is given by

$$\mathscr{C}x = x(1).$$

It should be noted that the parameter ε_u is allowed to be zero, such that $B_d = 0$, resulting in a pure boundary control model.

It can be shown that this model is a BCBO system.
Indeed, it is well-known that condition **[C1]** holds, i.e. the operator $A : D(A) \to X = L^2(0,1)$ defined by $Ax = \mathscr{A}x$ for all x in its domain $D(A) = D(\mathscr{A}) \cap \text{ Ker } \mathscr{B}$ is the infinitesimal generator of a C_0-semigroup $(T(t))_{t\geq 0}$ of bounded linear operators on $X = L^2(0,1)$.
The operator A is given by $Ax = \mathscr{A}x$ for all $x \in D(A) = D(\mathscr{A}) \cap \text{Ker } \mathscr{B}$, where

$$\begin{aligned} D(A) \quad = \quad & \left\{ x \in L^2(0,1) : x, \frac{dx}{dz} \text{ are a. c., } \frac{d^2x}{dz^2} \in L^2(0,1), \right. \\ & \left. D\frac{dx}{dz}(0) - vx(0) = 0 = \frac{dx}{dz}(1) \right\}. \end{aligned}$$

Moreover condition **[C2]** holds, i.e. the operator $\mathscr{B}$ is onto, such that there exists a bounded linear operator $B_b \in \mathscr{L}(\mathbb{C}, L^2(0,1))$ such that for all $u \in U_b = \mathbb{C}$, $B_b u \in D(\mathscr{A})$, the operator $\mathscr{A}B_b \in \mathscr{L}(\mathbb{C}, L^2(0,1))$ and for all $u \in U_b = \mathbb{C}$, $\mathscr{B}B_b u = u$.
It can easily be checked that this condition is satisfied with the operator B_b defined as the multiplication operator by the unit step function, i.e.

$$B_b u = 1(\cdot)u,$$

where $1(z) \equiv 1$ on $[0,1]$.
Finally, by arguments similar to those used in (Deutscher 2013), it can be shown that the operator $\mathscr{C}$ is A-bounded. More precisely, it can be shown that there exists $f \in L^2(0,1)$ such that, for all $x \in D(A)$,

$$\mathscr{C}x = x(1) = \langle f, (I - A)x \rangle. \tag{4.1.7}$$

Such a function f is given by

$$f = \sum_{n=1}^{+\infty} \frac{1}{1-\lambda_n} \psi_n(1)\phi_n,$$

where $(\phi_n)_{n\in\mathbb{N}}$ is a Riesz basis of eigenvectors of the operator A, $(\psi_n)_{n\in\mathbb{N}}$ is a corresponding dual Riesz basis such that the vectors ϕ_n and ψ_n are bi-orthonormal, and the real numbers λ_n are the eigenvalues of A. Then inequality (1.2.4) can be easily derived from (4.1.7). Hence condition (**C3**) holds.
It follows that the analysis and all the results of Part II are applicable to this model.

4.1.3 Analysis

The spectral properties of the operator A will be useful in the sequel and are recalled here. Since any Sturm-Liouville system is a Riesz-spectral system (Delattre et al. 2003), it is expected that the spectrum is real and discrete, and well-conditioned for the proposed methodology.
In fact, it is known that the eigenvalues $(\lambda_n)_{n\geq 1}$ of A are given for all $n \geq 1$ by

$$\lambda_n = -\frac{s_n^2 + v^2}{4D} - k \tag{4.1.8}$$

where the s_n, $n \geq 1$, are the solutions of the resolvent equation

$$\tan\left(\frac{s}{2D}\right) = \frac{2vs}{s^2 - v^2}, \quad s \in \mathbb{R}, \quad s > 0. \tag{4.1.9}$$

The Riesz basis of eigenvectors is given by $\{\phi_n : n \in \mathbb{N}_0\}$, where, for all $n \in \mathbb{N}_0$ and for all $z \in [0,1]$,

$$\phi_n(z) = K_n e^{\frac{v}{2D}z}\left[\cos\left(\frac{s_n}{2D}z\right) + \frac{v}{s_n}\sin\left(\frac{s_n}{2D}z\right)\right] \tag{4.1.10}$$

and the corresponding dual Riesz basis is $\{\psi_n : n \in \mathbb{N}_0\}$, where, for all $n \in \mathbb{N}_0$ and for all $z \in [0,1]$,

$$\psi_n(z) = K_n e^{-\frac{v}{2D}z}\left[\cos\left(\frac{s_n}{2D}z\right) + \frac{v}{s_n}\sin\left(\frac{s_n}{2D}z\right)\right].$$

In order to make this analysis complete, we study the reachability and stabilizability properties of the CDR system. First, we state the following lemma which shows that the pair (A, B_d) is reachable for an appropriate choice of the parameter ε_u.

Lemma 4.1.1 *Consider a CDR system with boundary control and observation described by (4.1.1). Assume that the distributed control operator B_d is given by (4.1.6), where the window width is*

$$\varepsilon_u := \frac{2}{j} \tag{4.1.11}$$

with $j \in \mathbb{N}_0$.
Then the pair (A, B_d) is reachable.

Proof. It is known (see (Winkin et al. 2000)) that the operator A is self-adjoint with respect to the equivalent inner product $\langle \cdot, \cdot \rangle_\rho$ defined for all $f, g \in L^2(0,1)$ by

$$\langle f, g \rangle_\rho = \int_0^1 e^{-\frac{v}{D}z} f(z) \overline{g(z)} dz, \tag{4.1.12}$$

and its eigenvectors $(\phi_n)_{n \in \mathbb{N}_0}$ form an orthonormal basis of $L^2(0,1)$ equiped with this inner product.
By (Curtain and Zwart 1995), the CDR system (4.1.1) is reachable if and only if for all $n \in \mathbb{N}_0$,

$$\langle b_d, \phi_n \rangle_\rho \neq 0, \tag{4.1.13}$$

where $b_d = \chi_{[1-\varepsilon_u, 1]}(\cdot)$.
Since for all $n \in \mathbb{N}_0$, ϕ_n is given by (4.1.10), two successive integrations by parts reveal that

$$\begin{aligned}
\langle b_d, \phi_n \rangle_\rho &= \int_0^1 e^{-\frac{v}{D}z} \chi_{[1-\varepsilon_u, 1]}(z) K_n e^{\frac{v}{2D}z} \left[\cos\left(\frac{s_n}{2D} z\right) + \frac{v}{s_n} \sin\left(\frac{s_n}{2D} z\right) \right] dz \\
&= K_n \int_{1-\varepsilon_u}^1 e^{-\frac{v}{2D}z} \left[\cos\left(\frac{s_n}{2D} z\right) + \frac{v}{s_n} \sin\left(\frac{s_n}{2D} z\right) \right] dz \\
&= \left[-K_n \frac{2D}{v} e^{-\frac{v}{2D}z} \left[2\cos\left(\frac{s_n}{2D} z\right) + \frac{v^2 - s_n^2}{v s_n} \sin\left(\frac{s_n}{2D} z\right) \right] \right]_{1-\varepsilon_u}^1 \\
&\quad -K_n \frac{s_n^2}{v^2} \int_{1-\varepsilon_u}^1 e^{-\frac{v}{2D}z} \left[\cos\left(\frac{s_n}{2D} z\right) + \frac{v}{s_n} \sin\left(\frac{s_n}{2D} z\right) \right] dz. \\
&= \left[-K_n \frac{2D}{v} e^{-\frac{v}{2D}z} \left[2\cos\left(\frac{s_n}{2D} z\right) + \frac{v^2 - s_n^2}{v s_n} \sin\left(\frac{s_n}{2D} z\right) \right] \right]_{1-\varepsilon_u}^1 \\
&\quad -\frac{s_n^2}{v^2} \langle b_d, \phi_n \rangle_\rho .
\end{aligned}$$

Hence,

$$\langle b_d, \phi_n \rangle_\rho = K_n \frac{v^2}{v^2 + s_n^2} \left[-\frac{2D}{v} e^{-\frac{v}{2D}z} \left[2\cos\left(\frac{s_n}{2D} z\right) + \frac{v^2 - s_n^2}{v s_n} \sin\left(\frac{s_n}{2D} z\right) \right] \right]_{1-\varepsilon_u}^1,$$

which shows that (4.1.13) is equivalent to

$$\left[e^{-\frac{v}{2D}z} \left[\frac{s_n^2 - v^2}{v s_n} \sin\left(\frac{s_n}{2D} z\right) - 2\cos\left(\frac{s_n}{2D} z\right) \right] \right]_{1-\varepsilon_u}^1 \neq 0.$$

Let us assume that there exists $n \in \mathbb{N}_0$ such that $\langle b, \phi_n \rangle_\rho = 0$.
Since the parameters s_n are the solutions of (4.1.9), it is easy to see that

$$e^{-\frac{v}{2D}} \left[\frac{s_n^2 - v^2}{v s_n} \sin\left(\frac{s_n}{2D}\right) - 2\cos\left(\frac{s_n}{2D}\right) \right] = 0.$$

By using (4.1.9) again, it follows that

$$\begin{aligned}
\langle b, \phi_n \rangle_\rho = 0 \quad &\Leftrightarrow \quad e^{-\frac{v}{2D}(1-\varepsilon_u)} \left[\frac{s_n^2 - v^2}{v s_n} \sin\left(\frac{s_n}{2D}(1-\varepsilon_u)\right) - 2\cos\left(\frac{s_n}{2D}(1-\varepsilon_u)\right) \right] = 0 \\
&\Leftrightarrow \quad \frac{s_n^2 - v^2}{v s_n} \sin\left(\frac{s_n}{2D}(1-\varepsilon_u)\right) - 2\cos\left(\frac{s_n}{2D}(1-\varepsilon_u)\right) = 0 \\
&\Leftrightarrow \quad \tan\left(\frac{s_n}{2D}(1-\varepsilon_u)\right) = \frac{2 v s_n}{s_n^2 - v^2} \\
&\Leftrightarrow \quad \tan\left(\frac{s_n}{2D}(1-\varepsilon_u)\right) = \tan\left(\frac{s_n}{2D}\right).
\end{aligned}$$

The last assertion holds if and only if there exists $m \in \mathbb{Z}$ such that

$$\frac{s_n}{2D}(1-\varepsilon_u) + m\pi = \frac{s_n}{2D},$$

or equivalently

$$\varepsilon_u s_n = 2Dm\pi,$$

i.e., in view of (4.1.11), $s_n = Dmj\pi$, where $mj \in \mathbb{Z}$.
It follows that

$$\frac{2 v s_n}{s_n^2 - v^2} = \tan\left(\frac{s_n}{2D}\right) = \tan\left(mj\frac{\pi}{2}\right).$$

The rightmost term of this equality is either zero if mj is even or undefined if mj is odd.
In any case, this is in contradiction with the fact that $s_n > 0$ and $v > 0$.

■

This result implies that the distributed control window for the CDR system, when located at the end of the spatial domain, can be chosen arbitrarily small while maintaining reachability.
The following result gives some sufficient conditions for the reachability and stabilizability of the extended CDR system.

Proposition 4.1.2 *a) If $0 \in \rho(A)$, the extended CDR system, i.e. the pair (A^e, B^e), is stabilizable.*

b) Under the assumptions of Lemma 4.1.1, the extended CDR system, i.e. the pair (A^e, B^e), is reachable.

Proof. a) Let us define $b = 1(\cdot)$. After two successive integrations by parts and by using the fact that the parameters s_n are the solutions of (4.1.9), we see that, for all

$n \in \mathbb{N}$,

$$\begin{aligned}
\langle b, \phi_n \rangle_\rho &= \int_0^1 e^{-\frac{v}{D}z} 1(z) K_n e^{\frac{v}{2D}z} \left[\cos\left(\frac{s_n}{2D}z\right) + \frac{v}{s_n} \sin\left(\frac{s_n}{2D}z\right) \right] dz \\
&= K_n \int_0^1 e^{-\frac{v}{2D}z} \left[\cos\left(\frac{s_n}{2D}z\right) + \frac{v}{s_n} \sin\left(\frac{s_n}{2D}z\right) \right] dz \\
&= K_n \frac{v^2}{v^2+s_n^2} \left[-\frac{2D}{v} e^{-\frac{v}{2D}z} \left[2\cos\left(\frac{s_n}{2D}z\right) + \frac{v^2-s_n^2}{vs_n} \sin\left(\frac{s_n}{2D}z\right) \right] \right]_0^1 \\
&= K_n \frac{v^2}{v^2+s_n^2} \left[\frac{2D}{v} e^{-\frac{v}{2D}} \left[\frac{s_n^2-v^2}{vs_n} \sin\left(\frac{s_n}{2D}z\right) - 2\cos\left(\frac{s_n}{2D}z\right) \right] - \frac{2D}{v}(-2) \right] \\
&= K_n \frac{4Dv}{v^2+s_n^2} \\
&\neq 0 \qquad (4.1.14)
\end{aligned}$$

where the weighted scalar product $\langle \cdot, \cdot \rangle_\rho$ is defined by (4.1.12).
Since A is a self-adjoint Riesz-spectral operator with respect to this scalar product, we deduce from (Curtain and Zwart 1995, Theorem 5.2.9, p. 237) that the pair (A, B_b) is stabilizable.
Now, we compute Ker $\begin{pmatrix} 0 & sI - A^* \end{pmatrix}$ for $s \in \overline{\mathbb{C}_0^+}$. We see that

$$\begin{aligned}
\begin{pmatrix} 0 & sI - A^* \end{pmatrix} \begin{pmatrix} x_1^e \\ x_2^e \end{pmatrix} = 0 \quad &\Leftrightarrow \quad A^* x_2^e = s x_2^e \\
&\Leftrightarrow \quad s = \lambda_n \quad \text{and} \quad x_2^e = \psi_n \qquad (4.1.15)
\end{aligned}$$

for some $n \in \mathbb{N}_0$.
If $s \neq \lambda_n$ for all $n \in \mathbb{N}_0$, it follows immediately that condition (3.2.12) holds.
Let us now assume that $s = \lambda_n \geq 0$ for some $n \in \mathbb{N}_0$. Let us consider $(x_1^e \ x_2^e)^T \in U_b \oplus X$ such that

$$\begin{pmatrix} x_1^e \\ x_2^e \end{pmatrix} \in \text{Ker } \begin{pmatrix} sI & (\mathscr{A}B_b)^* \end{pmatrix} \cap \text{Ker } \begin{pmatrix} 0 & sI - A^* \end{pmatrix} \cap \text{Ker } \begin{pmatrix} I & -B_b^* \end{pmatrix}.$$

If $x_2^e = 0$, it is easy to see that $x_1^e = 0$ as well and (3.2.12) holds. Otherwise, by (4.1.15), we have that $x_2^e = \psi_n$.
Moreover, since for all $u_b \in U_b$, $B_b u_b = 1(\cdot)$ and $\mathscr{A}B_b = -kB_b$, we see that

$$\begin{aligned}
&\begin{pmatrix} x_1^e \\ x_2^e \end{pmatrix} \in \text{Ker } \begin{pmatrix} sI & (\mathscr{A}B_b)^* \end{pmatrix} \cap \text{Ker } \begin{pmatrix} 0 & sI - A^* \end{pmatrix} \cap \text{Ker } \begin{pmatrix} I & -B_b^* \end{pmatrix} \\
\Leftrightarrow \quad &\begin{pmatrix} \lambda_n I & (\mathscr{A}B_b)^* \end{pmatrix} \begin{pmatrix} x_1^e \\ \psi_n \end{pmatrix} = 0 \quad \text{and} \quad \begin{pmatrix} I & -B_b^* \end{pmatrix} \begin{pmatrix} x_1^e \\ \psi_n \end{pmatrix} = 0 \\
\Leftrightarrow \quad &\lambda_n x_1^e - k B_b^* \psi_n = 0 \quad \text{and} \quad x_1^e - B_b^* \psi_n = 0 \\
\Rightarrow \quad &(\lambda_n - k) B_b^* \psi_n = 0,
\end{aligned}$$

which implies that

$$B_b^* \psi_n = 0 \qquad (4.1.16)$$

since $\lambda_n \neq k$.
But, by (4.1.14), it is also easy to see that

$$\begin{aligned} B_b^* \psi_n &= \int_0^1 \psi_n(z) dz \\ &= K_n \int_0^1 e^{-\frac{v}{2D}z} \left[\cos\left(\frac{s_n}{2D}z\right) + \frac{v}{s_n} \sin\left(\frac{s_n}{2D}z\right) \right] dz \\ &\neq 0, \end{aligned}$$

which is in contradiction with (4.1.16).
Hence x_2^e cannot be equal to ψ_n for some $n \in \mathbb{N}_0$ and must be zero, which shows that (3.2.12) holds in any case.
Since $0 \in \rho(A)$ by assumption and the pair (A, B_b) is stabilizable, it follows from Remark 2 that the pair $(\tilde{A}^e, \tilde{B}^e)$ given by (2.1.1) is stabilizable as well.
Finally, the conclusion follows by an argument similar to the one used in the proof of Proposition 2.1.2.

b) The result follows directly from Lemma 4.1.1 and Proposition 2.1.2. ■

It is interesting to notice that the proof of the stabilizability of the extended CDR system only depends on the operator B_b. This property can be established with boundary control only, i.e. when $B_d = 0$, even though the presence of a distributed input can make the choice of a stabilizing feedback easier provided that the pair (A, B_d) is stabilizable.

In view of the results stated in Part II, the LQ-optimal control problem is well-posed and solvable for CDR systems described by (4.1.1). This problem has been studied in e.g. (Mohammadi, Aksikas, Dubljevic and Forbes 2012).

Remark 3 *This part of the work focuses on the stabilizability analysis and the design of a stabilizing control law for the (extended) CDR system, which is useful for many applications, such as the chemical and biochemical reactors mentioned at the beginning of the chapter. However, it should be noted that the analysis of instabilities turns out to be very important for other applications based on CDR dynamics.*
A notable example is the study of Turing instabilities in diffusion-reaction processes where homogeneous equilibrium solutions can be destabilized with small inhomogeneous perturbations, leading the system to reach a spatially inhomogeneous equilibrium.
In particular, a topic of interest is the role of diffusion-reaction dynamics in pattern formation, including for example the processes in morphogenesis that lead to these patterns on animal skin or coat due to pigmentation.
Typically, such processes involve at least two interconnected diffusion-reaction equations of the form

$$\begin{cases} \frac{\partial x_1}{\partial t} &= f_1(x_1, x_2) + D_1 \frac{\partial^2 x_1}{\partial z} \\ \frac{\partial x_2}{\partial t} &= f_2(x_1, x_2) + D_2 \frac{\partial^2 x_2}{\partial z} \end{cases}$$

for all $t \geq 0$ on an interval $[0,L]$, or

$$\begin{cases} \frac{\partial x_1}{\partial t} &= f_1(x_1,x_2) + D_1^{(z_1)} \frac{\partial^2 x_1}{\partial z_1} + D_1^{(z_2)} \frac{\partial^2 x_1}{\partial z_2} \\ \frac{\partial x_2}{\partial t} &= f_2(x_1,x_2) + D_2^{(z_1)} \frac{\partial^2 x_2}{\partial z_1} + D_2^{(z_2)} \frac{\partial^2 x_2}{\partial z_2} \end{cases}$$

on a rectangular domain $[0,L_1] \times [0,L_2]$, where f_1 and f_2 are in general nonlinear functions and where the diffusion coefficients may be anisotropic, i.e. depend on the specific direction of migration, in the latter case.
In that context, a potential perspective could be the design of destabilizing control laws such that the system reaches an inhomogeneous equilibrium corresponding to a given pattern of interest.
See e.g. (Busiello, Planchon, Asllani, Carletti and Fanelli 2015) for a recent in depth analysis of pattern formation with interacting reactive species subject to anisotropic diffusion.

4.2 Comparison between the extended and nominal CDR system

In this section, we show that the results stated in section 2.2 can be applied to the CDR system. The main result states that the transfer function and approximate output of the extended system converge to the transfer function and output of the nominal system respectively, for almost every non negative time. This result motivates the use of the extended system in view of the resolution of a LQ-optimal control problem and the replacement of y by its Yosida approximation y_α in the cost functional for the CDR system.

Proposition 4.2.1 *The convection-diffusion-reaction system (4.1.1) is such that*

a) for all $s \in \rho(A)$,

$$\lim_{\alpha \to +\infty} \hat{\tilde{G}}^e_\alpha(s) = \hat{G}(s)$$

and

b) for a.e. $t \geq 0$, $y_\alpha(t) = C_\alpha x(t)$ converges in $\mathbb{C}$ as α goes to $+\infty$, and

$$\lim_{\alpha \to +\infty} y_\alpha(t) = \lim_{\alpha \to +\infty} C_\alpha x(t) = x(1,t).$$

Proof: The transfer function of the convection-diffusion-reaction system (4.1.1) is given by $\hat{G}(s) = \begin{pmatrix} \hat{G}_1(s) & \hat{G}_2(s) \end{pmatrix}$ where

$$\begin{aligned} \hat{G}_1(s) &= \mathscr{C}(sI - A)^{-1}(\mathscr{A}B_b - sB_b) + \mathscr{C}B_b \\ &= \frac{ve^{\frac{v}{2D}}\sqrt{\rho}}{g(s,1)} \end{aligned}$$

and

$$\begin{aligned}\hat{G}_2(s) &= \mathscr{C}(sI-A)^{-1}B_d \\ &= -\frac{e^{\frac{v}{2D}\varepsilon_u}}{s+k}\frac{g(s,1-\varepsilon_u)}{g(s,1)}+\frac{1}{s+k}\end{aligned}$$

with $\rho := \rho(s) := v^2+4D(k+s)$ and

$$g(s,z) = [v^2+2D(k+s)]\sinh\left(z\frac{\sqrt{\rho(s)}}{2D}\right)+v\sqrt{\rho(s)}\cosh\left(z\frac{\sqrt{\rho(s)}}{2D}\right).$$

This transfer function is strictly proper and thus admits a strong limit at $+\infty$ along the real axis, i.e. for all $(u_b,u_d)\in\mathbb{C}\oplus\mathbb{C}$,

$$\hat{G}(s)\,(u_b\,,u_d)^T = \hat{G}_1(s)u_b+\hat{G}_2(s)u_d \to 0$$

as $|s|\to+\infty$.
The input-output transfer function $\hat{\tilde{G}}^e_\alpha$ of the extended system defined by

$$\hat{y}_\alpha(s) = \hat{\tilde{G}}^e_\alpha(s)\,(\hat{u}_b(s)\,,\hat{u}_d(s))^T$$

for all $s\in\mathbb{C}$ is given by

$$\hat{\tilde{G}}^e_\alpha(s) = \begin{pmatrix}\hat{\tilde{G}}^e_{\alpha 1}(s) & \hat{\tilde{G}}^e_{\alpha 2}(s)\end{pmatrix}$$

where

$$\hat{\tilde{G}}^e_{\alpha_i}(s) = \frac{\alpha}{s-\alpha}[\hat{G}_i(\alpha)-\hat{G}_i(s)],$$

$i=1,2$, by the resolvent identity, see (Jacob and Zwart 2012, Proposition 5.2.4, p. 59).
Since

$$\lim_{\alpha\to+\infty}\mathscr{C}(\alpha I-A)^{-1}B_b = \lim_{\alpha\to+\infty}\mathscr{C}(\alpha I-A)^{-1}B_d = 0$$

and

$$\lim_{\alpha\to+\infty}C_\alpha B_b = \lim_{\alpha\to+\infty}\frac{\alpha}{k+\alpha}\left[-\frac{ve^{\frac{v}{2D}}\sqrt{\rho(\alpha)}}{g(\alpha,1)}+1\right] = 1,$$

it is easy to see that for all $s\in\mathbb{C}$,

$$\lim_{\alpha\to+\infty}\hat{\tilde{G}}^e_\alpha(s) = \hat{G}(s).$$

Now we show that the operators $(\mathscr{A}-A)B_b$ and $\mathscr{C}$ are admissible for $(T(t))_{t\geq 0}$. Since A is a Riesz-spectral operator, it is diagonalizable, i.e. isomorphic to a diagonal operator on l^2, see (Tucsnak and Weiss 2009, Section 2.6, pp. 49–56). This isomorphism is $Q\in\mathscr{L}(L^2(0,1),l^2)$, which is defined by

$$Qx = (\langle x,\psi_n\rangle)_{n\in\mathbb{N}_0}$$

for all $x \in L^2(0,1)$. Obviously, for all $n \geq 1$, $Q\phi_n = e_n$, where $\{e_n : n \in \mathbb{N}_0\}$ is the canonical basis of l^2. By this similarity transformation, the operator A can be seen as the diagonal operator $\tilde{A} : D(\tilde{A}) \subset l^2 \to l^2$ defined by

$$\tilde{A}w = (\lambda_n w_n)_{n\in\mathbb{N}_0}$$

for all $w \in D(\tilde{A})$, where

$$D(\tilde{A}) = \left\{ w \in l^2 : \sum_{n\in\mathbb{N}_0} (1+\lambda_n^2)|w_n|^2 < +\infty \right\}.$$

The operator $\mathscr{C} \in \mathscr{L}(X_1, \mathbb{C})$ can be seen as the operator $\tilde{\mathscr{C}} \in \mathscr{L}(l_1^2, \mathbb{C})$ defined by

$$\begin{aligned} \tilde{\mathscr{C}}w &= \langle w, \overline{c} \rangle \\ &= \sum_{n\in\mathbb{N}_0} c_n w_n \\ &= \sum_{n\in\mathbb{N}_0} \phi_n(1) w_n \end{aligned}$$

for all $w \in l_1^2$, where the sequence $(c_n)_{n\in\mathbb{N}_0} = (\phi_n(1))_{n\in\mathbb{N}_0} \in l_{-1}^2$.
We show that this sequence satisfies the Carleson measure criterion (see e.g. (Tucsnak and Weiss 2009, Definition 5.3.1., p. 159)) for the sequence $(\lambda_n)_{n\in\mathbb{N}_0}$, i.e. there exists $M > 0$ such that for all $h > 0$ and $\omega \in \mathbb{R}$,

$$\sum_{-\overline{\lambda}_n \in R(h,\omega)} |c_n|^2 \leq Mh, \tag{4.2.1}$$

where

$$R(h,\omega) = \{s \in \mathbb{C} : 0 < \operatorname{Re} s \leq h, |\operatorname{Im} s - \omega| \leq h\}.$$

This can be interpreted as the fact that the sum of the $|c_n|^2$ over all eigenvalues belonging to any rectangle centred around the real axis in the left-half plane is bounded by a value proportional to the height of the rectangle. Moreover, the discrete measure on $\mathbb{C}_0$ with weights $|c_n|^2$ in the points $-\overline{\lambda}_n$ is a Carleson measure (see e.g. (Tucsnak and Weiss 2009, The Carleson measure theorem, p. 406)). This criterion guarantees the admissibility of the equivalent observation operator $\tilde{\mathscr{C}}$.
Let $h > 0$ and $\omega \in \mathbb{R}$. Since all the eigenvalues of A are real, we see that, if $|\omega| > h$, then, for all $n \in \mathbb{N}_0$, $-\overline{\lambda}_n = -\lambda_n \notin R(h,\omega)$ and

$$\sum_{-\overline{\lambda}_n \in R(h,\omega)} |c_n|^2 = 0.$$

If $|\omega| \leq h$, then $-\overline{\lambda}_n = -\lambda_n \in R(h,\omega)$ if and only if $-\lambda_n \leq h$, which is true if and only if

$$s_n^2 \leq 4Dh - 4Dk - v^2.$$

Since the sequence $(s_n)_{n\in\mathbb{N}_0}$ is such that for all $n\in\mathbb{N}_0$, $s_{n+1}\geq s_n>0$, we can distinguish three cases.

1) If $h<\dfrac{s_1^2+v^2}{4D}+k$, then the condition $-\overline{\lambda}_n\in R(h,\omega)$ is never fulfilled, hence

$$\sum_{-\overline{\lambda}_n\in R(h,\omega)}|c_n|^2=0. \tag{4.2.2}$$

2) If $\dfrac{s_1^2+v^2}{4D}+k\leq h<\dfrac{s_2^2+v^2}{4D}+k$, then one observes that $-\overline{\lambda}_1=-\lambda_1\in R(h,\omega)$ and for all $n\geq 2$, $-\overline{\lambda}_n=-\lambda_n\notin R(h,\omega)$. Hence,

$$\sum_{-\overline{\lambda}_n\in R(h,\omega)}|c_n|^2=|c_1|^2=|\phi_1(1)|^2. \tag{4.2.3}$$

Observe that, by (4.1.10), for all $n\in\mathbb{N}_0$,

$$\begin{aligned}
|\phi_n(1)|^2 &= \left|K_n e^{\frac{v}{2D}}\left(\cos\frac{s_n}{2D}+\frac{v}{s_n}\sin\frac{s_n}{2D}\right)\right|^2\\
&= |K_n|^2 e^{\frac{v}{D}}\left(\cos\frac{s_n}{2D}\right)^2+\frac{2v}{s_n}\left(\cos\frac{s_n}{2D}\right)\left(\sin\frac{s_n}{2D}\right)+\frac{v^2}{s_n^2}\left(\sin\frac{s_n}{2D}\right)^2\\
&\leq |K_n|^2 e^{\frac{v}{D}}\left(1+\frac{2v}{s_n}+\frac{v^2}{s_n^2}\right)\\
&\leq e^{\frac{v}{D}}\sup_{i\in\mathbb{N}_0}|K_i|^2\left(1+\frac{2v}{s_1}+\frac{v^2}{s_1^2}\right)
\end{aligned} \tag{4.2.4}$$

since $(K_n)_{n\in\mathbb{N}_0}$ is a bounded sequence and for all $n\in\mathbb{N}_0$, $s_n\geq s_1>0$. Moreover,

$$h\geq\frac{s_1^2+v^2}{4D}+k>\frac{v^2}{4D}+k. \tag{4.2.5}$$

From (4.2.3), (4.2.4) and (4.2.5), we deduce that

$$\sum_{-\overline{\lambda}_n\in R(h,\omega)}|c_n|^2\leq m\leq\frac{m}{K}h \tag{4.2.6}$$

where

$$m=e^{\frac{v}{D}}\sup_{n\in\mathbb{N}_0}|K_n|^2\left(1+\frac{2v}{s_1}+\frac{v^2}{s_1^2}\right)$$

and

$$K=\frac{v^2}{4D}+k.$$

3) If $\frac{s_2^2+v^2}{4D}+k\leq h$, observe that, for all $n\geq 2$, $\frac{s_n}{2D\pi}\geq 1$ since $2D(n-1)\pi\leq s_n\leq 2Dn\pi$, which implies that for all $n\geq 2$,

$$\frac{s_n}{2D\pi}\leq\frac{s_n^2}{4D^2\pi^2}.$$

Now, we see that

$$\begin{aligned}
\sum_{-\overline{\lambda}_n\in R(h,\omega)}|c_n|^2 &= \sum_{s_n^2\leq 4Dh-4Dk-v^2}|\phi_n(1)|^2\\
&\leq \sum_{s_n^2\leq 4Dh}|\phi_n(1)|^2\\
&= \sum_{\frac{s_n^2}{4D^2\pi^2}\leq\frac{1}{D\pi^2}h}|\phi_n(1)|^2\\
&\leq \sum_{\frac{s_n}{2D\pi}\leq\frac{1}{D\pi^2}h}|\phi_n(1)|^2\\
&= \sum_{s_n\leq\frac{2}{pi}h}|\phi_n(1)|^2\\
&\leq \sum_{2D(n-1)\pi\leq\frac{2}{pi}h}|\phi_n(1)|^2\\
&= \sum_{n\leq\frac{h}{D\pi^2}+1}|\phi_n(1)|^2\\
&\leq \left\lfloor\frac{h}{D\pi^2}+1\right\rfloor m\\
&\leq \frac{m}{D\pi^2}h+m\\
&\leq \frac{m}{D\pi^2}h+\frac{m}{K}h\\
&= \left(\frac{m}{D\pi^2}+\frac{m}{K}\right)h, \qquad (4.2.7)
\end{aligned}$$

where $\left\lfloor\frac{h}{D\pi^2}+1\right\rfloor$ is the integer part of $\frac{h}{D\pi^2}+1$.

Finally, combining (4.2.2), (4.2.6) and (4.2.7), one concludes that there exists $M=\frac{m}{D\pi^2}+\frac{m}{K}>0$, which is independant of h and ω, such that (4.2.1) holds.
Since $(T(t))_{t\geq 0}$ is an exponentially stable C_0-semigroup, it follows from (Tucsnak and Weiss 2009, Theorem 5.3.2., p. 159) and (Tucsnak and Weiss 2009, Remark 5.3.4., p. 162) that $\mathscr{C}$ is an admissible observation operator for $(T(t))_{t\geq 0}$.

In order to show that $(\mathscr{A}-A)B_b$ is an admissible control operator for $(T(t))_{t\geq 0}$, we

show that its adjoint $[(\mathscr{A}-A)B_b]^*$ is an admissible observation operator for $(T(t)^*)_{t\geq 0}$. Let us consider again the operator $\tilde{A}$ and observe that it is a self-adjoint operator. Now we compute $[(\mathscr{A}-A)B_b]^*$ by using the identity

$$\langle \mathscr{A}x,\psi\rangle = \langle x,A^*\psi\rangle + \langle \mathscr{B}x,[(\mathscr{A}-A)B_b]^*\psi\rangle$$

for all $x\in D(\mathscr{A})$, $\psi\in D(A^*)$, see (Tucsnak and Weiss 2009, Remark 10.1.6., p. 330). In this case, the operator $A^*: D(A^*)\subset L^2(0,1)\to L^2(0,1)$ is given by

$$A^*x = D\frac{d^2x}{dz^2}+v\frac{dx}{dz}-kx$$

for all $x\in D(A^*)$, where

$$\begin{aligned} D(A^*) &= \left\{ x\in L^2(0,1) : x, \frac{dx}{dz} \text{ are a. c., } \frac{d^2x}{dz^2}\in L^2(0,1),\right. \\ &\quad \left. \frac{dx}{dz}(0)=0=D\frac{dx}{dz}(1)+vx(1)\right\}. \end{aligned}$$

Using integration by parts and the conditions of $D(\mathscr{A})$ and $D(A^*)$, we obtain

$$\begin{aligned} \langle \mathscr{A}x,\psi\rangle - \langle x,A^*\psi\rangle &= \int_0^1 \left[D\frac{d^2x}{dz^2}(z)-v\frac{dx}{dz}(z)-kx(z)\right]\overline{\psi(z)}dz \\ &\quad -\int_0^1 x(z)\overline{\left[D\frac{d^2\psi}{dz^2}(z)+v\frac{d\psi}{dz}(z)-k\psi(z)\right]}dz \\ &= D\int_0^1\left[\frac{d^2x}{dz^2}(z)\overline{\psi(z)}-x(z)\overline{\frac{d^2\psi}{dz^2}(z)}\right]dz \\ &\quad -v\int_0^1\left[\frac{dx}{dz}(z)\overline{\psi(z)}+x(z)\overline{\frac{d\psi}{dz}(z)}\right]dz \\ &= D\left[\frac{dx}{dz}(z)\overline{\psi(z)}\right]_0^1 - D\left[x(z)\overline{\frac{d\psi}{dz}(z)}\right]_0^1 - v\int_0^1\frac{dx}{dz}(z)\overline{\psi}dz \\ &= D\frac{dx}{dz}(1)\overline{\psi(1)}+Dx(0)\overline{\frac{d\psi}{dz}(0)}-x(1)\left[D\overline{\frac{d\psi}{dz}(1)}+v\overline{\psi(1)}\right] \\ &\quad +\left[-D\frac{dx}{dz}(0)+vx(0)\right]\overline{\psi(0)} \\ &= \left[-\frac{D}{v}\frac{dx}{dz}(0)+x(0)\right]v\overline{\psi(0)} \end{aligned} \tag{4.2.8}$$

for all $x\in D(\mathscr{A})$, $\psi\in D(A^*)$. But (4.2.8) should be equal to

$$\langle \mathscr{B}x,[(\mathscr{A}-A)B_b]^*\psi\rangle = \left[-\frac{D}{v}\frac{dx}{dz}(0)+x(0)\right]\overline{[(\mathscr{A}-A)B_b]^*\psi}.$$

Hence, for all $\psi \in D(A^*)$,

$$[(\mathscr{A}-A)B_b]^*\psi = v\psi(0).$$

The corresponding observation operator on l^2 is $\tilde{B} \in \mathscr{L}(l_1^2, \mathbb{C})$ defined by

$$\begin{aligned} \tilde{B}w &= \langle w, \overline{b} \rangle \\ &= \sum_{n\in\mathbb{N}_0} b_n w_n \\ &= \sum_{n\in\mathbb{N}_0} v\phi_n(0) w_n \end{aligned}$$

for all $w \in l_1^2$, where the sequence $(b_n)_{n\in\mathbb{N}_0} = (v\phi_n(0))_{n\in\mathbb{N}_0} \in l_{-1}^2$.
By an analysis similar to the one performed previously for the operator $\mathscr{C}$, one can show that the sequence $(b_n)_{n\in\mathbb{N}_0}$ satisfies the Carleson measure criterion for the sequence $(\lambda_n)_{n\in\mathbb{N}_0}$ with

$$\tilde{M} = \frac{\tilde{m}}{D\pi^2} + \frac{\tilde{m}}{K} > 0,$$

where

$$\tilde{m} = v \sup_{n\in\mathbb{N}_0} |K_n|^2.$$

Hence $(\mathscr{A}-A)B_b$ is an admissible control operator for $(T(t))_{t\geq 0}$.
The conclusion then follows from Proposition 2.2.1. ■

4.3 Numerical results

4.3.1 Numerical process and algorithm

This section provides an algorithm for the resolution of the LQ-optimal control problem via spectral factorization and gives some numerical results for stable and unstable convection-diffusion-reaction systems. The adaptability of the theory developped in Part II is demonstrated again since a LQ-optimal control problem is posed and solved for this class of systems with and without distributed control.
This problem is solved numerically by computing successively the eigenvalues of the operator A, the zeros of the spectral density and the spectral factors and by solving the diophantine equation with a residue computation.
Even though this process is described and illustrated in the context of a specific application, it is important to notice that the associated algorithm can be used for a much more general class of infinite-dimensional differential linear systems.

In this case, the diophantine equation (3.2.11) is equivalent to

$$(K^e - K_0^e)(sI - A^e - B^e K^e)^{-1} B^e = \hat{R}^e(s) - I \tag{4.3.1}$$

where the stabilizing feedback K^e is given by (3.3.2) or (3.2.2) depending on whether a distributed input is present in the model or not. In the former case, if the pair (A, B_d) is stabilizable, hence the prestabilizing feedback can be chosen as (3.3.3), the diophantine equation (4.3.1) becomes

$$\begin{cases} (K_1-k_{11})(sI-K_1)^{-1}+k_{12}(sI-A)^{-1}(sI-\mathscr{A})B_b(sI-K_1)^{-1} &= \hat{R}^e_{11}(s)-1 \\ -k_{12}(sI-A)^{-1}B_d &= \hat{R}^e_{12}(s) \\ -k_{21}(sI-K_1)^{-1}+k_{22}(sI-A)^{-1}(sI-\mathscr{A})B_b(sI-K_1)^{-1} &= \hat{R}^e_{21}(s)-1 \\ -k_{22}(sI-A)^{-1}B_d &= \hat{R}^e_{22}(s). \end{cases} \tag{4.3.2}$$

Since for all $x \in X$ and for all $s \in \rho(A)$,

$$(sI-A)^{-1}x = \sum_{n=1}^{+\infty} \frac{1}{s-\lambda_n}\langle x, \psi_n\rangle \phi_n,$$

the scalar feedback component(s) k_{0_1} (or k_{11} and k_{21}) and the decomposition of the functional component(s) k_{0_2} (or k_{12} and k_{22}) in the Riesz basis $(\phi_n)_{n\in\mathbb{N}_0}$ of eigenvectors of the operator A with corresponding dual Riesz basis $(\psi_n)_{n\in\mathbb{N}_0}$, can be found by computing the residues of the spectral factor at the pole K_1 and at each of the selected dominant eigenvalues λ_n, $n = 1, ..., N-1$, where $N \geq 2$, which can be computed numerically with standard algorithms.
The truncated modal decomposition of the solution is then integrated with the ODE solver ode45 in MATLAB. The numerical process is described by the following computational algorithm (inspired by (Winkin, Callier, Jacob and Partington 2005),(Vandewalle and Dewilde 1975)) of an approximate optimal feedback by symmetric extraction of elementary matrix spectral factors.
Even though this algorithm has been designed for the general case of MIMO CDR systems, it can be easily adapted and simplified for the case of a single boundary input, which is treated in Section 4.3.4.2.

ALGORITHM:

Step 1: Fix the number $N \geq 2$ of elementary spectral factors that will be computed. This number can be determined e.g. by performing an error analysis on the determinant of the spectral density, see (Winkin et al. 2005), or when the H^∞ norm of the difference between two consecutive estimated spectral factors becomes sufficiently small.

Step 2: Compute the $N-1$ first real solutions of the resolvent equation (4.1.9) and the $N-1$ associated eigenvalues of A given by (4.1.8).

Step 3: Compute the N dominant zeroes of the determinant of the spectral density

(3.2.4).

Step 4: Compute the elementary spectral factors $\hat{W}_n^e$, $n = 1,...,N$, associated to the N dominant pole-zero pairs (p_n, z_n) and given by

$$\hat{W}_n^e(s) = I - \frac{1}{s - p_n} uv^*,$$

where u is in the range of the Hankel matrix $H(\hat{F}^e, p_n)$, v^* is a linear combination of the lines of $H((\hat{F}^e)^{-1}, z_n)$ and

$$v^* u = z_n - p_n,$$

such that

$$(\det \hat{W}_n^e)(z_n) = 0.$$

The Hankel matrix of the spectral density $\hat{F}^e$ at the pole p_i is defined by

$$H(\hat{F}^e, p_i) = \begin{pmatrix} F_{i1} & F_{i2} & \cdots & F_{il_i-1} & F_{i1_i} \\ F_{i2} & F_{i3} & \cdots & F_{il_i} & 0 \\ \vdots & \vdots & \vdots & \vdots & \vdots \\ F_{i1_i} & 0 & \cdots & 0 & 0 \end{pmatrix}$$

where the F_{ik} are the coefficients of the Laurent series of $\hat{F}^e$ given by

$$\hat{F}^e(s) = \sum_{k=1}^{l_i} F_{ik}(s - p_i)^{-k} + F_{i0} + \sum_{k=1}^{+\infty} \tilde{F}_{ik}(s - p_i)^k$$

such that its elements correspond to the residues of $\hat{F}^e$ at p_i.
See (Vandewalle and Dewilde 1975) for the definition in the case of rational spectral densities.

Step 5: Compute the approximate spectral factor

$$\hat{R}_N^e(s) = \hat{W}_N^e(s)\hat{W}_{N-1}^e(s)...\hat{W}_1^e(s) \tag{4.3.3}$$

such that the sequence $(\det \hat{R}_N^e)_{N \in \mathbb{N}_0}$ converges to $\det \hat{R}^e$ in $\hat{\mathscr{A}_-}$.

Step 6: Solve the Diophantine equation

$$\mathscr{U}_N \hat{D}^e(s) + \mathscr{V}_N \hat{\mathscr{N}}^e(s) = \hat{R}_N^e(s)$$

by using modal decomposition with (4.3.1).

Step 7: Compute the approximate optimal feedback

$$K_{0_N}^e = \begin{pmatrix} k_{0_{11_N}} & k_{0_{12_N}} & 0 \\ k_{0_{21_N}} & k_{0_{22_N}} & 0 \end{pmatrix}$$

of the form (3.3.4) given by

$$K_{0_N}^e = -\mathscr{U}_N^{-1}\mathscr{V}_N = -\mathscr{U}_N^*\mathscr{V}_N,$$

where, for $i = 1, 2$,

$$k_{0_{i2_N}} = \sum_{n=1}^{N} \langle \tilde{k}_{i2_N}, \phi_n \rangle \psi_n. \tag{4.3.4}$$

END

This spectral factorization algorithm is semi-heuristic and is inspired by a method described in (Vandewalle and Dewilde 1975) for parahermitian rational spectral densities. Moreover, there is currently no proof of convergence of this algorithm for multiple input systems. However, it has been shown that, under suitable conditions, the method of spectral factorization by symmetric extraction is convergent for the determinant of the multidimensional spectral density (Winkin et al. 2005).

As mentioned before, the algorithm can be readily extended to a more general class of differential linear systems, where the determinant of the spectral density satisfies the assumptions described in (Winkin et al. 2005), i.e. more specifically, to the case of a Riesz-spectral operator A with discrete spectrum $\sigma(A) = \sigma_p(A) = \{\lambda_n : n \in \mathbb{N}\} \subset \mathbb{C}$ consisting of simple eigenvalues such that

$$\inf\{|\lambda_n - \lambda_m| : n, m \in \mathbb{N}, n \neq m\} > 0,$$

and

$$\sup\left\{ \sum_{\substack{l=1 \\ l \neq n}}^{+\infty} \frac{1}{|\lambda_l - \lambda_n|^2} : n \in \mathbb{N} \right\} < +\infty.$$

In fact, only step 2 is specific to the convection-diffusion-reaction system (4.1.1).

Even though this approach shares a connection with classical modal control (which is sometimes referred to as the direct approach), it should be noted that it is less prone to error propagation since the modal approximation is done in closed loop, after the prestabilization and computation of the spectral density (late lumping, or indirect approach), see e.g. (Balas 1986), (Balas 1988) and (Christofides and Daoutidis 1997). Moreover, the transfer function of the closed-loop system with the truncated feedback functionals (4.3.4) computed by the algorithm is given by $G_{\text{cl}}^e = N^e (R_N^e)^{-1}$, where R_N^e is the approximate spectral factor given by (4.3.3).

4.3.2 Implementation of the algorithm

This section mentions some of the choices that were made for the practical implementation of the algorithm for the CDR system. MATLAB was selected as the programming language for this purpose in view of using some of its routines and the built-in

plotting tools.

Step 2 was implemented by using the MATLAB function *fzero* on the resolvent equation (4.1.9). More precisely, the equation

$$\tan\left(\frac{s}{2D}\right) - \frac{2vs}{s^2 - v^2} = 0$$

is solved in $\mathbb{R}_0^+$ with this function. The fact that $s_n - 2D\pi(n-1) \to 0$ is used in order to provide an appropriate starting point for each use of *fzero*. However, the distance between the starting point and the corresponding $2D\pi(n-1)$ has to be increased carefully when the convection parameter itself increases, as seen in Figures 4.1 - 4.3.

For Step 3, many computations were done analytically before the implementation for optimization purposes. In fact, the resolvent operator, transfer function and right coprime fraction were computed by hand. Even though these computations were long and tedious, they were crucial in view of the limited computational power at hand. More precisely, the main motivation for this choice is the fact that the resolvent operator is an integral operator and is involved heavily in each evaluation of the spectral density, to which the program makes an important number of calls. Numerical integration was then prohibited at such a fundamental level in the program. Separate functions were created on the basis of the analytical computations.
The research of zeros of the determinant of the spectral density relies on the function *fzero* again. Due to the fact that the zeros quickly become close to the poles of the considered function, the roots research problem is badly conditioned and the algorithm eventually crashes if the starting point provided to the function *fzero* is not well chosen. Hence, a test had to be implemented manually in order to check the shape of the resolvent function around each pole and on which side of the pole the zero is located. The MATLAB routine then starts close to the solution, which allows for avoiding crashes and a faster execution of the program. Moreover, the variable s of the determinant of the spectral density has been scaled appropriately in order to improve the shape of the function around the poles.

For Steps 4 and 5, two methods were implemented for the computation of the residues F_{ik} of the spectral density $\hat{F}^e$ and its inverse, and the corresponding Hankel matrices.
The first method computes an approximate residue by letting s go to p_i in the function $(s-p_i)\hat{F}_n^e(s)$ until a given stopping criterion is met, where $\hat{F}_n^e$ is the reduced spectral density at the nth iteration.
The second method uses the *limit* routine on the same function. This method is more accurate but requires more computational power and hence is much slower.
The reduced spectral density is computed at each iteration by extracting the computed elementary spectral factors, i.e. by pre- and post-multiplying the spectral density by $(\hat{R}_n^e)^{-1}$ and $\hat{R}_n^e$, respectively, where $\hat{R}_n^e$ is the current approximate spectral factor. A similar method is applied to the inverse spectral density.

In Steps 6 and 7, the Diophantine equation was solved under the form (4.3.2). For

this purpose, another residue computation was implemented for each of the N poles of the approximate spectral factor. More precisely, the residues of the approximate spectral factor are computed in the right-hand side and the analytical form of the resolvent operator of A is used in the left-hand side in order to compute the truncated decomposition of the feedback functionals in the dual Riesz-basis $\{\psi_n\}_{n\in\mathbb{N}_0}$.

Finally, the integration of the closed-loop trajectories was implemented by computing the matrix corresponding to the truncated modal decomposition of the state and the feedback functionals in the first N modes of the CDR system. After the computation of the finite-dimensional trajectories given by $x(t) = e^{\tilde{A}t}x_0$, where $\tilde{A}$ is the truncated modal matrix of the system, the approximate state is reconstituted as a finite sum. This choice was rather natural due to the fact that the method relies heavily on the spectral structure of the dynamics generator. Moreover, it helps avoiding any dependence to a spatial discretization scheme and discretization step.

The MATLAB program is user-friendly and easy to configure. The parameters D, v, k, ε, ρ_1, ρ_2, ρ_3, η_1, η_2, α, k_1 and N, as well as the spatial discretization step, the time discretization step and the ending time, can be specified by the user at the beginning of the execution. The user can also choose whether a punctual perturbation or a Gaussian white noise is added in the dynamics of the dynamic compensator. It is also possible to tweak other parameters, such as the precision for the residue computations, and modify the initial condition for the trajectories directly in the code, which is well-documented for this purpose. Once every required parameter has been specified, the program generates the illustration of the computation of the solutions of the resolvent equation (4.1.9), the poles and zeros of the spectral density, the optimal feedback coefficients, the profiles of the optimal feedback functionals and the open-loop and closed-loop boundary and distributed input, state and output trajectories.

4.3.3 Computation of the solutions of the resolvent equation

In this short section, we show some numerical results that illustrate the numerical computations in Step 2 of the algorithm presented in the previous section.
Figures 4.1, 4.2 and 4.3 illustrate the computation of the solutions of the resolvent equation (4.1.9) for the CDR system (4.1.1) in Step 2 of the algorithm as the intersections between two curves with different values of the convection parameter. It should be noted that only the real solutions of the resolvent equation are computed for the spectrum of the operator A, even though this equation may have complex solutions as well. In Figures 4.1-4.3, both axes thus represent the set of real numbers $\mathbb{R}$.

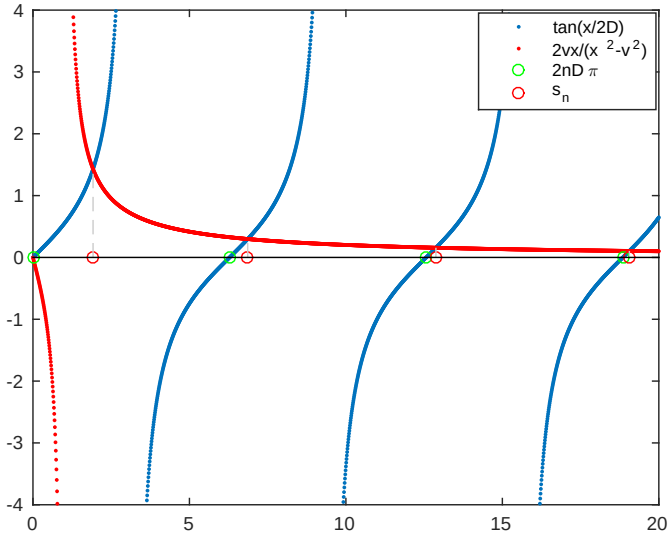

Figure 4.1: Solutions of the resolvent equation with $D = 1$, $v = 1$ and $k = 1$

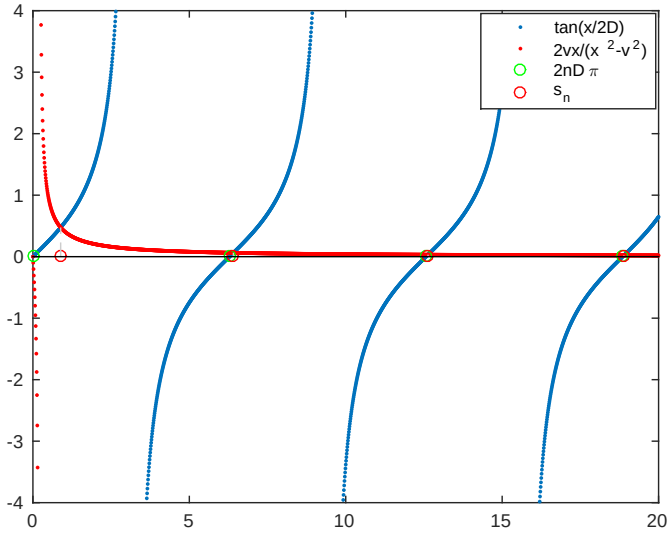

Figure 4.2: Solutions of the resolvent equation with $D = 1$, $v = 0.2$ and $k = 1$

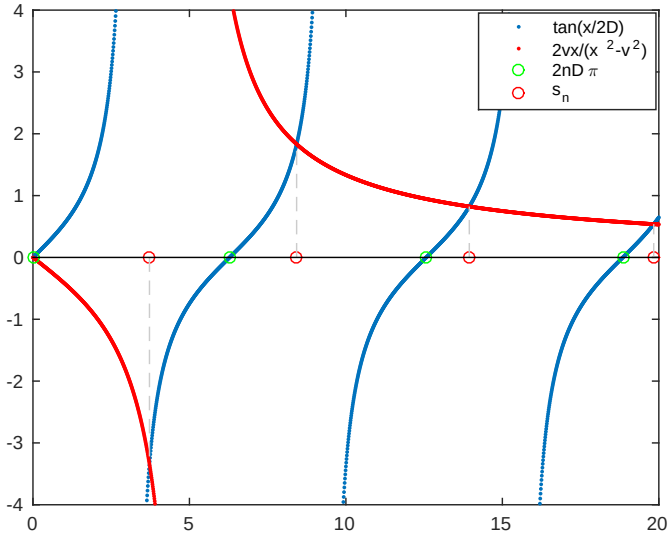

Figure 4.3: Solutions of the resolvent equation with $D = 1$, $v = 5$ and $k = 1$

In general, the distance between the solutions of the resolvent equation and the $2(n-1)D\pi$ is converging towards 0 at a fast rate. However, this speed of convergence is also heavily dependent on the ratio between the convection and diffusion parameters. In fact, the lower this ratio, the better the conditioning of the problem. This is explained by the fact that, when this ratio is small, the system is closer to a purely diffusive one, which is known to be very well conditioned. It is seen on figure 4.2 that, in this case, the solutions of the resolvent equation are even closer to the $2(n-1)D\pi$ than with the normalized parameters. They can take much more time to converge as the convection parameter grows however, as can be seen on Figure 4.3. In view of these results, it is expected that the extreme case of a convection-reaction system without diffusion is badly conditioned, at least for the computation of the spectrum, which is a crucial step in the proposed method of resolution. However, such a system cannot be seen directly as a particular case of (4.1.1) and has to be considered separately, with the diffusion coefficient D being zero from the start.

Figure 4.4 illustrates the evolution of the distance between an arbitrary solution of the resolvent equation (s_5 in this case) and the corresponding $2(n-1)D\pi$ ($= 8D\pi$). It is seen that this distance increases linearly with the convection parameter, which may decrease the speed of convergence of an algorithm of research of zeros.

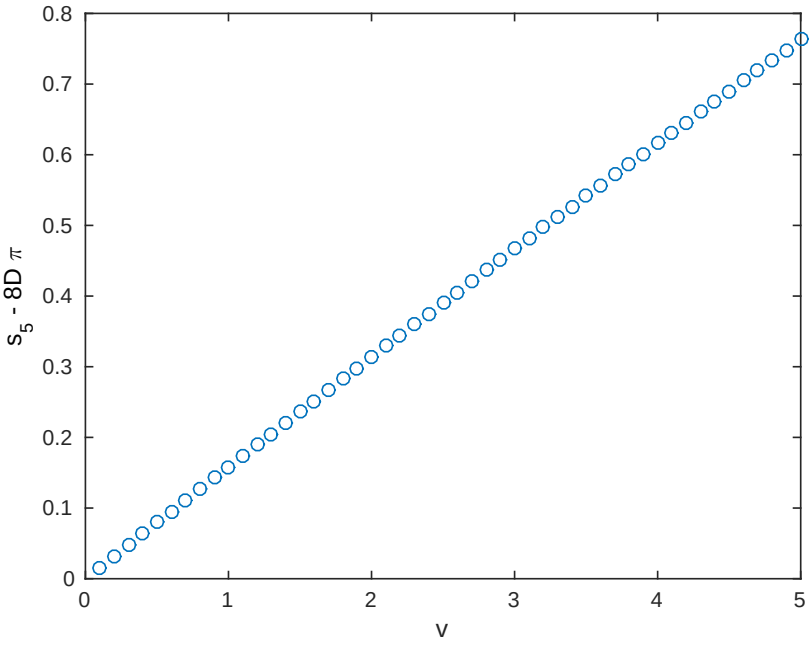

Figure 4.4: Distance between s_5 and $8D\pi$ against the convection parameter v ($D = 1$, $k = 1$)

4.3.4 Numerical simulations: stable and unstable CDR system

This section provides numerical results that illustrate the resolution of a LQ-optimal control problem for both stable and unstable convection-diffusion-reaction systems. Concerning the efficiency of the algorithm of spectral factorization by symmetric extraction, the convergence seems to be fast for the CDR system. In general, three elementary spectral factors are sufficient in order to obtain an accurate solution. It should be noted that the numerical conditioning heavily relies on the relative sizes of the diffusion and convection parameters. If the convection parameter is larger than the diffusion one, the model is numerically ill-conditioned and the numerical algorithm can fail quickly, especially when finding zeroes of the determinant of the spectral density. However, a relatively large diffusion parameter makes the numerical conditioning much better. A nearly purely diffusive system (close to the heat equation) allows the computation of more spectral factors and / or with a higher parameter α. Moreover, it is expected that the convergence may be noticeably slower with systems which are less well-conditioned than (4.1.1).

4.3.4.1 Stable case

In this section, we assume that the reaction parameter k is positive, which is the case in most applications. In this case, the CDR system is already exponentially stable. However, the closed-loop system with the optimal feedback control law can help bring additional robustness properties and is still useful. Sometimes, it may also help in stabilizing the system faster at the expense of a required control input over time.

The figures illustrate the computation of the eigenvalues of the operator A and the asymptotic behaviour of the state and input trajectories of the extended system with the application of the optimal feedback. The last figures show the response of the system to perturbations in the input of the dynamic compensator in order to illustrate the robustness properties of the feedback law.

Except when stated otherwise, the parameters used in the numerical simulations are $D = 8,\ v = 4,\ k = 1,\ \rho_1 = 2,\ \rho_2 = 1e-6,\ \rho_3 = 1.5,\ \eta_1 = 1,\ \eta_2 = 2,\ \varepsilon = 0.008,\ \alpha = 3100, N = 5$.
The prestabilizing feedback is given by (3.3.3) with $k_1 = -0.75$ and $k_2 = 0$.
Finally, the initial condition is given by $u_{b0} = u_b(0) = 0$ and for all $z \in [0,1]$,

$$v_0(z) = \sin\left(\frac{7\pi}{2}z\right) + \left(\frac{35D\pi}{v} - 20\right)\cos(6\pi z) + 20 \tag{4.3.5}$$

Note that $u_b(0) = 0$ must hold for the classical solution, since

$$u_b(0) = -\frac{D}{v}x_0(0) + x_0(0)$$

and $x_0 \in D(A)$. However, the mild solution is well defined for all $x_0 \in X$ and for the corresponding u_{b0}.

The poles and zeros of $\hat{F}^e$ are given below.

Poles	Zeros
-0.75	-1.05689
-3.02392	-3.00449
$-7.31085e+01$	$-7.31086e+01$
$-2.80381e+02$	$-2.80381e+02$
$-6.25819e+02$	$-6.25819e+02$

The first pole corresponds to the prestabilizing feedback parameter k_1 and the following four poles correspond to the dominant open-loop eigenvalues. It should be noted that the distance between the poles and zeros is converging towards 0 at a fast rate.

The optimal feedback approximate coefficients are

$$\begin{aligned} k_{11} &= -1.07453 \\ k_{21} &= -2.06711e-03 \\ \langle k_{12}, \phi_1 \rangle &= -3.81796e-02 \\ \langle k_{12}, \phi_2 \rangle &= 7.19369e-05 \\ \langle k_{12}, \phi_3 \rangle &= -1.25698e-06 \\ \langle k_{12}, \phi_4 \rangle &= 1.01735e-07 \\ \langle k_{22}, \phi_1 \rangle &= -2.10749e-03 \\ \langle k_{22}, \phi_2 \rangle &= 4.12753e-04 \\ \langle k_{22}, \phi_3 \rangle &= -1.36144e-04 \\ \langle k_{22}, \phi_4 \rangle &= 5.91680e-05. \end{aligned}$$

Figures 4.5 and 4.6 illustrate the numerical convergence of the optimal feedback when α goes to infinity.

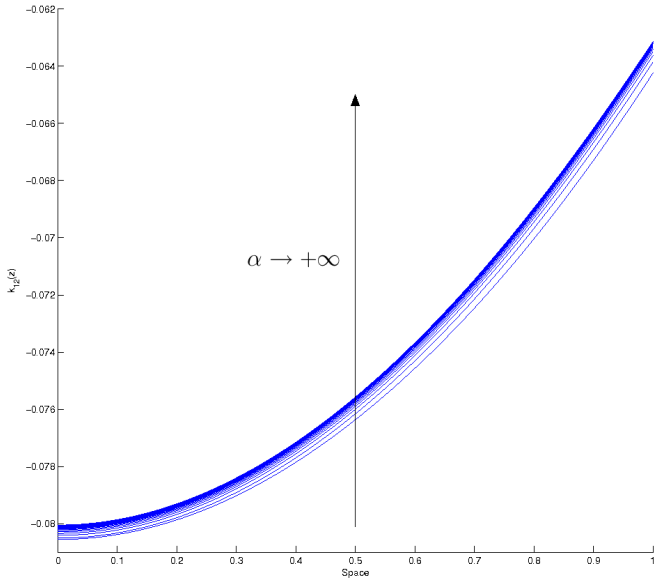

Figure 4.5: Profile of the feedback functional $k_{0_{12}}$ with varying α

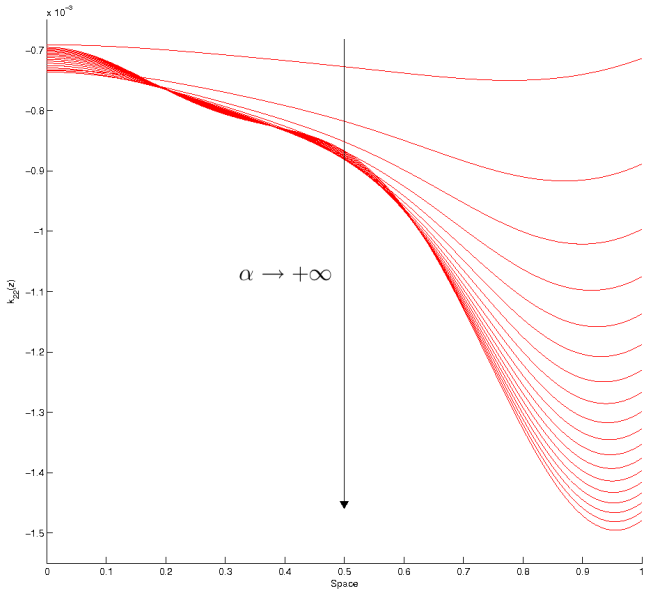

Figure 4.6: Profile of the feedback functional $k_{0_{22}}$ with varying α

As the parameter α increases, the distance between two successive feedback functionals becomes smaller as expected.

Figures 4.7-4.9 illustrate the behaviour of the closed-loop system. In Figure 4.8, it is seen that, as the ratio ρ_1/η_1 increases, the norm of the boundary input is reduced compared to its variation rate due to the higher weight in the cost functional, which leads to a faster stabilization at the cost of higher variations.

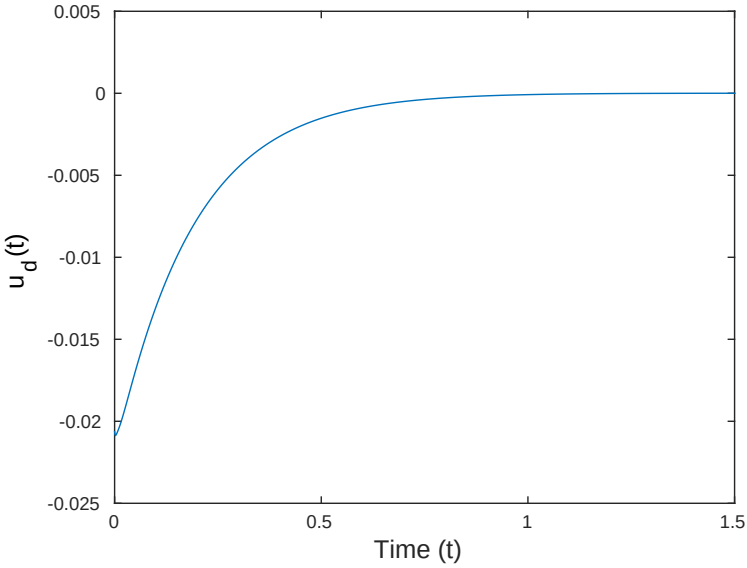

Figure 4.7: Closed-loop distributed input $u_d(t)$

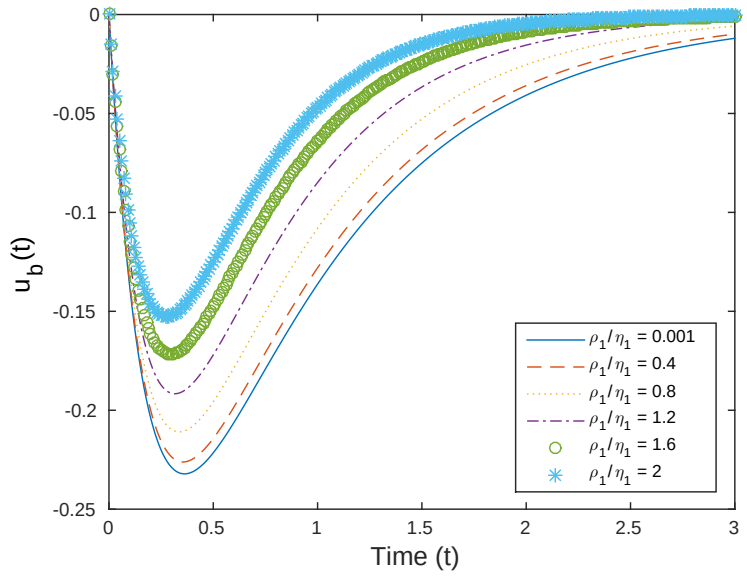

Figure 4.8: Closed-loop boundary input $u_b(t)$ with varying ratio ρ_1/η_1

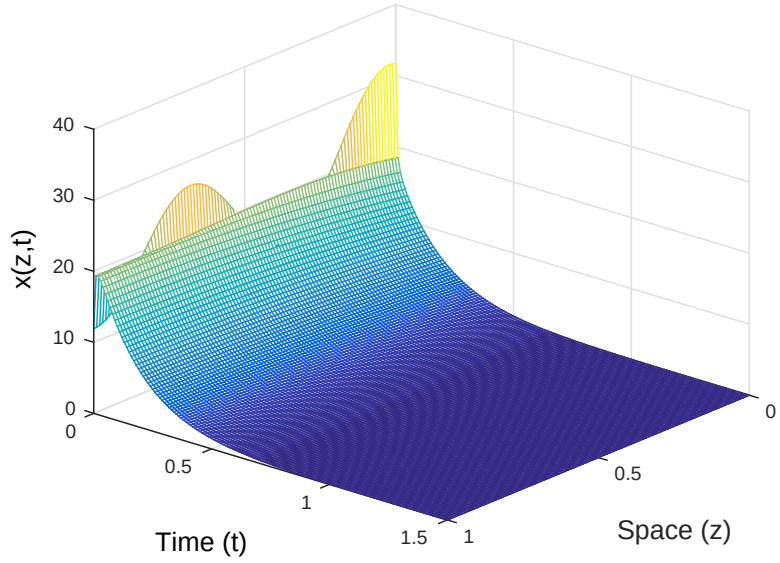

Figure 4.9: Closed-loop state trajectory $x(t)$

Figures 4.10-4.12 illustrate the behaviour of the closed-loop system with Gaussian white noise in the dynamics of the dynamic compensator.

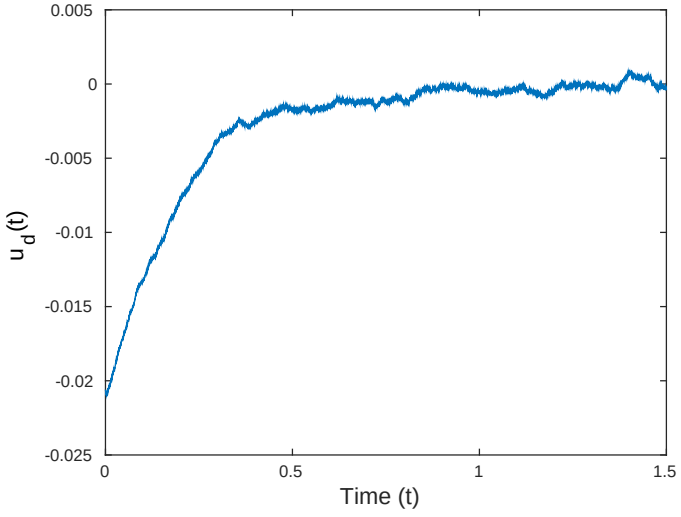

Figure 4.10: Closed-loop distributed input $u_d(t)$ with Gaussian white noise

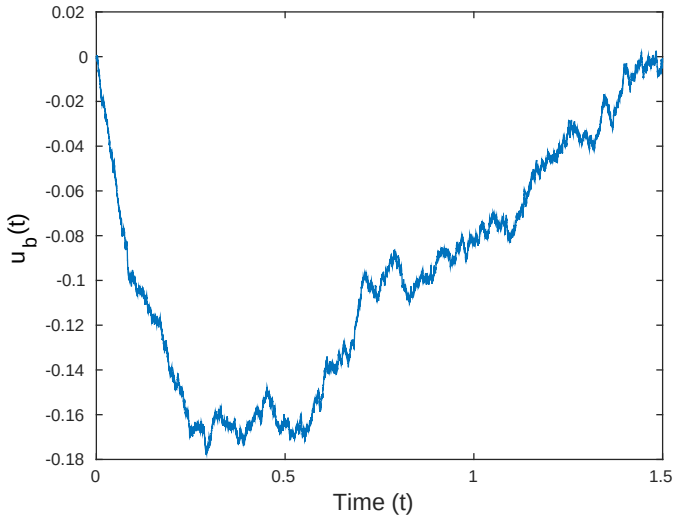

Figure 4.11: Closed-loop boundary input $u_b(t)$ with Gaussian white noise

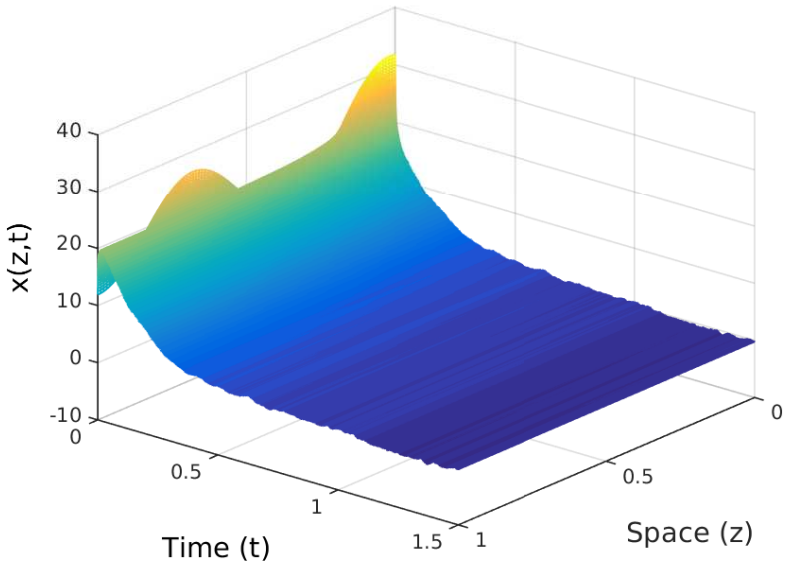

Figure 4.12: Closed-loop state trajectory $x(t)$ with Gaussian white noise

Figures 4.13-4.14 illustrate the behaviour of the closed-loop system with a punctual perturbation in the dynamics of the dynamic compensator at $t = 0.5$ and $t = 1.2$.

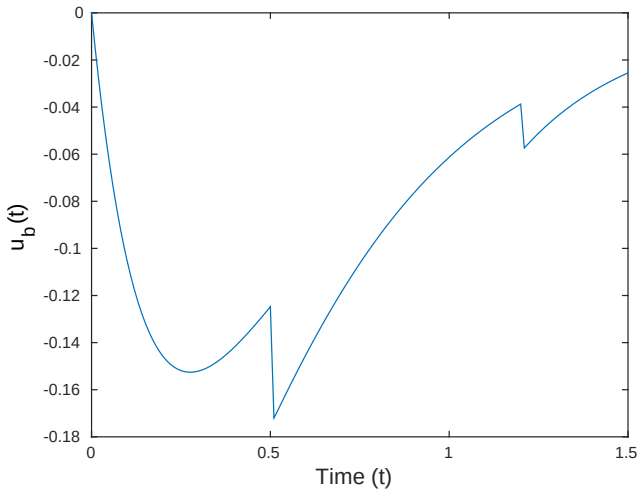

Figure 4.13: Closed-loop boundary input $u_b(t)$ with punctual perturbation at $t = 0.5$ and $t = 1.2$

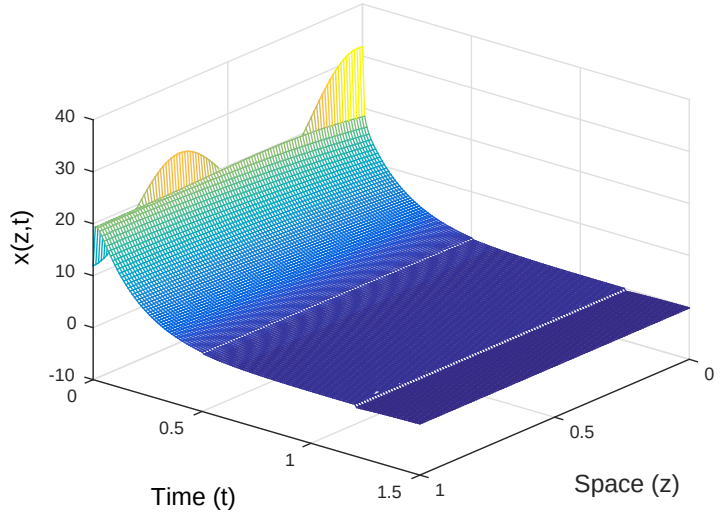

Figure 4.14: Closed-loop state trajectory $x(t)$ with punctual perturbation at $t = 0.5$ and $t = 1.2$

Some additional numerical simulations suggest that the optimal cost could be a monotonically convergent function of the parameter α.

4.3.4.2 Unstable case

In this section, the reaction parameter k is assumed to be negative enough such that the CDR system becomes open-loop unstable. Again, this can be done by considering e.g. the linearization of a chemical or biochemical system with a nonlinear reaction rate (based on e.g. Arrhenius equation, Haldane kinetics or others) around a non trivial unstable equilibrium. In this case, an appropriate feedback law is required in order to exponentially stabilize the system, which makes the resolution of the LQ-optimal control problem even more useful.
Moreover, in order to demonstrate the adaptability of the theory developed in Part II and of the algorithm, this problem is considered mainly with boundary control only in this section. It is also seen that the control input trajectories obtained with a distributed control whose associated window length becomes arbitrarily small converge numerically towards the input trajectories obtained with boundary control alone.

The following figures illustrate the asymptotic behaviour of the state and input trajectories of the extended system with the application of the optimal feedback with the following parameters: $D = 8$, $v = 4$, $k = -9$, $\rho_1 = 2$, $\rho_2 = 1e-6$, $\rho_3 = 1.5$, $\eta = 1$, $\varepsilon = 0$, $\alpha = 3100$, $N = 6$.
The initial condition is given by

$$v_0(z) = \sin\left(\frac{7\pi}{2}z\right) + \frac{7D\pi}{2v}\cos(6\pi z).$$

The prestabilizing feedback (whose existence is guaranteed, see Remark 4.1.2) is given by (3.2.2) with, in this case,

$$k_1 = 0.1 \quad \text{and} \quad k_2 = 20\langle \cdot, \psi_1 \rangle. \tag{4.3.6}$$

The stability of the corresponding closed-loop system has been checked numerically. As in Section 4.3.4.1, the initial condition is given by (4.3.5).

The poles and zeros of $\hat{F}^e$ are given below.

Poles	Zeros
-1.60295	1.90984
$-1.13281e+01$	$1.13086e+01$
$-7.82578e+01$	$-7.82579e+01$
$-3.15273e+02$	$-3.15273e+02$
$-7.10087e+02$	$-7.10087e+02$
$-1.26279e+03$	$-1.26279e+03$

The poles correspond to the dominant closed-loop eigenvalues with the prestabilizing feedback (3.2.2),(4.3.6). Again, the distance between the poles and zeros is converging towards 0 at a fast rate.

The optimal feedback approximate coefficients are

$$\begin{aligned} k_{0_1} &= 1.61244e-01 \\ \langle k_{0_2}, \phi_1 \rangle &= 1.35439e+01 \\ \langle k_{0_2}, \phi_2 \rangle &= -5.13287e-03 \\ \langle k_{0_2}, \phi_3 \rangle &= 3.44387e-04 \\ \langle k_{0_2}, \phi_4 \rangle &= -5.90957e-05 \\ \langle k_{0_2}, \phi_5 \rangle &= 1.55667e-05. \end{aligned}$$

Figures 4.15-4.8 illustrate the numerical convergence of the optimal feedback when α goes to infinity as well as the behaviour of the open-loop and closed-loop systems.

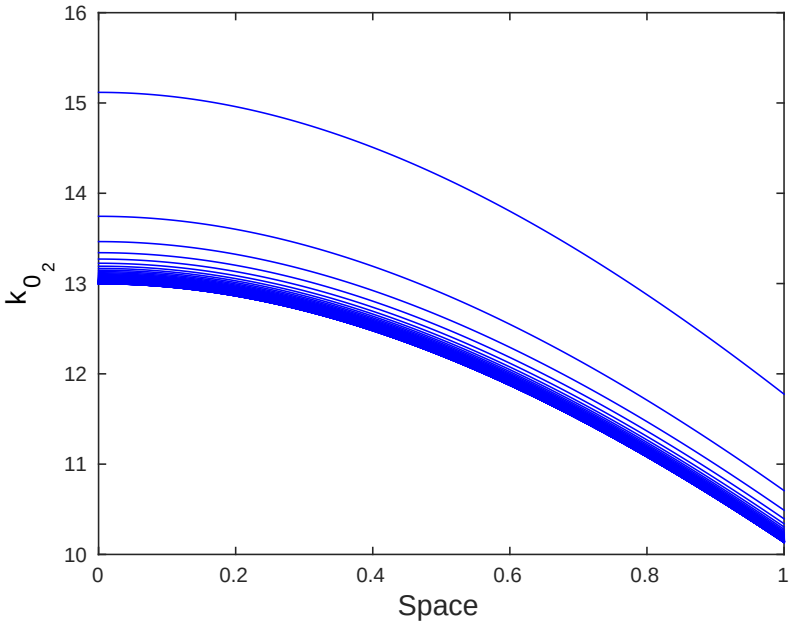

Figure 4.15: Profile of the feedback functional k_{0_2} with varying α

As observed in Section 4.3.4.1, the distance between two successive feedback functionals becomes smaller as the parameter α increases.

Figure 4.16 illustrates the open-loop trajectories while Figures 4.17, 4.18, 4.19 and 4.20 show the behaviour of the closed-loop system.

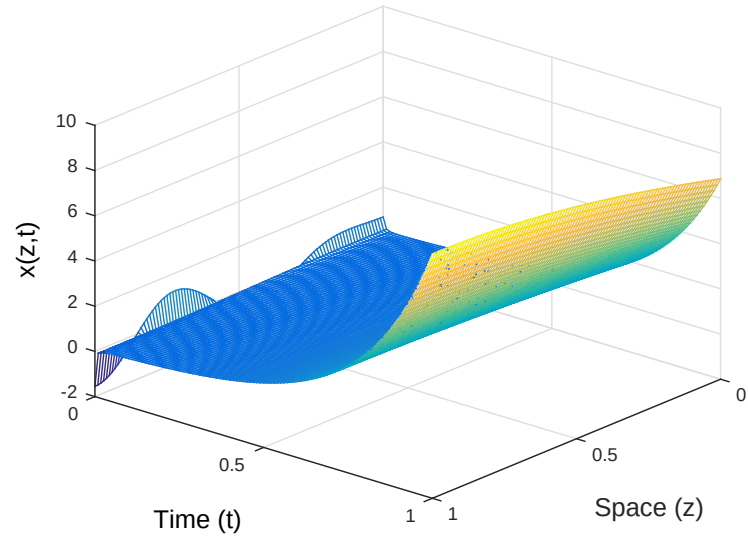

Figure 4.16: Open-loop state trajectory $x(t)$

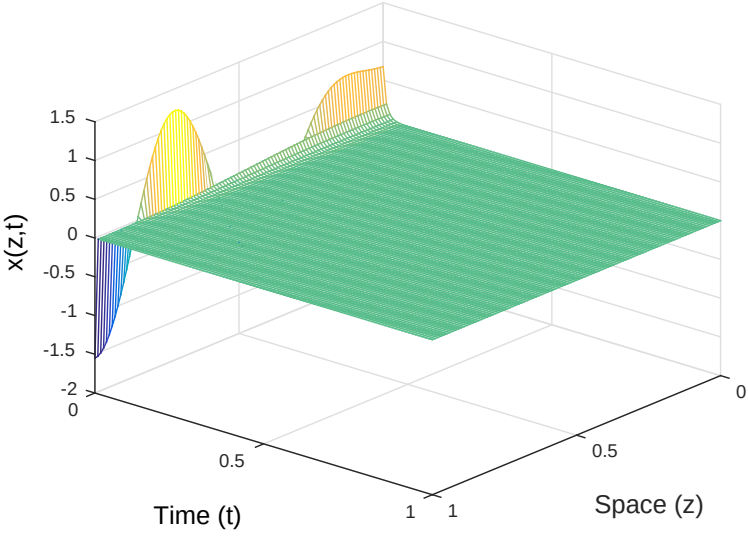

Figure 4.17: Closed-loop state trajectory $x(t)$

Figures 4.18 and 4.19 display a comparison between the closed-loop state trajectories with and without distributed control. One can clearly see the influence of the boundary and distributed actuation, respectively.

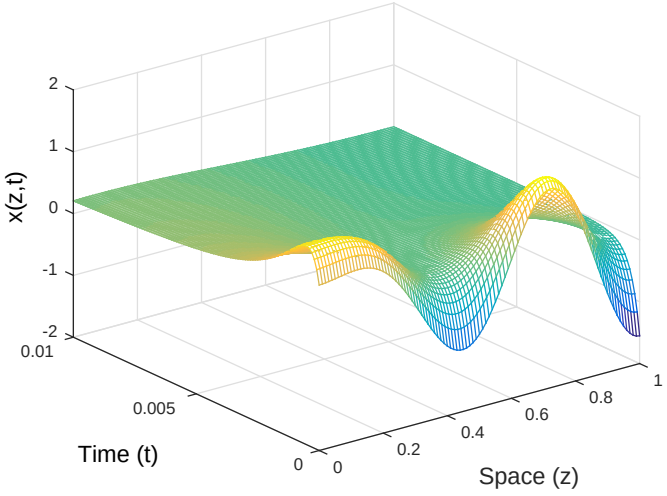

Figure 4.18: Closed-loop state trajectory $x(t)$ with pure boundary control

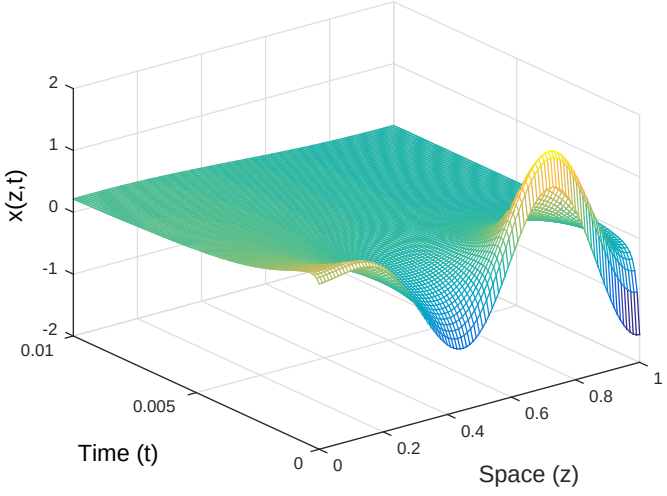

Figure 4.19: Closed-loop state trajectory $x(t)$ with mixed boundary-distributed control ($\varepsilon = 0.4$)

In Figure 4.20, it is seen again that, as the ratio ρ_1/η increases, the norm of the boundary input is reduced compared to its variation rate due to the higher weight in the cost functional.

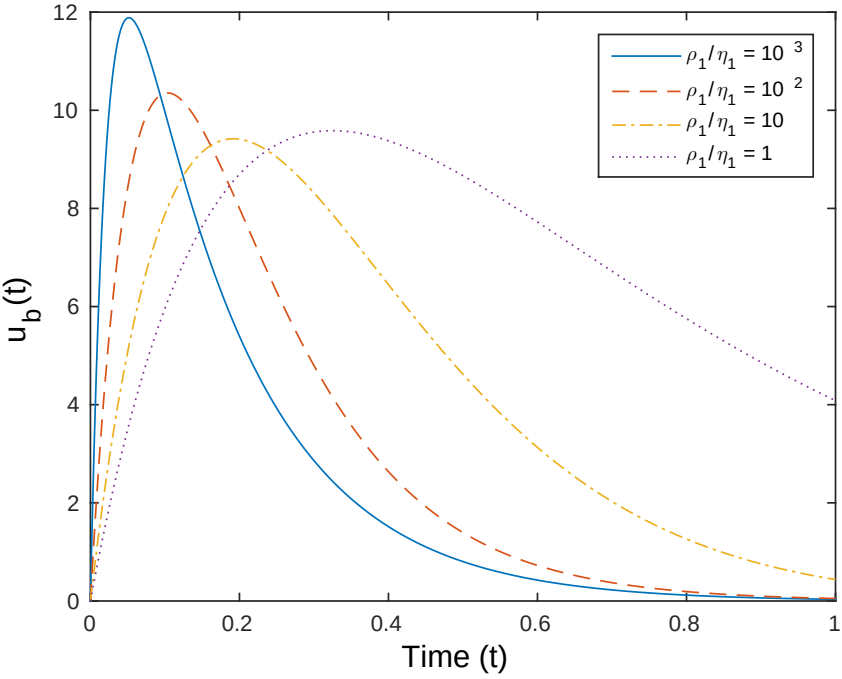

Figure 4.20: Closed-loop boundary input $u_b(t)$ with varying ratio ρ_1/η

Finally, it should be noted that, even though $B_d = 0$ in these simulations, considering a nonzero but suitably scaled distributed control window can be used as a way to obtain a good approximation of the solution while providing an easy mean to guarantee reachability, and hence uniqueness of the solution, see Lemma 4.1.1. Figure 4.21 shows the comparison between the boundary input and output trajectories obtained with $B_d = 0$ (bold blue line) and $B_d = \delta\chi_{[1-\varepsilon,1]}$, with δ and ε converging towards zero.
In this simulation, as $\delta = \varepsilon$ is going towards zero, the closed-loop boundary control trajectory under the optimal feedback law obtained with a distributed input becomes closer to the trajectory under the optimal feedback law obtained with a boundary input only. Moreover, as expected, pure boundary control is slightly slower to stabilize the output than when it is helped by distributed control.

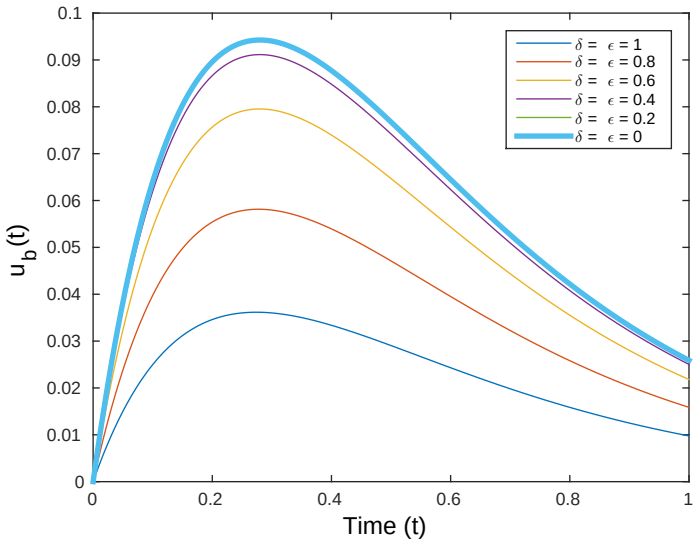

Figure 4.21: Closed-loop boundary input $u_b(t)$ with $B_d = 0$ and $B_d = \varepsilon\chi_{[1-\varepsilon,1]}$ for different values of ε

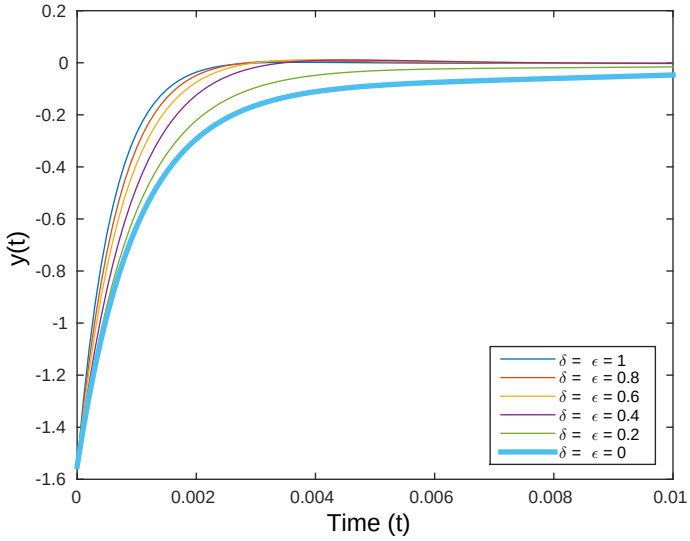

Figure 4.22: Closed-loop output $y(t)$ with $B_d = 0$ and $B_d = \varepsilon\chi_{[1-\varepsilon,1]}$ for different values of ε

Chapter 5

Hyperbolic system

Boundary control of hyperbolic differential systems is at the heart of many practical applications. Hyperbolic systems are heavily used in chemical engineering (tubular, reactors, heat exchangers, ...), in the modeling of irrigation canal systems with, in particular, the very popular Saint-Venant equations, and a wide range of other processes. They have been at the center of many studies and research topics during the past few decades, such as the analysis of well-posedness, stability or feedback stabilization of hyperbolic systems with boundary control, see e.g. (Witrant, D'Innocenzo, Sandou, Santucci, Di Benedetto, Isaksson, Johansson, Niculescu, Olaru, Serra, Tennina and Tiberi 2010), (Castillo et al. 2012), (Castillo et al. 2013), (Prieur, Winkin and Bastin 2008), (Bastin, Coron and d'Andréa Novel 2008), (Bounit 2003), (Besson, Tchousso and Xu 2006), (Chentouf and Wang 2009) and references therein.

5.1 Motivation: an experimental setup

The goal of this chapter is to design a controller for a Poiseuille flow model and implement this controller on an experimental setup. This system, or more precisely several variations of the associated model, have been considered and studied in (Castillo et al. 2012) and (Castillo et al. 2013).
The experiments were made possible mainly thanks to Christophe Prieur, Emmanuel Witrant, Felipe Castillo and Hassen Fourati, who granted access to the experimental setup in the GIPSA-lab in Grenoble and explained its primary uses.
The test bench has been manufactured by the company Soben. As mentioned in Chapter 1, it consists of a horizontal tube of one meter in which heat or moisture will be transported by an air flow. The tube is attached to a heating column in which a resistance is used in order to attain the desired heat level. The resistance has its own dynamics, which are relatively slow, and it takes some time to reach a given heat level. Near the heating column, at the entrance of the tube, a moisture injector can be found, which reacts much quicker than the heating column. Two fans, than can be controlled independently one from each other, are located at both ends of the tube and

are used to generate the air flow. Three sensors that can measure the temperature or moisture percentage in the air flow are placed along the tube, as well as one sensor that is used to measure the speed of the flow. Finally, the test bench is connected to an automaton, which is used to interact with the setup and implement control laws and / or state estimators. An adapted software developed and provided by Soben can be installed on a connected computer in order to run or reprogram the automaton. In "user mode", this software allows, among other things, manual control of the fans, the heating column or the humidity injector, monitoring and recording the data via the sensors and using two types of controllers (proportional-integral-derivative (PID) and R-S-T) that are already implemented, thanks to a graphical interface. In "programmer mode", the existing codes can be altered and new ones can be developed by using the specialized language LADDER, which is heavily used for the programming of programmable logic controllers (PLC) in the industry. Though not advised by the manufacturer, this mode allows for example the implementation of other control methods or observers. The latter is theoretical though since none has been implemented so far and there is no guarantee that the automaton is powerful enough to run the integrations required by an observer.
Figure 5.1 originates from (Castillo et al. 2013) and shows the schematic of the experimental setup.

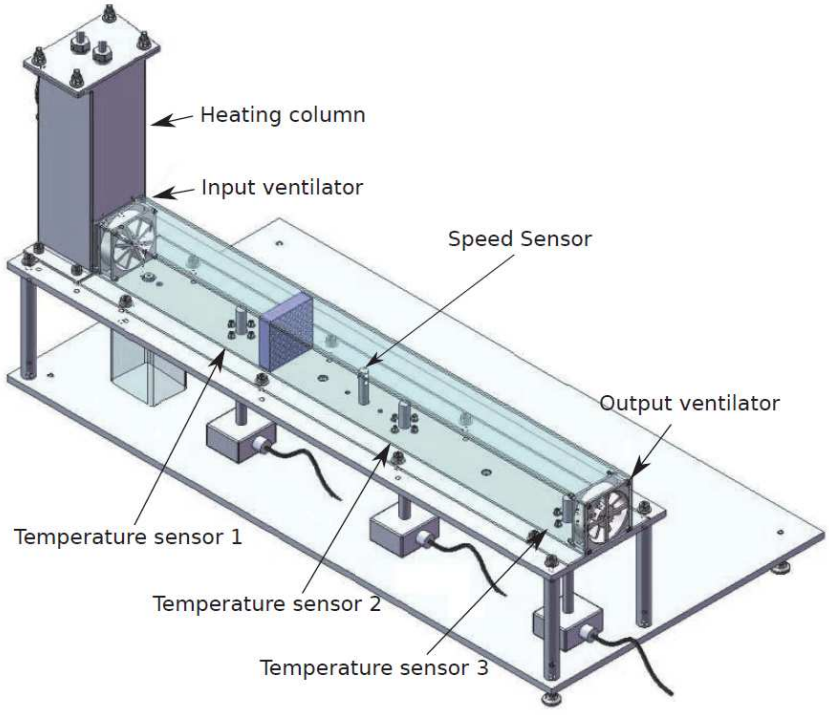

Figure 5.1: Schematic of the experimental setup

5.2 Modeling of the Poiseuille flow

This section introduces the hyperbolic Poiseuille flow control system, and how this system can be modeled, linearized and diagonalized.

The following table summarizes the notations for the parameters and variables that will be used through this chapter.

Notation	Interpretation	Unit
x	spatial position	m
t	time	s
$\rho(x,t)$	gas density	kg/m^3
$u(x,t)$	particle speed	m/s
$p(x,t)$	pressure	Pa
$\rho_{\text{in}}(t)$	inlet gas density	kg/m^3
$u_{\text{in}}(t)$	inlet particle speed	m/s
$p_{\text{in}}(t)$	inlet pressure	Pa
$p_{\text{out}}(t)$	outlet pressure	Pa
$dQ(t)$	heat exchange	J
$C_0(t)$	input fan rotating speed	1/s
$T_{\text{in}}(t)$	heating column input temperature	K
a	speed of sound in the gas	m/s
p_a	atmospheric pressure	Pa
C_v	specific heat constant at constant volume	J/(mol·K)
C_p	specific heat constant at constant pressure	J/(mol·K)
R	gas constant	J/(mol·K)
A	tube section	m^2
V_0	heating column volume	m^3
x_{ρ_i}	spatial position of the ith temperature/hygrometry sensor	m
x_s	spatial position of the speed sensor	m

Though the spatial variable will be denoted by x throughout this chapter in order to respect some notation conventions, it should not be confused with the BCBO state variable $x(t)$.

The modeling of the dynamics of the fluid inside the tube is based on one-dimensional quasilinear hyperbolic Euler equations for a perfect gas and a constant tube cross section. These equations are written in terms of the following primitive variables: the gas density (denoted by ρ), which is directly related to the temperature and the hygrometry of the gas, the particle speed (denoted by u, which should not be confused with the boundary input u_b) and the pressure (denoted by p). These equations represent the conservation of mass and the balance of momentum and energy. See e.g. (Winterbone and Pearson 2005).
It should be noted that the dynamics presented for the two models are rather general,

but the boundary conditions are really specific to the actuators used in the test bench.

5.2.1 First model

In this section, we consider all three aforementioned variables of the Poiseuille flow for the modeling.
By neglecting the heat exchanges and the friction in the tube, which are small for this application, the partial differential equations governing the dynamics of the system can be written as

$$\begin{cases} \frac{\partial \rho}{\partial t}(x,t) &= -u(x,t)\frac{\partial \rho}{\partial x}(x,t) - \rho(x,t)\frac{\partial u}{\partial x}(x,t) \\ \frac{\partial u}{\partial t}(x,t) &= -u(x,t)\frac{\partial u}{\partial x}(x,t) - \frac{1}{\rho(x,t)}\frac{\partial p}{\partial x}(x,t) \\ \frac{\partial p}{\partial t}(x,t) &= -a^2\rho(x,t)\frac{\partial u}{\partial x}(x,t) - u(x,t)\frac{\partial p}{\partial x}(x,t) \end{cases}$$

where $a = \sqrt{\frac{\gamma p}{\rho}}$ is the speed of sound in the gas, with

$$\gamma = \frac{C_p}{C_v}, \tag{5.2.1}$$

C_p and C_v being the specific heat constants at constant pressure and constant volume respectively.

The boundary conditions are

$$\begin{cases} \rho(0,t) &= \rho_{\text{in}}(t) \\ Au(0,t) &= K_f C_0(t)[p(0,t) - p_{\text{in}}] \\ Au(L,t) &= K_f C_1(t)[p_{\text{out}} - p(L,t)] \end{cases}$$

where A is the tube section, K_f (kg/m) is a coefficient depending on the fan specification map, p_{in} and p_{out} are the inlet and outlet pressures and C_0 and C_1 are the inlet and outlet fan rotating speeds.
The fan specification map establishes a relationship between the fan rotating speed, the flow rate and the pressure loss around the device. The map corresponding to the fans installed in the test bench has been computed and is available in the GIPSA-lab of Grenoble.
Moreover, it has been established in (Castillo et al. 2013) that the heating column has its own dynamics, which are described by

$$\dot{\rho}_{\text{in}}(t) = -\frac{R\gamma A T_{\text{in}}(t)u(0,t)\rho(0,t)}{V_0 p_{\text{in}}(t)}\rho_{\text{in}}(t) - \frac{R}{V_0 C_v p_{\text{in}}(t)}\rho_{\text{in}}(t)dQ(t) + \frac{\gamma A u(0,t)\rho(0,t)}{V_0} \tag{5.2.2}$$

where R is the gas constant, V_0 is the volume of the heating column, γ is given by (5.2.1), T_{in} is the heating column input temperature, dQ is the heat exchange, and $\rho_{\text{in}}(t) = \rho(0,t)$ for all $t \geq 0$.
These dynamics have been considered in (Castillo et al. 2013) and are based on the

first law of thermodynamics and the perfect gases law. They express the variation rate of the input density in terms of several other variables and parameters, including the heat exchange which is the actual control input.

An initial condition is given for all $x \in [0,1]$ by

$$(\rho(x,0)\ \ u(x,0)\ \ p(x,0))^T = (\rho_0(x)\ \ u_0(x)\ \ p_0(x))^T.$$

This system can be linearized around any constant equilibrium of the form $(\rho^*\ \ u^*\ \ p^*)^T$ and becomes

$$\left\{\begin{array}{lcl} \frac{\partial \tilde{\rho}}{\partial t}(x,t) & = & -u^*\frac{\partial \tilde{\rho}}{\partial x}(x,t) - \rho^*\frac{\partial \tilde{u}}{\partial x}(x,t) \\ \frac{\partial \tilde{u}}{\partial t}(x,t) & = & -u^*\frac{\partial \tilde{u}}{\partial x}(x,t) - \frac{1}{\rho^*}\frac{\partial \tilde{p}}{\partial x}(x,t) \\ \frac{\partial \tilde{p}}{\partial t}(x,t) & = & -(a^*)^2\rho^*\frac{\partial \tilde{u}}{\partial x}(x,t) - u^*\frac{\partial \tilde{p}}{\partial x}(x,t) \end{array}\right.$$

where the new variables $\tilde{\rho} = \rho - \rho^*$, $\tilde{u} = u - u^*$ and $\tilde{p} = p - p^*$ represent the distance between the actual state variables and the corresponding equilibria.

5.2.2 Second model

In this section, the Poiseuille flow model is simplified further and reduced to two PDE's with appropriate boundary conditions. The variables considered for the second model are the gas density and the speed of the flow. In fact, since the pressure is nearly constant (see e.g. (Castillo et al. 2013),(Castillo et al. 2012)), the model can be simplified in order to take only these two variables into account.

The dynamics of the system are described by the following partial differential equations:

$$\left\{\begin{array}{lcl} \frac{\partial \rho}{\partial t}(x,t) & = & -u(x,t)\frac{\partial \rho}{\partial x}(x,t) - \rho(x,t)\frac{\partial u}{\partial x}(x,t) \\ \frac{\partial u}{\partial t}(x,t) & = & -u(x,t)\frac{\partial u}{\partial x}(x,t). \end{array}\right. \tag{5.2.3}$$

By using Bernoulli's equation in order to describe the pressure variation induced by the rotation of the input fan, the boundary conditions can be modelled as

$$\left\{\begin{array}{rcl} \rho(0,t) & = & \rho_{\text{in}}(t) \\ p_a + \frac{1}{2}\rho(0,t)u(0,t)^2 & = & K_n C_0(t)^2 \end{array}\right.$$

where p_a is the atmosphere pressure and K_n (kg/m) is a coefficient depending on the fan specification map.
We add the initial condition given for all $x \in [0,1]$ by

$$(\rho(x,0)\ \ u(x,0))^T = (\rho_0(x)\ \ u_0(x))^T.$$

Now, observe that the only equilibria that are continuous with respect to space are constant functions on the spatial domain $[0,1]$. These equilibria correspond to constant density and speed profiles that can be used as objectives for tracking problems, which

will be considered in Section 5.4. The system can be linearized around a constant equilibrium $(\rho^* \ u^*)^T$ and rewritten as

$$\left\{ \begin{array}{rcl} \frac{\partial \tilde{\rho}}{\partial t}(x,t) & = & -u^* \frac{\partial \tilde{\rho}}{\partial x}(x,t) - \rho^* \frac{\partial \tilde{u}}{\partial x}(x,t) \\ \frac{\partial \tilde{u}}{\partial t}(x,t) & = & -u^* \frac{\partial \tilde{u}}{\partial x}(x,t) \end{array} \right. \tag{5.2.4}$$

where the new variables $\tilde{\rho} = \rho - \rho^*$ and $\tilde{u} = u - u^*$ represent the distance between the actual state variables and the corresponding equilibria.
In order to keep the notations as simple as possible, in the sequel, when considering the linearized system, the variables will simply be denoted by ρ and u.

Remark 4 *A more complex model involves an additional constant term associated with the friction losses in the second equation of (5.2.3). Considering this term can lead to non-constant density and speed equilibria profiles. However, we do not consider this case here since the friction in the tube is very small and can be neglected.*

The boundary conditions can be simplified further and rewritten as

$$\left\{ \begin{array}{rcl} \rho(0,t) & = & \rho_{\text{in}}(t) \\ u(0,t) & = & u_{\text{in}}(t) \end{array} \right. \tag{5.2.5}$$

where u_{in} is an input depending on the fan specification map.

For technical reasons, we consider the slightly modified system

$$\left\{ \begin{array}{rcl} \frac{\partial \rho}{\partial t}(x,t) & = & -u^* \frac{\partial \rho}{\partial x}(x,t) - \rho^* \frac{\partial u}{\partial x}(x,t) \\ \frac{\partial u}{\partial t}(x,t) & = & -v^* \frac{\partial u}{\partial x}(x,t) \end{array} \right. \tag{5.2.6}$$

as an approximation of (5.2.4), where v^* is close to (but different from) u^*. The motivation for this choice will be detailed in Section 5.3.

5.3 Description: the Poiseuille flow as a BCBO system

This section aims at showing that one of the models for the Poiseuille flow system is well-posed and is a BCBO system (see Section 1.2).

5.3.1 BCBO formalism

As previously mentioned, in the sequel, we focus on the second model since the pressure variations inside the system can be neglected, though similar developments could be made for the first model. The system (5.2.4) with the corresponding boundary conditions can be written as the infinite-dimensional linear system (1.2.1)-(1.2.3) with $B_d = 0$ and where, for all $t \geq 0$,

$$x(t) = (\rho(\cdot,t) \ u(\cdot,t))^T,$$

$$u_b(t) = (\rho_{\text{in}}(t) \;\; u_{\text{in}}(t))^T$$

and

$$y(t) = (\rho(x_{\rho_1},t) \;\; \rho(x_{\rho_2},t) \;\; \rho(x_{\rho_3},t) \;\; u(x_s,t))^T,$$

with x_{ρ_1}, x_{ρ_2}, x_{ρ_3} the spatial positions of the density sensors and x_s the spatial position of the speed sensor.

We consider the state space $X = L^2(0,1) \oplus L^2(0,1)$, the boundary input space $U_b = \mathbb{R}^2$ and the output space $Y = \mathbb{R}^4$.
The operator $\mathscr{A} : D(\mathscr{A}) \subset X \to X$ is defined by

$$\mathscr{A} = \begin{pmatrix} -u^* \frac{d}{dx} & -\rho^* \frac{d}{dx} \\ 0 & -u^* \frac{d}{dx} \end{pmatrix}$$

on its domain

$$D(\mathscr{A}) = \{(\rho \;\; u)^T \in X : \rho, u \text{ are a. c., } \frac{d\rho}{dx}, \frac{du}{dx} \in L^2(0,1)\},$$

the boundary control operator $\mathscr{B} : D(\mathscr{B}) = D(\mathscr{A}) \to \mathbb{R}^2$ is defined by

$$\mathscr{B} \begin{pmatrix} \rho \\ u \end{pmatrix} = \begin{pmatrix} \rho(0) \\ u(0) \end{pmatrix}$$

for all $(\rho, u) \in D(\mathscr{B})$, and the observation operator $\mathscr{C} : D(\mathscr{C}) = D(\mathscr{A}) \to \mathbb{R}^4$ is given, for all $(\rho, u) \in D(\mathscr{C})$, by

$$\mathscr{C} \begin{pmatrix} \rho \\ u \end{pmatrix} = \begin{pmatrix} \rho(x_{\rho_1}) \\ \rho(x_{\rho_2}) \\ \rho(x_{\rho_3}) \\ u(x_s) \end{pmatrix}.$$

5.3.2 BCBO conditions

Unfortunately, the operator A corresponding to this differential system is not diagonalizable and it seems hard to show that it is the infinitesimal generator a C_0-semigroup on X. Several attempts have been made in order to demonstrate this, but none of them proved successful. The main tools that were used consist of the central results for the generation of contraction C_0-semigroups (Hille-Yosida, Lumer-Phillips) and the theory of perturbations of generators by unbounded operators, see e.g. (Engel and Nagel 2000), (Engel and Nagel 2006).

In order to solve this problem, we consider the system (5.2.6), for which the operator $\tilde{\mathscr{A}} : D(\tilde{\mathscr{A}}) \to X$ is defined by

$$\tilde{\mathscr{A}} = \begin{pmatrix} -u^* \frac{d}{dx} & -\rho^* \frac{d}{dx} \\ 0 & -v^* \frac{d}{dx} \end{pmatrix},$$

where $u^* \neq v^*$, and the dynamics generator $A : D(A) \subset X \to X$ is given by $Ax = \tilde{\mathscr{A}}x$ for all $x \in D(A)$, where

$$D(A) = \{(\rho,u) \in X : \rho,u \text{ are a. c., } \frac{d\rho}{dx}, \frac{du}{dx} \in L^2(0,1),\ \rho(0) = u(0) = 0\}.$$

Let us define the invertible transformation matrix

$$S = \begin{pmatrix} 1 & \frac{\rho^*}{v^*-u^*} \\ 0 & 1 \end{pmatrix}. \tag{5.3.1}$$

It is well-known that the operator

$$S^{-1}AS = \begin{pmatrix} -u^* \frac{d}{dx} & 0 \\ 0 & -v^* \frac{d}{dx} \end{pmatrix} \tag{5.3.2}$$

on its domain

$$\begin{aligned} D(S^{-1}AS) &= \{(\rho,u) \in X : S(\rho,u) \in D(A)\} \\ &= D(A) \end{aligned}$$

is the infinitesimal generator of a contraction C_0-semigroup on X, see e.g. (Jacob and Zwart 2012), (Curtain and Zwart 1995).
Hence A is the generator of a C_0-semigroup as well, see e.g. (Jacob and Zwart 2012, Exercise 5.4., p. 63), and condition **[C1]** holds.

Moreover, condition **[C2]** is satisfied with $B_b \in \mathscr{L}(\mathbb{R}^2, X)$ defined for all $u_b = (\rho_{\text{in}}\ u_{\text{in}})^T \in \mathbb{R}^2$ by

$$\begin{aligned} B_b u_b &= B_b \begin{pmatrix} \rho_{\text{in}} \\ u_{\text{in}} \end{pmatrix} \\ &= \begin{pmatrix} 1(\cdot)\rho_{\text{in}} \\ 1(\cdot)u_{\text{in}} \end{pmatrix}. \end{aligned}$$

In fact, it is easy to see that for all $u_b = (\rho_{\text{in}}\ u_{\text{in}})^T \in U_b = \mathbb{R}^2$, $B_b u_b \in D(\mathscr{A})$ and

$$\begin{aligned} \mathscr{B}B_b u_b &= \mathscr{B} \begin{pmatrix} 1(\cdot)\rho_{\text{in}} \\ 1(\cdot)u_{\text{in}} \end{pmatrix} \\ &= \begin{pmatrix} 1(0)\rho_{\text{in}} \\ 1(0)u_{\text{in}} \end{pmatrix} \\ &= \begin{pmatrix} \rho_{\text{in}} \\ u_{\text{in}} \end{pmatrix} \\ &= u_b. \end{aligned}$$

Moreover,

$$\mathscr{A}B_b = 0 \in \mathscr{L}(U_b, X),$$

which shows that the associated extended dynamics generator has the rather simple structure

$$A^e = \begin{pmatrix} 0 & 0 & 0 \\ 0 & A & 0 \\ 0 & C_\alpha A & 0 \end{pmatrix}.$$

It should be noted that one entry of the operator B_b can be zero if the corresponding input variable is fixed (e.g. at some equilibrium value) and is not used as a control variable. Moreover, as is usually the case for BCBO systems, the choice for B_b is not unique. In fact, any function f on $[0,1]$ satisfying $f(0) = 1$ and $\frac{df}{dx} \in L^2(0,1)$ could be used instead of the step function. However, a choice other than the simple step functions may lead to additional difficulties, including the fact that the operator $\mathscr{A}B_b$ could be different from zero.

Finally, observe that for all $i \in \{1,2,3\}$, there exists $f_i \in X$ such that

$$\rho(x_{\rho_i}) = \langle f_i, (I-A)(\rho,u)\rangle. \tag{5.3.3}$$

For that purpose, observe that, if $f_i = (f_{i_1}, f_{i_2}) \in X$ is such that f_{i_1} and f_{i_2} are differentiable functions with support on $[0,x_{\rho_i}]$, (5.3.3) can be rewritten as

$$\int_0^{x_{\rho_i}} \left[\rho(x) + u^* \frac{d\rho}{dx}(x) + \rho^* \frac{du}{dx}(x)\right] f_{i_1}(x)dx + \int_0^{x_{\rho_i}} \left[u(x) + v^* \frac{du}{dx}(x)\right] f_{i_2}(x)dx = \rho(x_{\rho_i}),$$

which becomes, after an integration by parts of the terms involving the derivatives of ρ and u and using the conditions of $D(A)$,

$$\begin{aligned} &\int_0^{x_{\rho_i}} \rho(x) f_{i_1}(x)dx + u^* f_{i_1}(x_{\rho_i})\rho(x_{\rho_i}) - u^* \int_0^{x_{\rho_i}} \rho(x) \frac{df_{i_1}}{dx}(x)dx + \rho^* f_{i_1}(x_{\rho_i}) u(x_{\rho_i}) \\ -\rho^* &\int_0^{x_{\rho_i}} u(x) \frac{df_{i_1}}{dx}(x)dx + \int_0^{x_{\rho_i}} u(x) f_{i_2}(x)dx + v^* f_{i_2}(x_{\rho_i}) u(x_{\rho_i}) - v^* \int_0^{x_{\rho_i}} u(x) \frac{df_{i_2}}{dx}(x)dx \\ &= \rho(x_{\rho_i}). \end{aligned}$$

Hence, we look at a function $f_i \in X$ such that, for all $x \in [0,x_{\rho_i}]$,

$$\begin{cases} f_{i_1}(x) - u^* \frac{df_{i_1}}{dx}(x) = 0 \\ u^* f_{i_1}(x_{\rho_i}) = 1 \end{cases}$$

and

$$\begin{cases} f_{i_2}(x) - v^* \frac{df_{i_2}}{dx}(x) = \rho^* \frac{df_{i_1}}{dx}(x) \\ v^* f_{i_2}(x_{\rho_i}) + \frac{\rho^*}{u^*} = 0. \end{cases}$$

Using the general solution of the first homogeneous differential equation in the second inhomogeneous one, we obtain $f_i = (f_{i_1}, f_{i_2})$ where, for almost all $x \in [0,x_{\rho_i}]$,

$$f_{i_1}(x) = \frac{1}{u^*} e^{\frac{x-x_{\rho_i}}{u^*}},$$

and

$$f_{i_2}(x) = \frac{\rho^*}{v^*(v^*-u^*)} e^{\frac{x-x_{\rho_i}}{v^*}} - \frac{\rho^*}{u^*(v^*-u^*)} e^{\frac{x-x_{\rho_i}}{u^*}},$$

and, for almost all $x \in [x_{\rho_i}, 1]$,

$$f_{i_1}(x) = f_{i_2}(x) = 0.$$

Similarly, there exists $f = (f_1, f_2) \in X$ given, for almost all $x \in [0, x_s]$ by

$$f_1(x) = 0$$

and

$$f_2(x) = \frac{1}{v^*} e^{\frac{x-x_s}{v^*}},$$

and, for almost all $x \in [x_s, 1]$,

$$f_1(x) = f_2(x) = 0,$$

such that

$$u(x_s) = \langle f, (I-A)(\rho, u) \rangle.$$

Then, by taking the max norm on Y, we see that, for all $(\rho, u) \in D(A)$,

$$\begin{aligned} \left\| \mathscr{C} \begin{pmatrix} \rho \\ u \end{pmatrix} \right\| &= \max \left\{ \left| \left\langle \begin{pmatrix} f_{1_1} \\ f_{1_2} \end{pmatrix}, (I-A) \begin{pmatrix} \rho \\ u \end{pmatrix} \right\rangle \right|, \left| \left\langle \begin{pmatrix} f_{2_1} \\ f_{2_2} \end{pmatrix}, (I-A) \begin{pmatrix} \rho \\ u \end{pmatrix} \right\rangle \right|, \\ &\quad \left| \left\langle \begin{pmatrix} f_{3_1} \\ f_{3_2} \end{pmatrix}, (I-A) \begin{pmatrix} \rho \\ u \end{pmatrix} \right\rangle \right|, \left| \left\langle \begin{pmatrix} f_1 \\ f_2 \end{pmatrix}, (I-A) \begin{pmatrix} \rho \\ u \end{pmatrix} \right\rangle \right| \Bigg\} \\ &\leq \max\{\|f_1\|, \|f_2\|, \|f_3\|, \|f\|\} \left(\left\| A \begin{pmatrix} \rho \\ u \end{pmatrix} \right\| + \left\| \begin{pmatrix} \rho \\ u \end{pmatrix} \right\| \right). \end{aligned}$$

Hence, condition **[C3]** holds.

Concerning the dynamical properties of the extended system, it can be shown that the spectrum of the operator A is empty and the nominal system is stable, which implies that $\sigma(A^e) = \{0\}$. The instability of the extended system only originates from the dynamics corresponding to the boundary inputs.
Moreover, with both boundary inputs, the nominal system is exactly controllable and this property is transmitted to the main part of the dynamics of the extended system. Again, as for the parabolic CDR system, this property is of particular interest since solving the problem of spectral factorization of an appropriate spectral density and the corresponding Diophantine equation provides the restriction of the optimal feedback to the reachable subspace.

Similar developments can be made for the second model, which can be diagonalized and expressed in the BCBO formalism as well. However, in the sequel, we focus on the second model since, as mentioned earlier, it can be observed that the pressure is nearly constant and can be removed from the model without losing any significant information.

5.4 Control

Fluid or gas transport is at the heart of many industrial applications, including for example gas flow in pipelines or ventilation systems in deep pits and mines that regulate air quality and temperature for workers. These processes require adapted control in order to ensure proper behaviour or people's safety. We are now interested in designing control laws for the nominal and extended models presented in the previous sections. These control laws will be based on the resolution of a LQ-optimal control problem again. As previously mentioned, the tools related to this problem and its resolution are relatively well-understood and mastered in the framework of distributed parameter systems. The main objective here consists of regulating the temperature or hygrometry of the gas transported by the air flow in the tube. In addition, by controlling the rotating speed of one or both fans, the speed of the flow can be regulated as well. More precisely, the goal is to track desired temperature, hygrometry or speed profiles and measuring the effectiveness of this tracking with the sensors in the tube.
This section provides control laws derived from the nominal Poiseuille flow model or from its BCBO model.

5.4.1 First approach: boundary control extension with bounded observation

In this section, we consider that the fans operate at a constant speed and the only control action is the inlet temperature which is regulated via the heating column. In addition, we consider that the whole state is penalized in the cost functional. This implies that the extension can be performed in order to include the boundary input in the extended state, but the approximate output operator C_α is not required.

The first step consists of considering the diagonalized system based on the operator (5.3.2), where the change of variables is given by (5.3.1). Observe that, with only the inlet temperature being controlled directly, the boundary control operator $\mathscr{B}$ is not affected by the change of variables and is given by

$$\mathscr{B}\begin{pmatrix}\rho\\ u\end{pmatrix} = \rho(0).$$

Lemma 5.4.1 *Consider the extended Poiseuille flow system with the bounded observation operator given by*

$$C^e = \begin{pmatrix}\rho_1 I & 0\\ \rho_2 B_b & \rho_2 S\end{pmatrix}.$$

Then the spectral density (3.2.4) associated with an appropriate right coprime fraction of the form (3.2.5)-(3.2.6) is

$$\hat{F}^e(s) = \frac{\rho_1^2+\rho_2^2-s^2}{k^2-s^2}, \tag{5.4.1}$$

where $k > 0$, and the standard (i.e. such that $\hat{R}^e(\infty) = I$) spectral factor of $\hat{F}^e(s)$ is given by

$$\hat{R}^e(s) = \frac{s + \sqrt{\rho_1^2 + \rho_2^2}}{s+k}. \tag{5.4.2}$$

Proof. In this case, the operator B_b is given by

$$B_b \begin{pmatrix} \rho_{\text{in}} \\ u_{\text{in}} \end{pmatrix} = \begin{pmatrix} 1(\cdot)\rho_{\text{in}} \\ 0 \end{pmatrix}.$$

Since $\mathscr{A}B_b = 0$, the extended dynamics generator is given by

$$A^e = \begin{pmatrix} 0 & 0 \\ 0 & A \end{pmatrix},$$

and the bounded control operator is

$$B^e = \begin{pmatrix} I \\ -B_b \end{pmatrix}.$$

A straightforward computation reveals that the resolvent operator of A (from which we easily deduce the resolvent operator of A^e) has the form

$$\left[(sI - A)^{-1} \begin{pmatrix} \rho \\ u \end{pmatrix} \right](x) = \begin{pmatrix} \frac{1}{u^*} \int_0^x e^{\frac{s}{u^*}(\xi - x)} \rho(\xi) d\xi \\ \frac{1}{v^*} \int_0^x e^{\frac{s}{v^*}(\xi - x)} u(\xi) d\xi \end{pmatrix}$$

for all $(\rho \ \ u)^T \in X$ and all $x \in [0,1]$.
Then we find, for all $u_b \in U_b$ and all $x \in [0,1]$,

$$\begin{aligned} \left[(sI - A)^{-1} B_b u_b \right](x) &= \begin{pmatrix} \frac{1}{u^*} \left[\int_0^x e^{\frac{s}{u^*}(\xi - x)} 1(\xi) d\xi \right] u_b \\ 0 \end{pmatrix} \\ &= \begin{pmatrix} \frac{1}{s} \left(1 - e^{-\frac{s}{u^*}x} \right) u_b \\ 0 \end{pmatrix}. \end{aligned}$$

We can then compute

$$\begin{aligned} \hat{G}^e(s) &= C^e (sI - A^e)^{-1} B^e \\ &= \begin{pmatrix} \rho_1 \frac{1}{s} I \\ \rho_2 \left(\frac{1}{s} S B_b - S(sI - A)^{-1} B_b \right) \end{pmatrix} \\ &= \begin{pmatrix} \rho_1 \frac{1}{s} I \\ \rho_2 \frac{1}{s} e^{-\frac{s}{u^*} \cdot} \\ 0 \end{pmatrix}. \end{aligned}$$

A right coprime fraction of $\hat{G}^e(s)$ is given by

$$\begin{aligned}\hat{N}^e(s) &= \begin{pmatrix} \rho_1 \frac{1}{s+k} I \\ \rho_2 \frac{1}{s+k} e^{-\frac{s}{u^*}\cdot} \\ 0 \end{pmatrix} \\ \hat{D}^e(s) &= \frac{s}{s+k}\end{aligned}$$

with $k > 0$, and the corresponding spectral density is

$$\begin{aligned}\hat{F}^e(s) &= \hat{N}^e_*(s)\hat{N}^e(s) + \hat{D}^e_*(s)\hat{D}^e(s) \\ &= \rho_1 \frac{1}{k-s}\rho_1 \frac{1}{k+s} + \rho_2 \frac{1}{k-s}\rho_2 \frac{1}{k+s} \int_0^1 e^{\frac{s}{u^*}x} e^{-\frac{s}{u^*}x} dx + \frac{-s}{k-s}\frac{s}{k+s} \\ &= \frac{\rho_1^2 + \rho_2^2 - s^2}{k^2 - s^2},\end{aligned}$$

which shows (5.4.1).

Finally, it can easily be seen that the spectral factor $\hat{R}^e \in H^\infty(\mathscr{L}(U_b))$ given by (5.4.2) satisfies $(\hat{R}^e)^{-1} \in H^\infty(\mathscr{L}(U_b))$ and for all $\omega \in \mathbb{R}$,

$$\hat{F}^e(j\omega) = \hat{R}^e_*(j\omega)\hat{R}^e(j\omega).$$

■

The following results provide the solution of the LQ-optimal control problem for the extended Poiseuille flow system. Moreover, the optimal dynamical feedback law can easily be converted into a nonlinear static state feedback law due to the the fact that the heating column has its own dynamics. In fact, this dynamical feedback establishes a direct link between the inlet density and its derivative with respect to time and can be plugged in the dynamics of the heating column given by (5.2.2) in order to establish a static relationship.

Lemma 5.4.2 *The solution of the LQ-optimal control control problem (3.1.1) with the cost functional (3.1.2) for the extended Poiseuille flow system is given by the optimal feedback*

$$K_0^e = \begin{pmatrix} -\sqrt{\rho_1^2 + \rho_2^2} & 0 & 0 \end{pmatrix}. \tag{5.4.3}$$

Proof. With the spectral factor (5.4.2), the Diophantine equation reads

$$\mathscr{U}\frac{s}{s+k} + \begin{pmatrix} \mathscr{V}_1 & \mathscr{V}_2 & \mathscr{V}_3 \end{pmatrix} \begin{pmatrix} \frac{1}{s+k} \\ \frac{1}{s+k}\left(e^{-\frac{s}{u^*}\cdot} - 1(\cdot)\right) \\ 0 \end{pmatrix} = \frac{s + \sqrt{\rho_1^2 + \rho_2^2}}{s+k}$$

where $\mathscr{U} = 1$ is a scalar unitary operator, $\mathscr{V}_1$ is a scalar operator and $\mathscr{V}_2$ and $\mathscr{V}_3$ are operators from $L^2(0,1)$ to $\mathbb{R}$.

This equation is equivalent to

$$\mathscr{V}_1 + \mathscr{V}_2 \left(e^{-\frac{s}{u^*}\cdot} - 1(\cdot) \right) = \sqrt{\rho_1^2 + \rho_2^2}. \tag{5.4.4}$$

Since $\mathscr{V}$ cannot depend on s, an obvious solution to this equation is

$$\mathscr{V}_1 = \sqrt{\rho_1^2 + \rho_2^2}, \quad \mathscr{V}_2 = \mathscr{V}_3 = 0,$$

which gives the optimal feedback operator (5.4.3). ■

Since only the heating column is used as an actuator in this case, the system is not reachable and the solution of the Diophantine equation is not unique. However, the system is reachable if at least one fan is used as an actuator as well, which guarantees the uniqueness of the solution.

Theorem 5.4.3 *The dynamical feedback law for the extended system can be interpreted as the non-linear static boundary state feedback for the nominal system*

$$dQ(t) = \frac{1}{R} \left(\sqrt{\rho_1^2 + \rho_2^2} V_0 C_v p_{in}(t) - RC_p A T_{in}(t) u(0,t) \rho(0,t) + C_p A p_{in}(t) u(0,t) \right) \tag{5.4.5}$$

for all $t \geq 0$.

Proof. By Lemma 5.4.2 combined with 3.2.14, the optimal feedback law is given by the dynamic compensator

$$\dot{\rho}_{\text{in}}(t) = -\sqrt{\rho_1^2 + \rho_2^2} \rho_{\text{in}}(t)$$

for all $t \geq 0$.
Hence we deduce from (5.2.2) that the corresponding heat exchange control input dQ must be given by (5.4.5). ■

In a standard testing environment, the inlet temperature T_{in} is the ambient temperature and the inlet pressure p_{in} is the atmospheric pressure, so both can be easily measured. The speed and density at 0 can be computed with the knowledge of the current heating column and fan inputs, or with a state observer.

Remark 5 *It should be noted that, thanks to the diagonalization process, the problem can be easily solved with the inlet air flow being controlled as well. In fact, even though the spectral density becomes a* 2×2 *matrix-valued function, it is diagonal as well, with the diagonal entries having the same structure as (5.4.1). More precisely, the spectral density is given by*

$$\hat{F}^e(s) = \begin{pmatrix} \frac{\rho_1^2 + \rho_2^2 - s^2}{k^2 - s^2} & 0 \\ 0 & \frac{\rho_1^2 + \rho_2^2 - s^2}{k^2 - s^2} \end{pmatrix}$$

and a spectral factor can be computed as

$$\hat{R}^e(s) = \begin{pmatrix} \frac{s+\sqrt{\rho_1^2+\rho_2^2}}{s+k} & 0 \\ 0 & \frac{s+\sqrt{\rho_1^2+\rho_2^2}}{s+k} \end{pmatrix}.$$

With $\mathscr{U} = I$, solving the corresponding Diophantine equation amounts to solving (5.4.4) for both inputs.
The optimal feedback operator is then given by

$$K_0^e = \begin{pmatrix} -\sqrt{\rho_1^2+\rho_2^2} & 0 & 0 & 0 \\ 0 & -\sqrt{\rho_1^2+\rho_2^2} & 0 & 0 \end{pmatrix}.$$

Again, since this feedback operator has been designed for the extended system, it also establishes a link between the input air speed and its derivative with respect to time. Hence, in a practical application, a dynamical feedback law has to be implemented for the regulation of the fan rotating speed.

Figures 5.2 - 5.5 illustrate the numerical behaviour of the closed-loop trajectories for the linearized and the nonlinear system. In figures 5.2 and 5.4, it is seen that the closed-loop trajectories converge to a desired constant equilibrium profile represented by the zero function. When applied to the nonlinear system, the feedback law yields similar results, though the state trajectories are more prone to sharp variations, which can be explained partially by the nonlinearities themselves and partially by the sensitivity of the chosen integration scheme with respect to the spatial discretization.

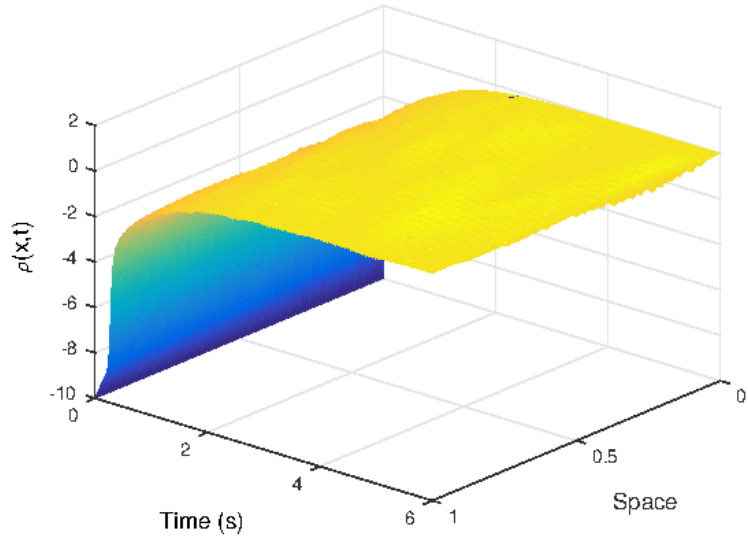

Figure 5.2: Closed-loop density $\rho(t)$ for the linearized model

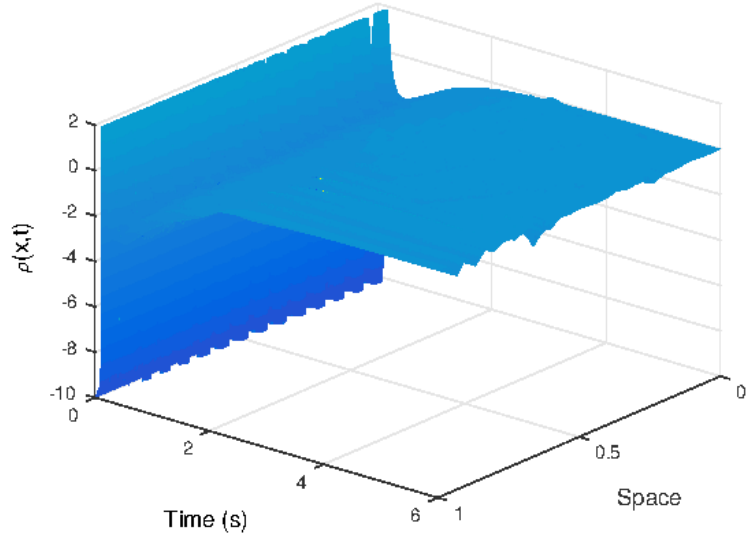

Figure 5.3: Closed-loop density $\rho(t)$ for the nonlinear model

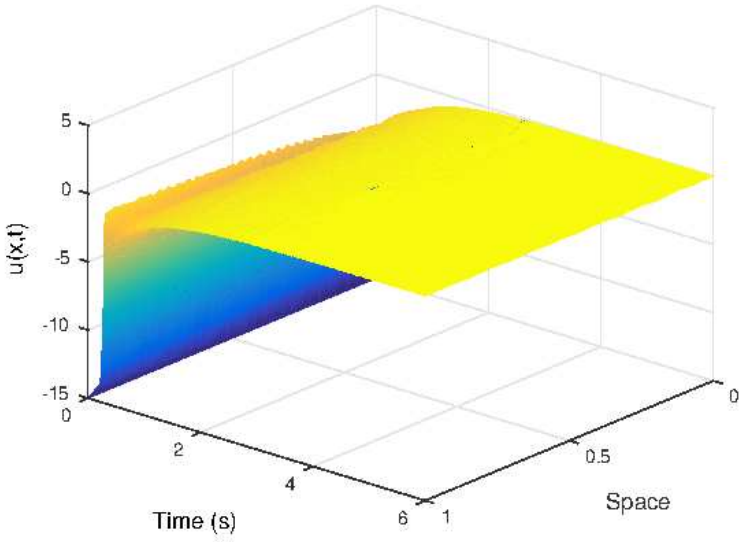

Figure 5.4: Closed-loop speed $u(t)$ for the linearized model

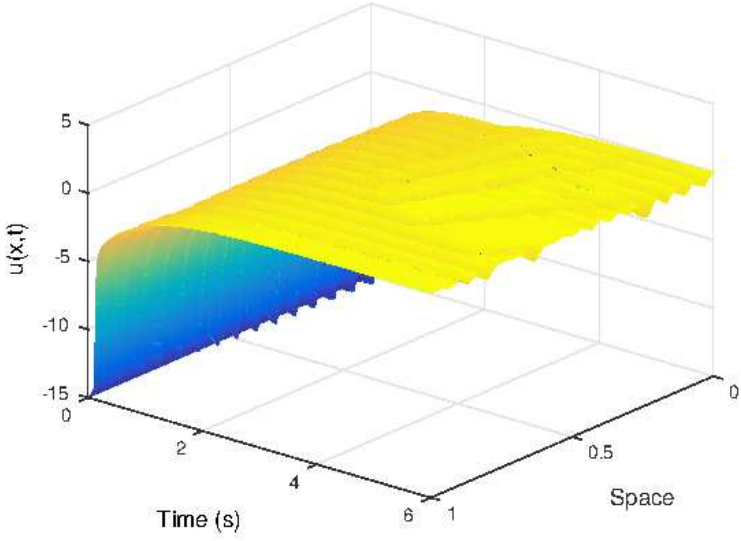

Figure 5.5: Closed-loop speed $u(t)$ for the nonlinear model

5.4.2 Second approach: nominal system

In this section, we follow the general methodology of resolution of the LQ-optimal control problem by performing formal computations on the nominal system with unbounded operators. More precisely, we penalize the density measured at the end of the tube by the third temperature/hygrometry sensor (located at x_{ρ_3}) and the particle speed measured by the speed sensor (located at x_s). No extension of the system is involved here.

The transfer function, right coprime fraction and spectral density can be computed explicitely for the second model.
In fact, taking the Laplace transform of the second equation of (5.2.6) and combining it with the second input equation of (5.2.5) yields

$$\hat{u}(x,s) = e^{-\frac{s}{v^*}x}\hat{u}_{\text{in}}(s). \tag{5.4.6}$$

By taking the Laplace transform of the first equation of (5.2.6) and plugging (5.4.6) into it, we obtain the differential equation

$$\frac{d\hat{\rho}(x,s)}{dx} + \frac{s}{u^*}\hat{\rho}(x,s) + \frac{\rho^*}{u^*v^*}se^{-\frac{s}{v^*}x}\hat{u}_{\text{in}}(s) = 0.$$

Solving this differential equation yields

$$\hat{\rho}(x,s) = Ce^{-\frac{s}{u^*}x} + \frac{\rho^*}{v^*-u^*}e^{-\frac{s}{v^*}x}\hat{u}_{\text{in}}(s),$$

which, combined with the first input equation of (5.2.5), gives

$$\hat{\rho}(x,s) = e^{-\frac{s}{u^*}x}\hat{\rho}_{\text{in}}(s) + \frac{\rho^*}{v^*-u^*}\left(e^{-\frac{s}{v^*}x} - e^{-\frac{s}{u^*}x}\right)\hat{u}_{\text{in}}(s).$$

By taking the Laplace transform of the output equation

$$y(t) = \begin{pmatrix} \rho(x_{\rho_3}) \\ u(x_s) \end{pmatrix},$$

we can then compute the transfer function, which is given by

$$\hat{G}(s) = \begin{pmatrix} \rho_1 e^{-\frac{x_{\rho_3}}{u^*}s} & \rho_1\frac{\rho^*}{v^*-u^*}\left(e^{-\frac{x_{\rho_3}}{v^*}s} - e^{-\frac{x_{\rho_3}}{u^*}s}\right) \\ 0 & \rho_2 e^{-\frac{x_s}{v^*}s} \end{pmatrix}.$$

Since this transfer function is stable, the spectral density is given by

$$\hat{F}(s) = I + \hat{G}_*(s)\hat{G}(s) =$$

$$\begin{pmatrix} 1+\rho_1^2 & \rho_1^2\frac{\rho^*}{u^*-v^*}\left(e^{\frac{(u^*-v^*)x_{\rho_3}}{u^*v^*}s} - 1\right) \\ \rho_1^2\frac{\rho^*}{u^*-v^*}\left(e^{-\frac{(u^*-v^*)x_{\rho_3}}{u^*v^*}s} - 1\right) & 1+\rho_1^2\frac{(\rho^*)^2}{(u^*-v^*)^2}\left(2 - e^{-\frac{(u^*-v^*)x_{\rho_3}}{u^*v^*}s} - e^{\frac{(u^*-v^*)x_{\rho_3}}{u^*v^*}s}\right) + \rho_2^2 \end{pmatrix}.$$

One can easily check that a spectral factor $\hat{R}$ satisfying $\hat{R} \in H^\infty(\mathscr{L}(\mathbb{R}^2))$, $\hat{R}^{-1} \in H^\infty(\mathscr{L}(\mathbb{R}^2))$ and for all $\omega \in \mathbb{R}$,

$$\hat{F}(j\omega) = \hat{R}_*(j\omega)\hat{R}(j\omega)$$

is given by

$$\hat{R}(s) = \begin{pmatrix} \sqrt{1+\rho_1^2}e^{-\frac{x\rho_3}{u^*}s} & \frac{\rho_1^2}{\sqrt{1+\rho_1^2}}\frac{\rho^*}{v^*-u^*}\left(e^{-\frac{x\rho_3}{v^*}s} - e^{-\frac{x\rho_3}{u^*}s}\right) \\ 0 & \sqrt{1+\rho_2^2}e^{-\frac{(u^*+v^*)x\rho_3}{2u^*v^*}s} + \frac{\rho_1}{\sqrt{1+\rho_1^2}}\frac{\rho^*}{v^*-u^*}\left(e^{-\frac{x\rho_3}{v^*}s} - e^{-\frac{x\rho_3}{u^*}s}\right) \end{pmatrix}.$$

The Diophantine equation then reads

$$\begin{pmatrix} \mathscr{U}_{11} & \mathscr{U}_{12} \\ \mathscr{U}_{21} & \mathscr{U}_{22} \end{pmatrix} + \begin{pmatrix} \mathscr{V}_{11} & \mathscr{V}_{12} \\ \mathscr{V}_{21} & \mathscr{V}_{22} \end{pmatrix} \begin{pmatrix} e^{-\frac{s}{u^*}\cdot} & \frac{\rho^*}{v^*-u^*}\left(e^{-\frac{s}{v^*}\cdot} - e^{-\frac{s}{u^*}\cdot}\right) \\ 0 & e^{-\frac{s}{v^*}\cdot} \end{pmatrix}$$

$$= \begin{pmatrix} \sqrt{1+\rho_1^2}e^{-\frac{x\rho_3}{u^*}s} & \frac{\rho_1^2}{\sqrt{1+\rho_1^2}}\frac{\rho^*}{v^*-u^*}\left(e^{-\frac{x\rho_3}{v^*}s} - e^{-\frac{x\rho_3}{u^*}s}\right) \\ 0 & \sqrt{1+\rho_2^2}e^{-\frac{(u^*+v^*)x\rho_3}{2u^*v^*}s} + \frac{\rho_1}{\sqrt{1+\rho_1^2}}\frac{\rho^*}{v^*-u^*}\left(e^{-\frac{x\rho_3}{v^*}s} - e^{-\frac{x\rho_3}{u^*}s}\right) \end{pmatrix}.$$

This time, since we are working with the nominal system with unbounded operators, we are looking for an unbounded solution of the Diophantine equation. Such a solution is given by the unitary operator

$$\mathscr{U} = \begin{pmatrix} \frac{\sqrt{2}}{2} & \frac{\sqrt{2}}{2} \\ \frac{\sqrt{2}}{2} & -\frac{\sqrt{2}}{2} \end{pmatrix}$$

and the unbounded operator $\mathscr{V}$ described by

$$\begin{aligned}
\mathscr{V}_{11}f &= \sqrt{1+\rho_1^2}f(x_{\rho_3}) - \frac{\sqrt{2}}{2}f(0) \\
\mathscr{V}_{12}f &= -\frac{1}{\sqrt{1+\rho_1^2}}\frac{\rho^*}{v^*-u^*}\left[f(x_{\rho_3}) - f\left(\frac{v^*}{u^*}x_{\rho_3}\right)\right] - \frac{\sqrt{2}}{2}f(0) \\
\mathscr{V}_{21}f &= -\frac{\sqrt{2}}{2}f(0) \\
\mathscr{V}_{22}f &= \sqrt{1+\rho_2^2}f\left(\frac{u^*+v^*}{2u^*}x_{\rho_3}\right) + \frac{\rho_1}{\sqrt{1+\rho_1^2}}\frac{\rho^*}{v^*-u^*}\left[f(x_{\rho_3}) - f\left(\frac{v^*}{u^*}x_{\rho_3}\right)\right] \\
&\quad + \frac{\sqrt{2}}{2}f(0).
\end{aligned}$$

Even though the corresponding feedback seems rather complicated at first glance, it can be approximated by a much simpler operator. Indeed, the speed equilibria u^* and

v^* are supposed to be close and were only considered as different for technical reasons. By letting v^* go to u^*, the operators $\mathscr{V}_{12}$ and $\mathscr{V}_{22}$ can be approximated as

$$\mathscr{V}_{12} f \approx -\frac{\sqrt{2}}{2} f(0).$$

and

$$\mathscr{V}_{22} f \approx \sqrt{1+\rho_2^2} f(x_{\rho_3}) + \frac{\sqrt{2}}{2} f(0).$$

The feedback operator can then be approximated as

$$\begin{aligned} K_0 \begin{pmatrix} \rho \\ u \end{pmatrix} &= -\mathscr{U}^* \mathscr{V} \begin{pmatrix} \rho \\ u \end{pmatrix} \\ &\approx \begin{pmatrix} -\frac{\sqrt{2}}{2}\sqrt{1+\rho_1^2}\rho(x_{\rho_3}) - \frac{\sqrt{2}}{2}\sqrt{1+\rho_2^2}u(x_{\rho_3}) + \rho(0) \\ -\frac{\sqrt{2}}{2}\sqrt{1+\rho_1^2}\rho(x_{\rho_3}) - \frac{\sqrt{2}}{2}\sqrt{1+\rho_2^2}u(x_{\rho_3}) + u(0) \end{pmatrix}. \end{aligned}$$

Finally, we obtain the following effective feedback law:

$$\begin{pmatrix} \rho_{\text{in}}(t) \\ u_{\text{in}}(t) \end{pmatrix} = \begin{pmatrix} -\frac{\sqrt{2}}{2}\sqrt{1+\rho_1^2}[\rho(x_{\rho_3},t) - \rho^*] - \frac{\sqrt{2}}{2}\sqrt{1+\rho_2^2}[u(x_{\rho_3},t) - u^*] + \rho(0,t) \\ -\frac{\sqrt{2}}{2}\sqrt{1+\rho_1^2}[\rho(x_{\rho_3},t) - \rho^*] - \frac{\sqrt{2}}{2}\sqrt{1+\rho_2^2}[u(x_{\rho_3},t) - u^*] + u(0,t) \end{pmatrix}.$$

Even though these relations make sense from a purely mathematical point of view, they are not realistic for a practical implementation. Indeed, both $\rho_{\text{in}}(t)$ and $u_{\text{in}}(t)$ are cancelled in these equations due to the boundary conditions (5.2.5), forcing the outlet density and speed to go to the corresponding equilibria immediately, which is physically impossible. However, around the equilibrium, the inlet density and speed can be estimated by ρ^* and u^*, respectively, yielding a physically realistic control law at the expense of a slightly suboptimal behaviour during the rise time (and the peak time when applicable).
Finally, the proportional output feedback law given by

$$\begin{pmatrix} \rho_{\text{in}}(t) \\ u_{\text{in}}(t) \end{pmatrix} = \begin{pmatrix} -\frac{\sqrt{2}}{2}\sqrt{1+\rho_1^2}[\rho(x_{\rho_3},t) - \rho^*] - \frac{\sqrt{2}}{2}\sqrt{1+\rho_2^2}[u(x_{\rho_3},t) - u^*] + \rho^* \\ -\frac{\sqrt{2}}{2}\sqrt{1+\rho_1^2}[\rho(x_{\rho_3},t) - \rho^*] - \frac{\sqrt{2}}{2}\sqrt{1+\rho_2^2}[u(x_{\rho_3},t) - u^*] + u^* \end{pmatrix} \tag{5.4.7}$$

can be implemented and the behaviour of the closed-loop system can be observed by using the available sensors.
This feedback law can be interpreted as the fact that the input hygrometry and particle speed (and thus the inlet fan speed) must be proportional to the distance between the outlet hygrometry and speed and the chosen equilibria, where the proportionality coefficients depend on the weighting parameters in the cost functional.
The corresponding controller has been implemented on the test bench and yielded the results presented in Section 5.5. These results illustrate the stabilization properties of the obtained static feedback for the nominal system.

5.5 Experimental results

This section shows some of the experimental results obtained with the experimental setup of the GIPSA-LAB in Grenoble.

Several difficulties were encountered while working with this setup. First, due to the heat melting some plastic parts in the heating column, it was heavily discouraged to use it as an actuator. This technical problem combined with the very slow dynamics of the heating column motivated the choice of moisture control instead. Moreover, though relatively close to the C programming language, the LADDER language required some learning before being used to reprogram the provided tools. In addition, the graphical interface is not intended to be modified easily in order to incorporate additional control methods or other tools. Doing so would have required learning the Visual Basic language from scratch. A compromise then had to be found, which involved the reprogramming of the existing PID and R-S-T methods and altering their input variables in order to use the fans as actuators, since this is not allowed by the provided tools.

Despite these technical hurdles, the feedback law computed in the previous section proved effective when implemented on the test bench. It allowed the tracking of a desired hygrometry profile while using both the rotation speed of the first fan and the moisture injector as actuators.

The experiments were performed by using the following methodology, with which they can easily be reproduced. Note that it is highly recommended to make a backup copy of the original program implemented in the automaton before overwriting it.

1. Activate the power supply of the test bench and the automaton by turning the general switch on the side of the test bench to ON.
2. Start up the system by pressing the green switch on the front of the test bench.
3. Boot up the computer connected to the automaton.
4. Launch the *CX-programmer* software in programmer mode and select the file "FlowControl.cxp". Then replace the contents of the PID functional block called "BlocFunction_Controleur_PID" by the new code for the control law given by (5.4.7). Note that the equilibrium u^*, as well as the weighting parameters ρ_1 and ρ_2, have to be modified in the code if necessary.
5. Successively click on the buttons called "Travail Online" and "Transférer vers API" in the task bar in order to transfer the modified program to the automaton.
6. Launch the *Flow control test bench* software and choose "PID" in the box called "Type of control".

7. Configure the equilibrium ρ^* by entering the desired value in the box called "Setpoint", click on "Validation" and then on "Run / Stop".

Between each test, it is recommended to click on the button called "Cooling demand", which activates both fans at their fastest rotating speed in order to eliminate any residual artificial humidity in the tube.

The experiments were realized in standard environmental conditions (temperature around 25 C$^\circ$ with slight variations during the experimental process, humidity around 26.3% and no external perturbations around the test bench).
Three experiments were performed with different values of the tracked hygrometry and speed profiles, denoted by ρ^* and u^*, respectively, as well as different values of the weighting parameters ρ_1 and ρ_2 penalizing the hygrometry and speed components of the state, respectively.
The following figures illustrate the convergence of the hygrometry of the Poiseuille flow towards the selected equilibria profiles, represented by horizontal red lines, with normalized weight parameters for the inputs in the cost functional, as well as the behaviour of the gas velocity measured by the speed sensor and of the corresponding inputs. The results are systematically illustrated first on a time interval of 30 seconds, which is the fastest time in which a steady state was attained in the fourth experiment, in order to allow a direct comparison between the results. Longer time intervals are also presented here for the slower three first experiments.
Due to the physical limitations of the process (including limitations of the mist injector), it is difficult to reach hygrometry values above around 31%.
For each experiment, the parameters, limitations and environmental conditions are summarized in a table before the corresponding figures. The fan rotating speed is expressed in revolutions per minute (RPM).

First experiment:

Parameter	Value
ρ^*	29%
u^*	0.65 m/s
ρ_1	3
ρ_2	0.1
η	1
Limiting fan rotating speed	900 RPM
Full experimental time	130 s
Approximate external temperature	25 C$^\circ$
External hygrometry	26.3%

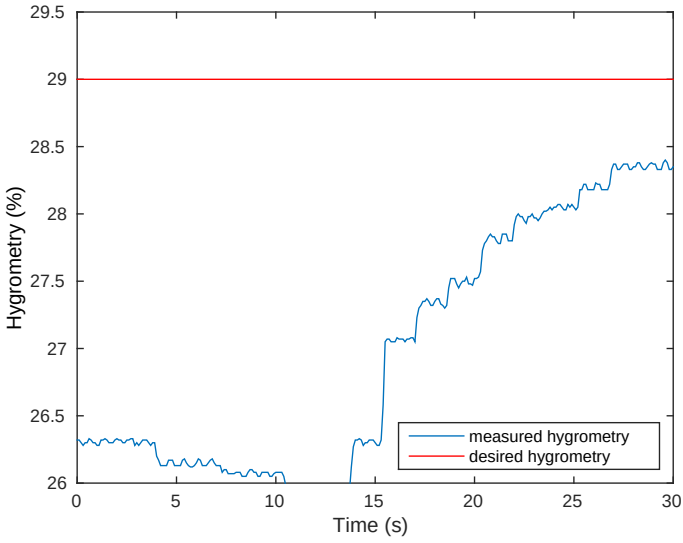

Figure 5.6: Evolution of the hygrometry measured by the third sensor towards the tracked profile of 29% in closed loop with $\rho_1 = 3$ and $\rho_2 = 0.1$

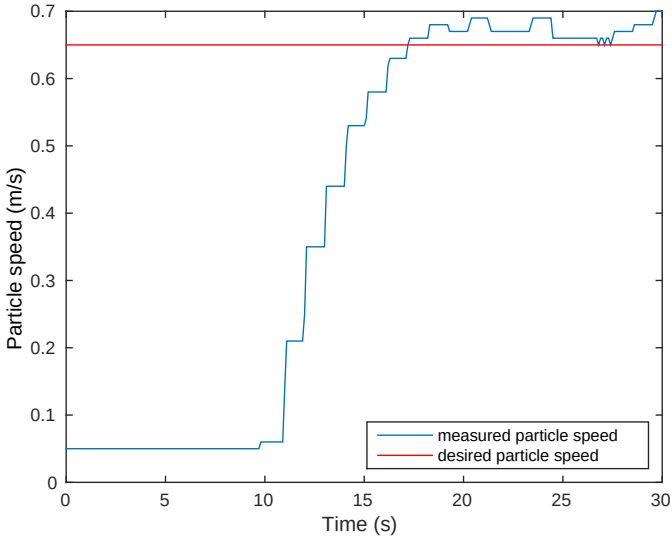

Figure 5.7: Evolution of the gas velocity measured by the speed sensor in closed loop with a tracked profile of 0.65 m/s, $\rho_1 = 3$ and $\rho_2 = 0.1$

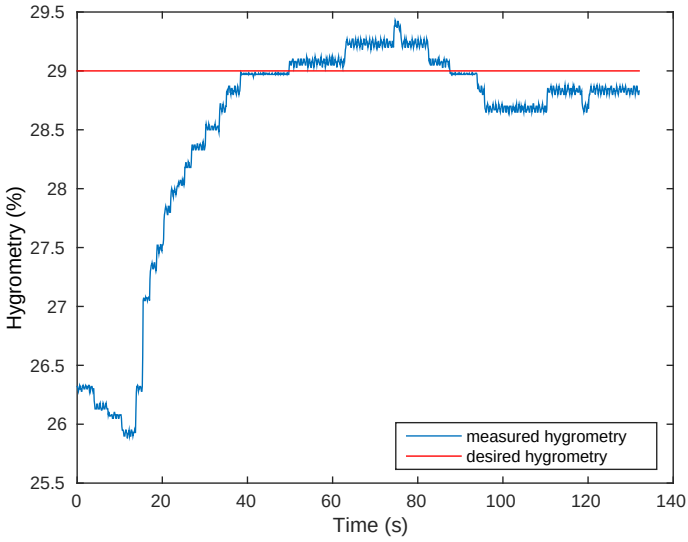

Figure 5.8: Evolution of the hygrometry measured by the third sensor towards the tracked profile of 29% in closed loop with $\rho_1 = 3$ and $\rho_2 = 0.1$

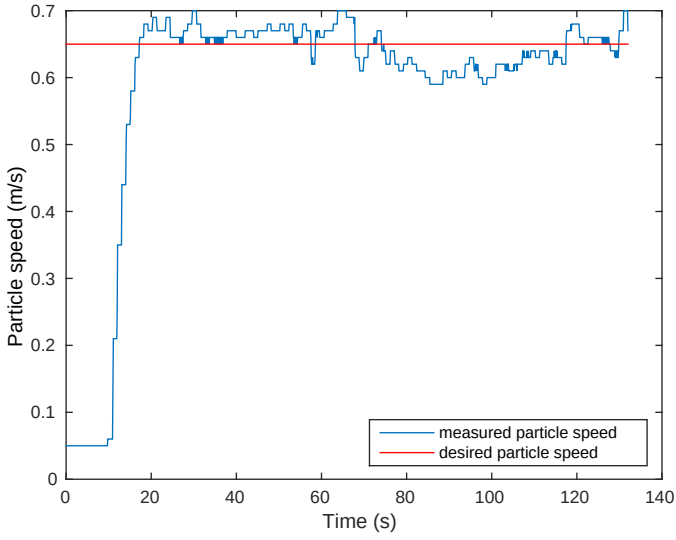

Figure 5.9: Evolution of the gas velocity measured by the speed sensor in closed loop with a tracked profile of 0.65 m/s, $\rho_1 = 3$ and $\rho_2 = 0.1$

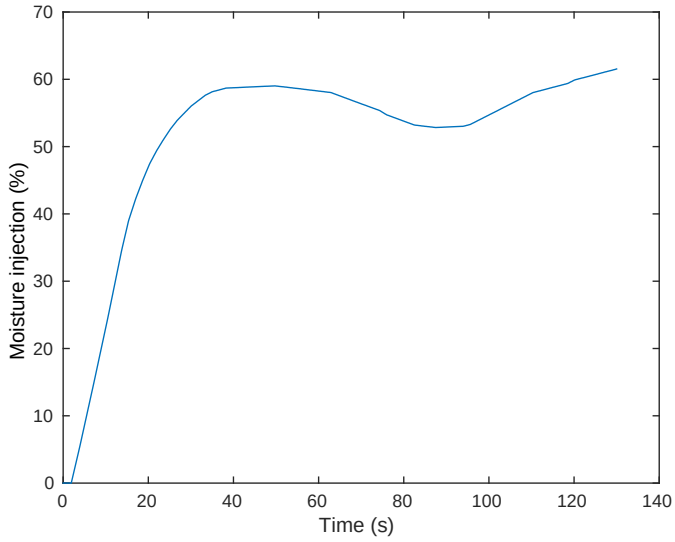

Figure 5.10: Evolution of the moisture injection in closed loop with a tracked profile of 29%, $\rho_1 = 3$ and $\rho_2 = 0.1$

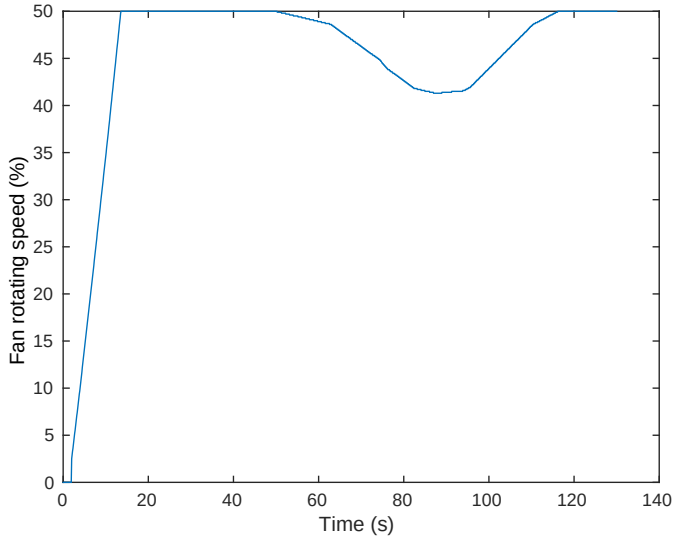

Figure 5.11: Evolution of the fan speed in closed loop with a tracked profile of 0.65 m/s, $\rho_1 = 3$ and $\rho_2 = 0.1$

As seen in Figures 5.6 and 5.7, 30 seconds are not enough in order to reach the tracked hygrometry and speed equilibria. This conclusion holds for the second and third experiments as well. Figures 5.8 and 5.9, however, show that these profiles, and in particular the hygrometry one, can be approached with a steady behaviour in about 115 seconds. One can see on Figures 5.10 and 5.11 that the moisture injector is relatively steady after 30 seconds, while the inlet fan operates at 50% of its maximal rotating speed most of the time.
At first glance, Figure 5.8 seems to exhibit two interesting characteristics: a non-minimum phase behaviour and a static error. However, both could be explained by measurement errors due to the temperature / hygrometry sensors which, according to the manufacturer Soben, may be subject to errors of up to 2 C° or 1% of relative humidity (even though errors of such amplitude should only occur in rare circumstances under fast and high variations in the temperature of hygrometry profile). The absence of integral action in the implemented controller may also explain the static error. Finally, the non-minimum phase behaviour happens in some situations where it has a simple physical explanation. Such a situation arises when there is some residual moisture which has not been properly cleared by the air flow in the tube between two tests. Activation of the inlet fan before the moisture injector then results in a brief drop in measured hygrometry before the injected moisture flows through the tube again. This behaviour was observed several times during the experimental process and it may have been the case in particular at this point in the experiment.

Second experiment:

Parameter	Value
ρ^*	29%
u^*	0.65 m/s
ρ_1	10
ρ_2	0.1
η	1
Limiting fan rotating speed	900 RPM
Full experimental time	110 s
Approximate external temperature	25 C°
External hygrometry	26.3%

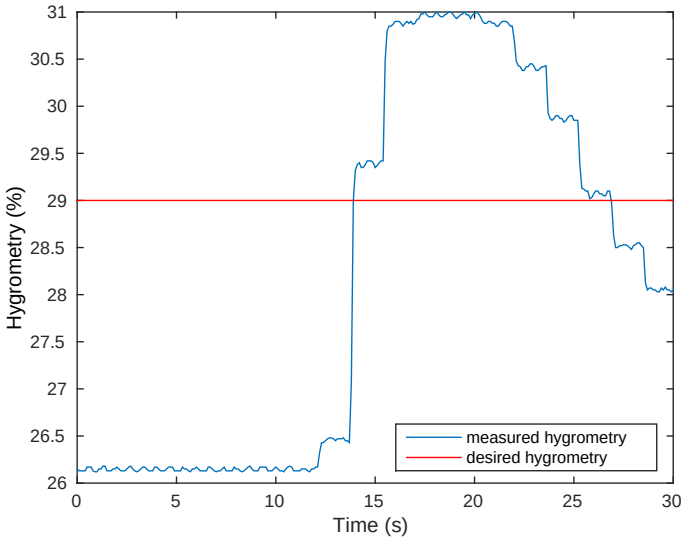

Figure 5.12: Evolution of the hygrometry measured by the third sensor towards the tracked profile of 29% in closed loop with $\rho_1 = 10$ and $\rho_2 = 0.1$

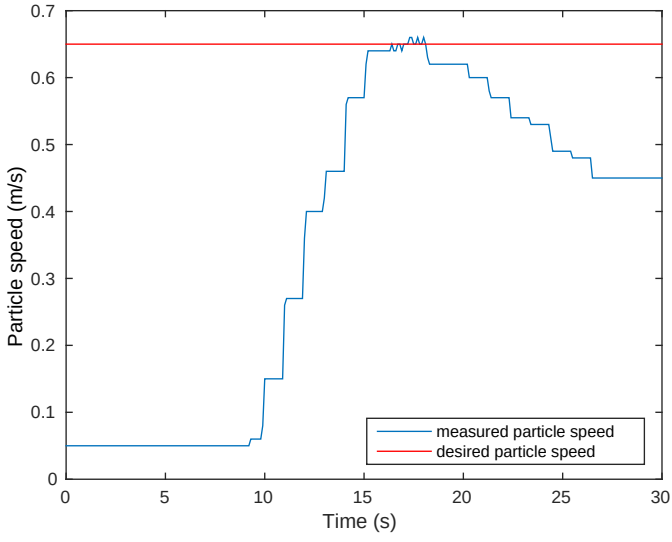

Figure 5.13: Evolution of the gas velocity measured by the speed sensor in closed loop with a tracked profile of 0.65 m/s, $\rho_1 = 10$ and $\rho_2 = 0.1$

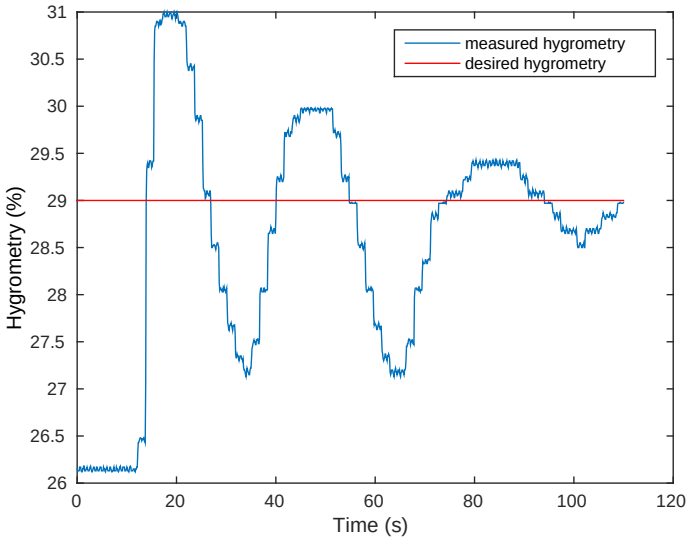

Figure 5.14: Evolution of the hygrometry measured by the third sensor towards the tracked profile of 29% in closed loop with $\rho_1 = 10$ and $\rho_2 = 0.1$

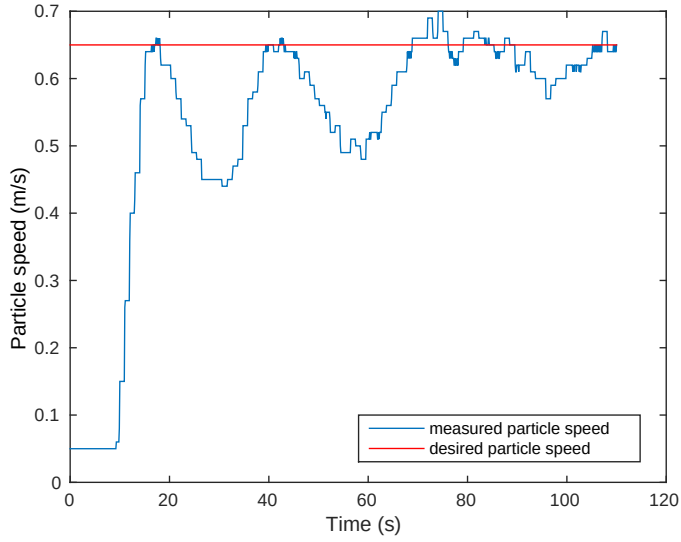

Figure 5.15: Evolution of the gas velocity measured by the speed sensor in closed loop with a tracked profile of 0.65 m/s, $\rho_1 = 10$ and $\rho_2 = 0.1$

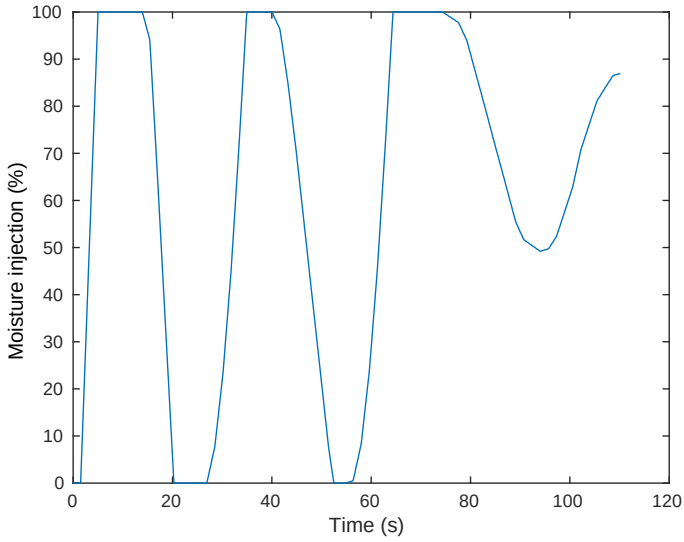

Figure 5.16: Evolution of the moisture injection in closed loop with a tracked profile of 29%, $\rho_1 = 10$ and $\rho_2 = 0.1$

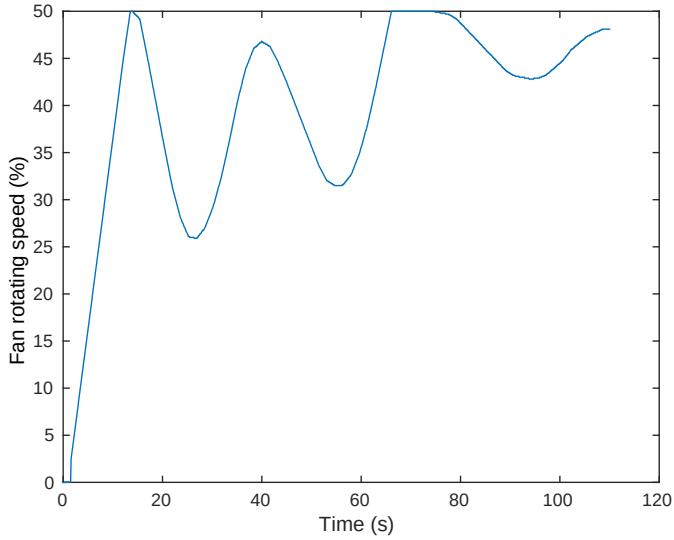

Figure 5.17: Evolution of the fan speed in closed loop with a tracked profile of 0.65 m/s, $\rho_1 = 10$ and $\rho_2 = 0.1$

The second experiment was performed with parameters and operational conditions similar to those for the first one, except for the first weighting parameter ρ_1, which is higher. This difference results in oscillations of much higher amplitude around the tracked hygrometry profile, as seen in Figure 5.14, and a hygrometry trajectory which is still not stabilized at the end of the experimental time. Figure 5.15 shows that the particle speed is also much more oscillating than in the first experiment, even though the steady behaviour is nearly attained after 110 seconds. These important variations can be observed in Figures 5.16 and 5.17 for the moisture injector and the fan rotating speed as well.

Third experiment:

Parameter	Value
ρ^*	29%
u^*	0.2 m/s
ρ_1	1
ρ_2	0.1
η	1
Limiting fan rotating speed	900 RPM
Full experimental time	115 s
Approximate external temperature	25 C$^\circ$
External hygrometry	26.3%

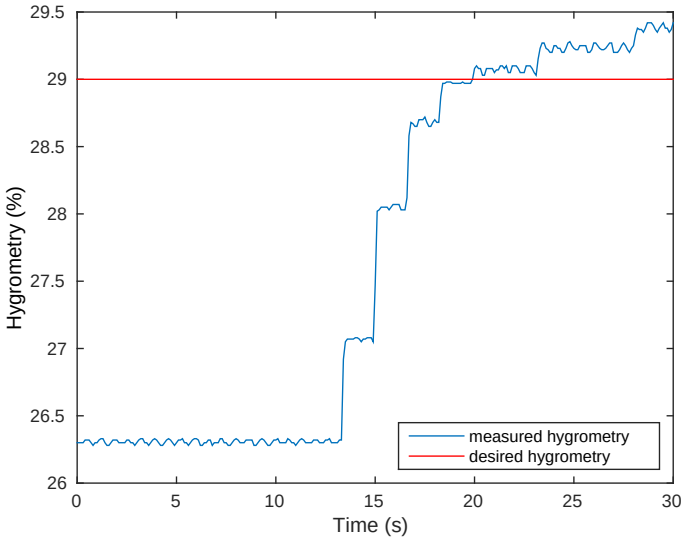

Figure 5.18: Evolution of the hygrometry measured by the third sensor towards the tracked profile of 29% in closed loop with $\rho_1 = 1$ and $\rho_2 = 0.1$

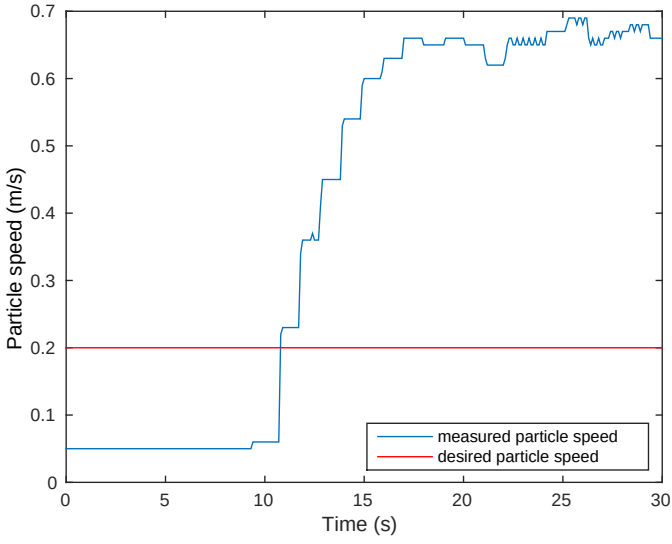

Figure 5.19: Evolution of the gas velocity measured by the speed sensor in closed loop with a tracked profile of 0.2 m/s, $\rho_1 = 1$ and $\rho_2 = 0.1$

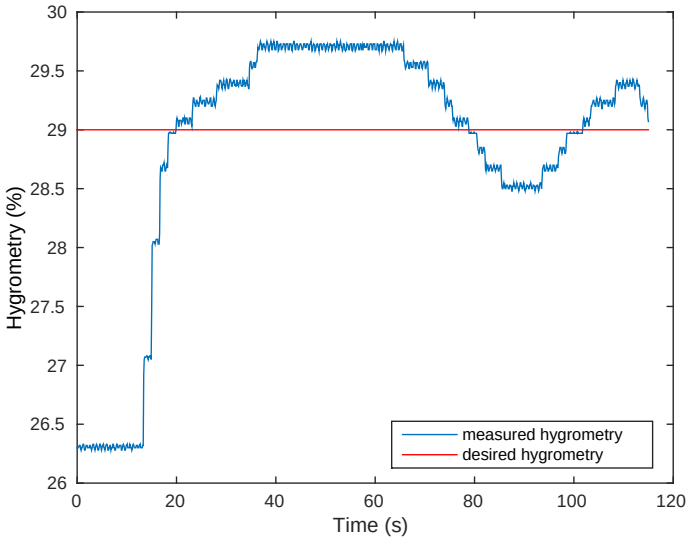

Figure 5.20: Evolution of the hygrometry measured by the third sensor towards the tracked profile of 29% in closed loop with $\rho_1 = 1$ and $\rho_2 = 0.1$

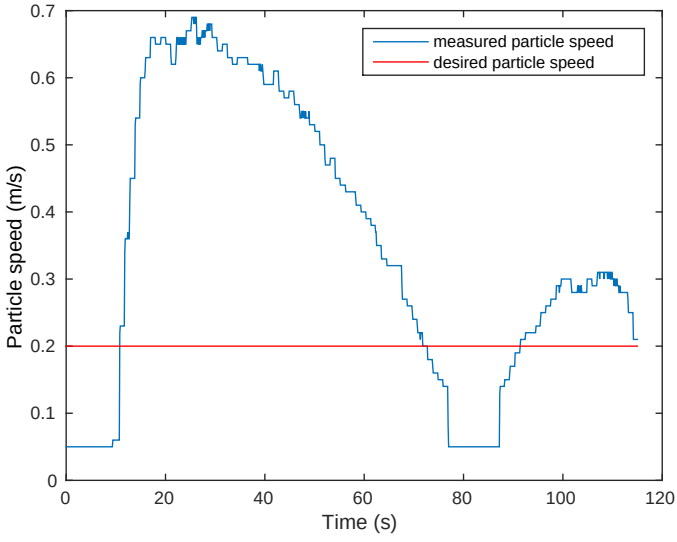

Figure 5.21: Evolution of the gas velocity measured by the speed sensor in closed loop with a tracked profile of 0.2 m/s, $\rho_1 = 1$ and $\rho_2 = 0.1$

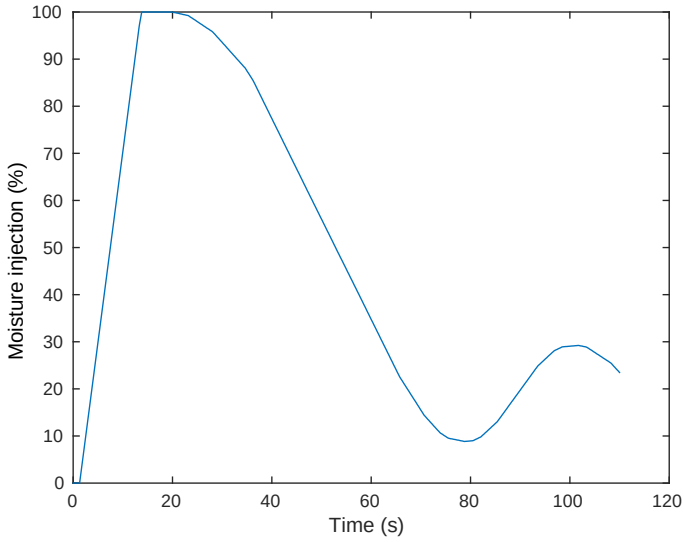

Figure 5.22: Evolution of the moisture injection in closed loop with a tracked profile of 29%, $\rho_1 = 1$ and $\rho_2 = 0.1$

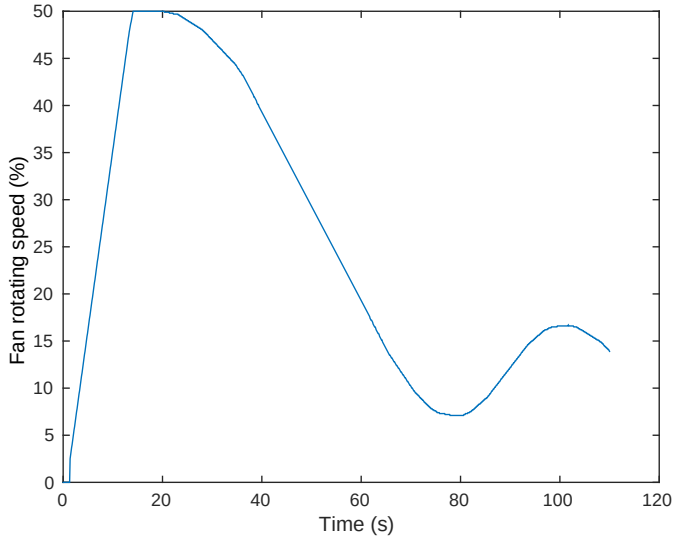

Figure 5.23: Evolution of the fan speed in closed loop with a tracked profile of 0.2 m/s, $\rho_1 = 1$ and $\rho_2 = 0.1$

In the third experiment, both the weighting parameter ρ_1 and the tracked speed profile u^* have been lowered with respect to the first two tests. As a consequence of the smaller weighting parameter, the amplitude of the oscillations shown in Figure 5.20 is reduced as well. However, the settling time is not lower than in the second experiment. This can be explained by the different tracked speed profile of only 0.2 m/s, which drastically reduces the air flow in the tube and slows the whole process down. Despite the limitation of the rotating speed to 50% of its maximal value, the inlet fan is almost never saturated, as seen in Figure 5.23. For an efficient transportation of the moisture in the tube, it seems that the fan should at least operate around $800 - 900$ RPM, which is not a restrictive requirement but is almost never met here nevertheless. Note that, around the 80 s mark, the particle speed temporarily drops to zero (the speed sensor does not go below 0.05 m/s). This is due to another limitation of the test bench. Indeed, as can be seen in Figure 5.23, the required fan rotating speed drops below 10%, which effectively causes the fan to shut down completely until that threshold is met again.

Fourth experiment:

Parameter	Value
ρ^*	31%
u^*	0.9 m/s
ρ_1	10
ρ_2	0.5
η	1
Limiting fan rotating speed	1800 RPM
Full experimental time	30 s
Approximate external temperature	25 C°
External hygrometry	26.3%

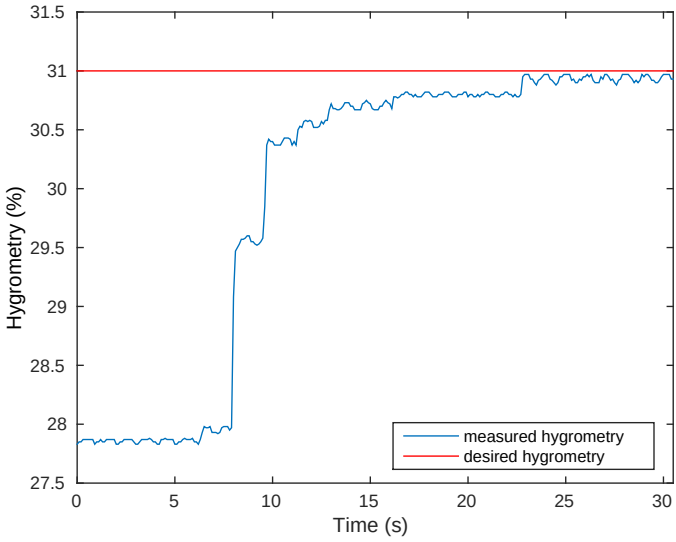

Figure 5.24: Evolution of the hygrometry measured by the third sensor towards the tracked profile of 31% in closed loop with $\rho_1 = 10$ and $\rho_2 = 0.5$

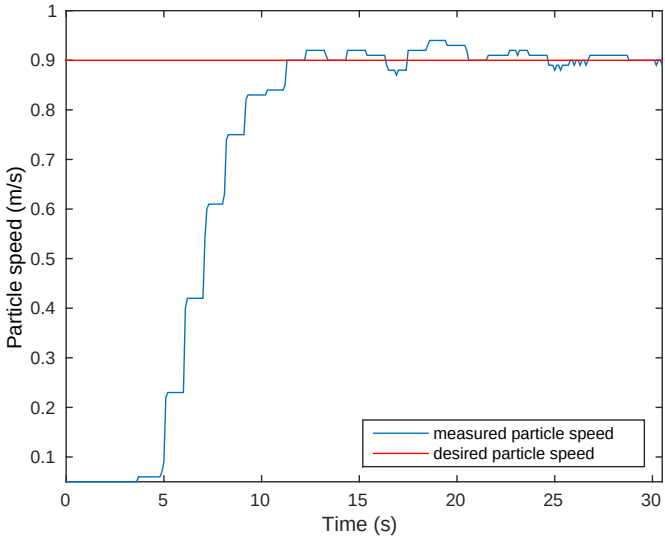

Figure 5.25: Evolution of the gas velocity measured by the speed sensor in closed loop with a tracked profile of 0.9 m/s, $\rho_1 = 10$ and $\rho_2 = 0.5$

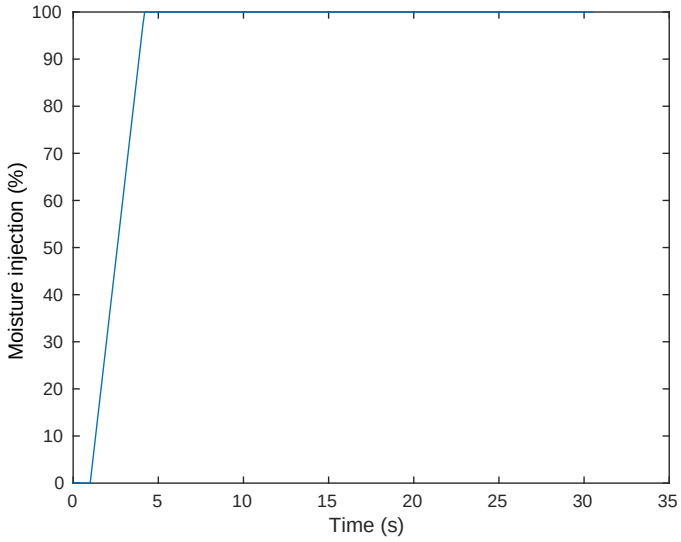

Figure 5.26: Evolution of the moisture injection in closed loop with a tracked profile of 31%, $\rho_1 = 10$ and $\rho_2 = 0.5$

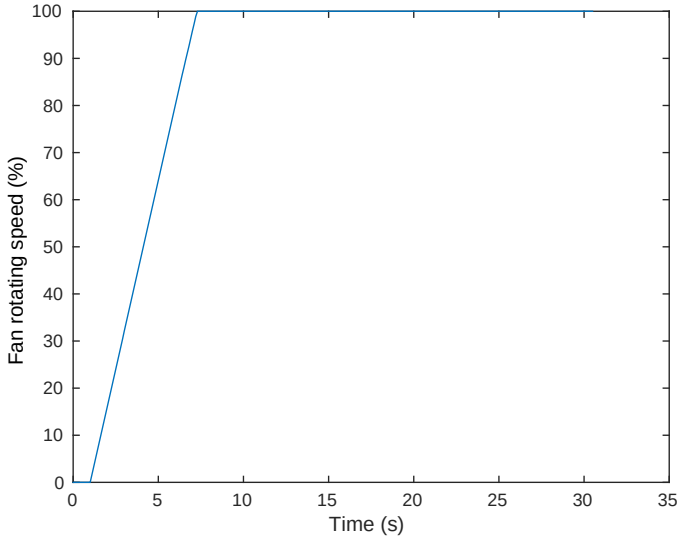

Figure 5.27: Evolution of the fan speed in closed loop with a tracked profile of 0.9 m/s, $\rho_1 = 10$ and $\rho_2 = 0.5$

The fourth experiment is the only one in which both tracked equilibria were reached with a steady behaviour in less than 30 seconds. This result can be explained by several factors. First, the weighting parameters ρ_1 and ρ_2 were higher than in the previous experiments, resulting in a faster convergence at the cost of much steeper input trajectories. This can be observed in Figures 5.26 and 5.27 which show that both the fan and the moisture injector are quickly saturated. Second, the tracked speed profile of 0.9 m/s is the highest possible value allowed by the fans when they reach their maximal rotating speed, which was required in order to reach the hygrometry profile of 31% but allows the whole convergence process to be faster. Third, this hygrometry profile is the highest that could be reached during the whole experimental process and does not seem to allow for overshoots, as observed in Figure 5.24, which makes the process faster as well.

A brief comparison between the experiments can be made at this point.
As can be seen on figures 5.8, 5.14 and 5.20, for a given tracked value, the overshoot and the settling time are heavily dependent on the choice of the weighting parameters and of the tracked speed equilibrium, and can be much higher if the output is not penalized enough in the cost functional. Figure 5.24 shows that even a higher tracked profile can be approached in less time and without any overshoot at the cost of a higher penalization, which has consequences on the inputs of the system.
It can also be observed that the behaviour of the particle speed in Figures 5.9, 5.15 and 5.25 is steadier than in Figure 5.21 due to the better choice of the tracked speed profile and the weighting parameters. Indeed, a desired speed of 0.2 m/s is too low for an efficient transportation of the mist in the tube and makes the whole process much slower and less effective. The value reached by the speed in Figure 5.25 is the maximal speed allowed by the fans.Concerning the evolution of the fan rotating speed shown in Figures 5.11, 5.17 and 5.23, because of physical restrictions, the fan was manually limited to 50% of its maximal rotation speed when tracking a hygrometry profile of 29% in the first three experiments. In fact, in these conditions, the quantity of injected mist is too low and the moisture is mostly carried out of the system by the higher air flow. However, in the fourth experiment, the fan was allowed to reach its maximal speed of 1800 RPM in order to allow a (relatively quick) stabilization of the hygrometry around the higher desired profile of 31%.

Even though the impact of the tracked profiles and parameters seems to be important through these experiments, it should be noted that the amplitude of the oscillations and the length of the settling time can also be explained partially by the limitations of the physical inputs of the test bench. These limitations include the RPM range of the installed fans, the fact that the fans completely shut down when the required voltage input goes below a fixed threshold and the fact that the moisture injection process in the tube is limited in speed and intensity itself.
As previously mentioned, using the heating column for temperature regulation instead would make the control process even more difficult since the dynamics of the column are much slower than those of the moisture injector, while the acceptable temperature range for safe operating conditions is also relatively limited.

Part IV

Conclusion and perspectives

Whatever you do in this life,
it's not legendary,
unless your friends are there to see it.

– Barney Stinson

Conclusion

In this work, a class of infinite-dimensional linear differential systems, featuring in general both boundary and distributed control along with boundary observation, was introduced. The main goal consisted of posing and solving a LQ-optimal control problem for this class of systems, with practical applications in mind.
In order to tackle the difficulties inherent to the unboundedness of the involved operators, a specific change of variables was performed and an extended mathematical model was presented. Under suitable initial conditions and sufficiently regular inputs, this model was shown to be related to the nominal one. More precisely, the boundary input and a Yosida-type approximation of the output based on the resolvent operator were introduced in the extended state, while the time derivative of the former acts as the extended input.
It has been shown that this model is well-posed. More precisely, under our initial assumptions, the operator associated to the extended dynamics is the infinitesimal generator of a C_0-semigroup of bounded linear operators on the extended state space. An interesting related characteristic of this extended system is that it preserves the analyticity when the nominal system has this property. This fact is especially useful when one needs regularity of the state, input and / or (approximate) output trajectories. Moreover, the model was built such that it preserves many other interesting properties of the nominal system, such as the spectral structure, while adding some crucial ones. In particular, we have seen that the extended system is reachable and detectable, and that reachability and stabilizability with respect to the distributed input are transmitted from the nominal system. Other criteria for testing reachability or stabilizability for a pure boundary control system were also presented.
We also had an interesting insight on the comparison between the extended and nominal systems, and more precisely between the approximate and effective outputs as the parameter α goes to infinity. Under suitable assumptions that are satisfied for most practical applications, the extended model was validated further thanks to the fact that the Yosida-type approximate output and the extended transfer function converge in some sense to their respective nominal counterpart when the parameter α goes to infinity.

After introducing and studying the general framework, we have successfully described a general methodology of resolution of a LQ-optimal control problem for the extended model of a BCBO system. This approach is based on the computation of a right coprime fraction of the transfer function, the resolution of a problem of spectral factorization of an associated operator-valued spectral density along the imaginary axis

and the resolution of a Diophantine equation. An important advantage of the method is that it deals with both pure boundary control and mixed boundary and distributed control. We have seen that in both cases, under suitable assumptions, the problem is solvable and its (unique) solution can be interpreted as a dynamical feedback law for the nominal system. This control law is stabilizing, i.e. the state, input and output trajectories of the closed-loop nominal system converge to zero exponentially fast. It is also optimal with respect to a given cost functional for the extended system, which can be interpreted as a cost functional for the nominal system involving non-standard terms corresponding to a penalization of the variation rate of the boundary input and the approximate output. We emphasized the fact that the associated weighting parameters can be tuned depending on the situation and the current objectives.

In the second part of this work, a numerical algorithm of spectral factorization by symmetric extraction was developed and summarized. Two classes of mathematical models of boundary control systems with boundary observation, that can be used in a relatively wide range of applications or processes, have been considered in order to illustrate the theoretical results and the general methodology of the first part, as well as the algorithm.
The first application is a class of convection-diffusion-reaction systems that is typically used for the modeling of chemical or biochemical reactors, for example, or may correspond to the linearization of such a system around an unstable equilibrium. It shows how a LQ-optimal control problem can be solved numerically for a class of parabolic systems with a spectrum composed of simple eigenvalues. In order to bring as much diversity in the results as possible, this part covers both the stable and unstable cases, and the problem is solved successively with mixed boundary and distributed control and then with pure boundary control.

Perspectives

Further investigations could include the convergence of the method of spectral factorization by symmetric extraction for a class of MIMO distributed parameter systems including parabolic systems such as convection-diffusion-reaction systems, extending to the multi-input case the one studied in (Winkin et al. 2005). This would provide a guarantee that the solution generated by the semi-heuristic algorithm will converge to the spectral factor. We hope that this analysis could provide an estimate of the rate of convergence.
Moreover, in view of the promising numerical results obtained in the application (see e.g. Figures 4.5, 4.6 and 4.15), it is expected that, possibly under additional conditions, the closed-loop stable transfer function $(\hat{u}_b, \hat{u}_d) \mapsto \hat{y}_\alpha$ (which depends on α) will converge to a certain closed-loop transfer function corresponding to the nominal system with respect to an appropriate norm as α tends to $+\infty$. This conjecture could also be studied in detail and proved, potentially resulting in a proof of convergence of the optimal feedback for the extended system towards the solution of an appropriate LQ-optimal control problem for the nominal system as α tends to $+\infty$ and η_1 tends to

0, see (1.2.5) and (3.3.1). This question is an interesting topic for future research. The continuity of the spectral factorization with respect to a parameter could also play an important role here, see (Jacob, Winkin and Zwart 1999).
Moreover, since one of the advantages of the proposed methodology is the fact that this is an indirect approach (late lumping), it would be interesting to compare the numerical results obtained in Chapter 4 with a priori discretization methods, such as finite differences and the resolution of the finite-dimensional LQ-optimal control problem by the resolution of the Riccati equation.
Finally, though the results obtained with the test bench simulating the Poiseuille flow were promising, there is still much room for improvement. Other types of control laws could be tested. More precisely, we could consider the more complicated design of a LQ-optimal control law for the full extended BCBO system. Similar computations as for the previous cases reveal that, in this case, the spectral density is given by

$$\hat{F}^e(s) = \frac{1}{k^2 - s^2}\left[\rho_1^2 + \rho_2^2 \frac{\alpha^2}{\alpha^2 - s^2}\left(e^{-\frac{\gamma}{u^*}\alpha} - e^{-\frac{\gamma}{u^*}s}\right)\left(e^{-\frac{\gamma}{u^*}\alpha} - e^{\frac{\gamma}{u^*}s}\right) - s^2\right]$$

where $\gamma \in [0,1]$ is the spatial position of the penalized density in the cost functional. Unfortunately, this spectral density is not rational anymore and finding an analytic spectral factor turns out to be much more difficult than in the previous cases. Clearly, the spectral density becomes rational as α goes to infinity, and more precisely becomes the same density as for the extreme cases with an unbounded punctual observation and a bounded weighted identity. If the spectral factorization is continuous with respect to the parameter α, this could indicate that the resolution of the Diophantine equation for the rational spectral density actually provides the optimal feedback for the LQ-optimal control problem with an unbounded observation operator. This is still an open question and is beyond the scope of this work. A state observer could also be implemented in order to make state feedback laws more efficient.

Nomenclature

List of notations

t	The time variable
z	The space variable (CDR system)
x	The space variable (Poiseuille flow system)
$\dot{x}(t)$	The derivative of x with respect to t
x^T	The transpose of the vector x
$X \oplus Y$	The direct sum between X and Y
$\overline{E}$	The closure of the set E
$D(A)$	The domain of the operator A
Ker A	The kernel (or null space) of the operator A
Ran A	The range of the operator A
$\rho(A)$	The resolvent set of the operator $A : D(A) \subset X \to X$, i.e. the set of all complex values λ such that $(\lambda I - A)^{-1}$ is a bounded linear operator on X
$R(\lambda, A)$	The resolvent operator of A, given by $(\lambda I - A)^{-1}$, with $\lambda \in \rho(A)$
$\mathscr{L}(X,Y)$	The vector space of all bounded linear operators from X to Y
$\mathscr{L}(X)$	The vector space of all bounded linear operators from X to Y
$(T(t))_{t\geq 0}$	C_0-semigroup of bounded linear operators
A^*	The topological adjoint of the operator A
$\hat{F}_*$	The parahermitian adjoint of the operator valued function $\hat{F}$, i.e. $\hat{F}_*(s) = \hat{F}(-\overline{s})^*$
$\langle x, y \rangle$	The scalar product between x and y
$H^\infty(\mathscr{L}(\mathscr{H}))$	The usual Hardy space of $\mathscr{L}(\mathscr{H})$-valued functions that are holomorphic and bounded on the open right half-plane, where $\mathscr{H}$ is a Hilbert space
$L^p(a,b)$	The usual Lebesgue space of complex-valued p-integrable functions defined on $[a,b]$
$L^p([0,t],W)$	The usual Lebesgue space of p-integrable functions defined on $[0,t]$ and with values in W
$L^p([0,+\infty),W)$	The usual Lebesgue space of p-integrable functions defined on $[0,+\infty)$ and with values in W

List of abbreviations

a.c.	absolutely continuous
BCBO	boundary control and boundary observation
CDR	convection-diffusion-reaction
LQ	linear quadratic
MIMO	multiple-input and multiple-output
ODE	ordinary differential equation
PDE	partial differential equation
PID	proportional-integral-derivative
RPM	revolutions per minute

Bibliography

I. Aksikas, J. Winkin, and D. Dochain. Optimal lq-feedback regulation of a non-isothermal plug flow reactor model by spectral factorization. *IEEE Transactions on Automatic Control*, **52 (7)**, 1179–1193, 2007.

A. Alizadeh Moghadam, I. Aksikas, S. Dubljevic, and J. F. Forbes. Boundary optimal (lq) control of coupled hyperbolic pdes and odes. *Automatica*, **49 (2)**, 526–533, 2013.

M. J. Balas. Exponentially stabilizing finite-dimensional controllers for linear distributed parameter systems: Galerkin approximation of infinite dimensional controllers. *J. Math. Anal. Appl.*, **117**, 358–384, 1986.

M. J. Balas. Finite-dimensional controllers for linear distributed parameter systems: exponential stability using residual mode filters. *J. Math. Anal. Appl.*, **133**, 283–296, 1988.

G. Bastin, J.-M. Coron, and B. d'Andréa Novel. Using hyperbolic systems of balance laws for modeling, control and stability analysis of physical networks. *in* 'Lecture notes for the Pre-Congress Workshop on Complex Embedded and Networked Control Systems, 17th IFAC World Congress', Seoul, 2008.

T. Besson, A. Tchousso, and C.-Z. Xu. Exponential stability of a class of hyperbolic pde models from chemical engineering. *in* 'Proceedings of the 45th IEEE Conference on Decision and Control', pp. 3974–3978, San Diego, 2006.

H. Bounit. The stability of an irrigation canal system. *Int. J. Appl. Math. Comput. Sci.*, **13 (4)**, 453–468, 2003.

D. M. Busiello, G. Planchon, M. Asllani, T. Carletti, and D. Fanelli. Pattern formation for reactive species undergoing anisotropic diffusion. *Eur. Phys. J. B*, **88:222**, 2015.

F. M. Callier and J. Winkin. Lq-optimal control of infinite-dimensional systems by spectral factorization. *Automatica*, **28 (4)**, 757–770, 1992.

F. M. Callier and J. Winkin. The spectral factorization problem for multivariable distributed parameter systems. *Integr. equ. oper. theory*, **34 (3)**, 270–292, 1999.

F. Castillo, E. Witrant, and L. Dugard. Dynamic boundary stabilization of linear parameter varying hyperbolic systems: application to a poiseuille flow. *in* 'IFAC Joint Conference SSSC - 11th Workshop on Time-Delay Systems', pp. 344–349, Grenoble, 2013.

F. Castillo, E. Witrant, C. Prieur, and L. Dugard. Dynamic boundary stabilization of linear and quasi-linear hyperbolic systems. *in* 'Proceedings of the 51st IEEE Conference on Decision and Control', pp. 2952–2957, Maui, 2012.

B. Chentouf and J.-M. Wang. Boundary feedback stabilization and riesz basis property of a 1-d first order hyperbolic linear system with l^∞-coefficients. *J. Differential Equations*, **246**, 1119–1138, 2009.

P. D. Christofides and P. Daoutidis. Finite-dimensional control of parabolic pde systems using approximate inertial manifolds. *J. Math. Anal. Appl.*, **216**, 398–420, 1997.

R. Curtain and H. J. Zwart. *An introduction to infinite-dimensional linear systems theory*. Springer-Verlag, New York, 1995.

J. R. Dehaye and J. Winkin. Boundary control systems with yosida type approximate boundary observation. *in* 'Proceedings of the first IFAC Workshop on Control of Systems Modeled by Partial Differential Equations (CPDE)', number 61, Paris, 2013*a*.

J. R. Dehaye and J. Winkin. Lq-optimal control by spectral factorization of extended semigroup boundary control systems with approximate boundary observation. *in* 'Proceedings of the 52nd IEEE Conference on Decision and Control (CDC)', pp. 1071–1076, Florence, 2013*b*.

C. Delattre, D. Dochain, and J. Winkin. Sturm-liouville systems are riesz-spectral systems. *Int. J. Appl. Math. Comput. Sci.*, **13 (4)**, 481–484, 2003.

J. Deutscher. Finite-dimensional dual state feedback control of linear boundary control systems. *Int. J. Control*, **86 (1)**, 41–53, 2013.

B. D. Doytchinov, W. J. Hrusa, and S. J. Watson. On perturbations of differentiable semigroups. *Semigroup Forum*, **54 (1)**, 100–111, 1997.

A. K. Dramé, D. Dochain, and J. J. Winkin. Asymptotic behavior and stability for solutions of a biochemical reactor distributed parameter model. *IEEE Transactions on Automatic Control*, **53 (1)**, 412–416, 2008.

K.-J. Engel and R. Nagel. *One-parameter semigroups for linear evolution equations*. Springer-Verlag, New York, 2000.

K.-J. Engel and R. Nagel. *A short course on operator semigroups*. Springer-Verlag, New York, 2006.

H. O. Fattorini. Boundary control systems. *SIAM J. Control Optim.*, **6**, 349–388, 1968.

P. Grabowski and F. M. Callier. Boundary control systems in factor form: Transfer functions and input-output maps. *Integr. equ. oper. theory*, **41 (1)**, 1–37, 2001.

J. R. Grad and K. A. Morris. Solving the linear quadratic optimal control problem for infinite-dimensional systems. *Computers Math. Applic.*, **32 (9)**, 99–119, 1996.

M. Ikeda and D. D. Šiljak. Optimality and robustness of linear quadratic control for nonlinear systems. *Automatica*, **26 (3)**, 499–511, 1990.

B. Jacob and H. J. Zwart. *Linear port-Hamiltonian systems on infinite-dimensional spaces*. Birkhäuser, Basel, 2012.

B. Jacob, J. Winkin, and H. J. Zwart. Continuity of the spectral factorization on a vertical strip. *Systems & Control Letters*, **37 (4)**, 183–192, 1999.

Y. Le Gorrec, B. M. J. Maschke, J. A. Villegas, and H. J. Zwart. Dissipative boundary control systems with application to distributed parameters reactors. *in* 'Proceedings of the 2006 IEEE International Conference on Control Applications', pp. 668–673, Munich, 2006.

L. Mohammadi, I. Aksikas, S. Dubljevic, and J. F. Forbes. Lq-boundary control of a diffusion-convection-reaction system. *Int. J. Control*, **85 (2)**, 171–181, 2012.

J. B. Moore and B. D. O. Anderson. Optimal linear control systems with input derivative constraints. *in* 'Proceedings of the Institution of Electrical Engineers', Vol. 114 (12), pp. 1987–1990, 1967.

K. A. Morris and C. Navasca. Approximation of low rank solutions for linear quadratic control of partial differential equations. *Comput. Optim. Appl.*, **46 (1)**, 93–111, 2010.

M. R. Opmeer. The algebraic riccati equation for infinite-dimensional systems. *in* 'Proceedings of the 21st International Symposium on Mathematical Theory of Networks and Systems', pp. 1610–1614, Groningen, 2014.

C. Prieur, J. Winkin, and G. Bastin. Robust boundary control of systems of conservation laws. *Math. Control Signals Syst.*, **20**, 173–197, 2008.

A. J. Pritchard and D. Salamon. The linear quadratic control problem for infinite dimensional systems with unbounded input and output operators. *SIAM J. Control Optim.*, **25 (1)**, 121–144, 1987.

M. Rosenblum and J. Rovnyak. *Hardy classes and operator theory*. Oxford University Press, New York, 1985.

O. Staffans. *Well-posed linear systems*. Cambridge University Press, Cambridge, 2005.

M. Tucsnak and G. Weiss. *Observation and control for operator semigroups*. Birkhäuser, Basel, 2009.

J. P. Vandewalle and P. Dewilde. On the minimal spectral factorization of nonsingular positive rational matrices. *IEEE Transactions on Information Theory*, **21 (6)**, 612–618, 1975.

J. A. Villegas. *A port-hamiltonian approach to distributed parameters systems*. Wöhrmann Print Service, Zutphen, 2007.

G. Weiss. Transfer functions of regular linear systems. part 1: characterizations of regularity. *Trans. American Math. Society*, **342 (2)**, 827–854, 1994.

M. Weiss and G. Weiss. Optimal control of stable weakly regular linear systems. *Mathematics of Control, Signals and Systems*, **10 (4)**, 287–330, 1997.

J. Winkin, F. M. Callier, B. Jacob, and J. Partington. Spectral factorization by symmetric extraction for distributed parameter systems. *SIAM J. Control Optim.*, **43 (4)**, 1435–1466, 2005.

J. Winkin, D. Dochain, and P. Ligarius. Dynamical analysis of distributed parameter tubular reactors. *Automatica*, **36 (3)**, 349–361, 2000.

D. E. Winterbone and R. J. Pearson. *Theory of engine manifold design: wave action methods for IC engines*. Wiley, London, 2005.

E. Witrant, A. D'Innocenzo, G. Sandou, F. Santucci, M. D. Di Benedetto, A. J. Isaksson, K. H. Johansson, S.-I. Niculescu, S. Olaru, E. Serra, S. Tennina, and U. Tiberi. Wireless ventilation control for large-scale systems: the mining industrial case. *Int. J. Robust Nonlinear Control*, **20**, 226–251, 2010.